Galvanic Cathodic Protection of Steel Reinforcement Using Metallized Zinc Coatings

by

Yan Chen, B.Eng.

A Thesis Submitted to
the School of Graduate Studies and Research
in Partial Fulfillment of
the Requirements for the Degree of

Master of Applied Sciences

Department of Civil Engineering
Faculty of Engineering
University of Ottawa
Ottawa, Ontario, Canada, K1N 6N5

October, 1994

ISBN 0-612-00603-4

UNIVERSITÉ D'OTTAWA
UNIVERSITY OF OTTAWA

Abstract

Corrosion of steel reinforcement in concrete bridges and parking garages due to the intrusion of chloride ions from deicing salt is a serious problem in northern climates. A number of approaches have been used in the past to mitigate steel corrosion. Cathodic protection is considered to be the only technique to slow down corrosion in salt contaminated concrete to a negligible rate. This is accomplished by either an impressed current anode or a sacrificial anode in the system. The impressed current anode system, with metallized zinc as the anode material, has been used with success on a number of bridges. The sacrificial anode system has been used on a limited number of bridges under marine environment.

An impressed current system is difficult to apply to parking garages because of the thickness of concrete cover in these structures. Cover in concrete parking garages is typically much thinner than that used in bridges, and may easily cause electrical shorts between the anode and the reinforcing bar. Systems with sacrificial anodes, commonly referred to as galvanic cathodic protection systems, instead, take advantage of the reduced thickness of concrete cover, thus becoming a feasible form of protection for parking structures.

The goal of this research project is to develop a sacrificial anode for cathodic protection of steel reinforcement in parking garages and bridges.

Although it is too early to draw conclusions, certain trends have been reported on performance of sacrificial anode systems. So far the results indicate that the effectiveness of galvanic cathodic protection increases with decreasing the thickness of concrete cover. Salt contamination and moisture also increase the effectiveness of galvanic cathodic protection of reinforcement.

Acknowledgments

I wish to express my appreciation to Dr. M. Saatcioglu and Dr. R. Brousseau for their guidance, advice and financial support throughout this research program.

I also wish to thank Mr. Qian, Mr. B. Baldock, Mr. R. Evraire and the technical staffs of the Material Laboratory of the Institute for Research in Construction at the National Research Council of Canada for their assistance during the experimental part of this project.

Contents

List of Figures

List of Tables

Acronyms

AC	Alternating current
CP	Cathodic protection
CSE	Copper/copper Sulphate reference Electrode
DC	Direct current
FDOT	Florida Department of Transportation
FHWA	Federal Highway Administration
NHE	Normal Hydrogen Electrode
PVC	Polyvinyl chloride
SCE	Saturated Calomel Electrode
SHE	Standard Hydrogen Electrode

List of Symbols

Al	Aluminum
Cl-	Chloride ion
$CaCO_3$	Calcium carbonate
$Ca(OH)_2$	Calcium hydroxide
CO_2	Carbonate dioxide
Cu	Copper
$Cu/CuSO_4$	Copper/copper sulphate
E	Potential
E_a	Anode potential
E_c	Cathode potential
$E_o.a$	Open circuit potential
E_{corr}	Corrosion potential
Fe	Steel
$Fe(OH)_3$	Ferric hydroxide
Fe_2O_3	Ferric oxide
H_2O	Water
I	Current flow
$I_o.a$	Exchange current density of anode
I_a	Anode current
I_c	Cathode current
I_{corr}	Corrosion current
ne	Electron
O_2	Oxygen
OH^-	Hydroxide ion
Zn	Zinc

Chapter 1

Introduction

1.1 Introduction

1.1.1 Reinforcement Corrosion in Salt Contaminated Concrete

Reinforced concrete is a widely used construction material. Concrete and steel form a composite action to resist stresses caused by exterior loads. Concrete is poor in tension and strong in compression, while steel is strong both in tension and compression. Reinforcing bars are used as tension steel in most applications, and are placed in the cracked tension zone where they are susceptible to corrosion. The corrosion of reinforcement in concrete is a serious problem in North America. Concrete normally provides excellent corrosion protection for embedded steel because of high alkalinity (pH value around 12) of cement which facilitates the formation of a protective oxide film on the surface of encased steel. This protection environment will easily be destroyed, however, due to the intrusion of chloride ions from deicing salt. The protective oxide film around the reinforcement may be broken at certain rate of chloride concentration and in presence of a certain concentration of oxygen and moisture, the embedded steel may start to corrode, damaging the concrete structure [1].

Electrochemical Background

Most metals are not found as pure materials in nature. Ores are refined to obtain a metal and the metal is then shaped to a final product. During this process, energy

is added to the metal. This energy is released as a result of corrosion. The release of energy is an electrochemical process in which the metal reverts back to its more stable oxide film.

Steel reverts to the thermodynamically more stable oxides according to the following reactions [2].

$$4Fe + 6H_2O + 3O_2 \rightarrow 4Fe(OH)_3, \tag{1.1}$$

and

$$2Fe(OH)_3 \rightarrow Fe_2O_3 + 3H_2O, \tag{1.2}$$

where $Fe(OH)_3$ is ferric hydroxide, and Fe_2O_3 is ferric oxide.

The process of a metal to release energy and revert bake to its natural ore is an electrochemical process called **corrosion**. Corrosion occurs in most of metals at their natural state. Some description of the corrosion process is given in this section.

Corrosion is an electrochemical process which includes four basic elements: anode, cathode, conductor, and electrolyte, and involves an anodic reaction and a cathodic reaction. Fig. 1.1 illustrates these four basic elements in a corrosion cell. The anodic reaction is the oxidation of a metal (anode) to its cation with the release of electrons. The cathodic reaction, on the other hand, is an electrochemical reduction where the electrons are consumed with oxygen and water to form hydroxyl ions. These two types of reactions must proceed in parallel and at an equal rate on the two electrodes. Therefore the electrons released from anodic reaction are subsequently consumed by cathodic reaction. The conductor connects anode and cathode to close the circuit for the flow of electric current. The electrolyte is the solution that surrounds the electrodes, and contains necessary elements to react with the immersed metal. The ionic current between the anode and cathode flows through the electrolyte [3].

Corrosion of Steel in Concrete

Reinforced concrete may exhibit conditions similar to those of a corrosion cell described in the previous section. Due to the refinement of the ore, different energy levels may exist on the surface of a single reinforcement. With these different potentials, a galvanic cell is formed as illustrated in Fig. 1.2. While the areas of high

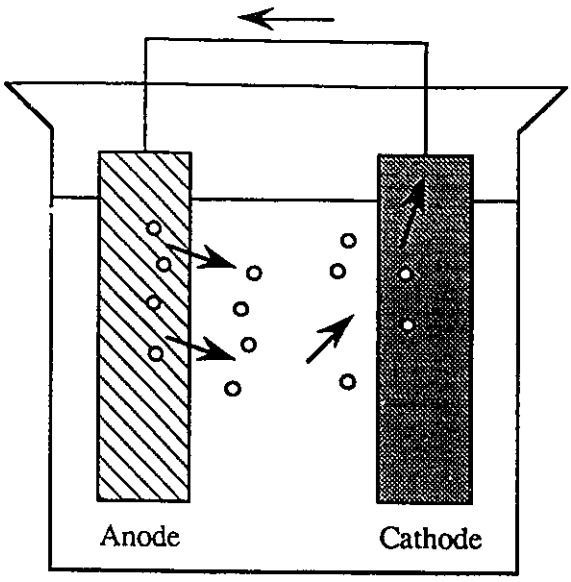

$$Fe \rightarrow Fe^{2+} + 2e^{-} \qquad O_2 + H_2O + 4e^{-} \rightarrow 4OH^{-}$$

Figure 1.1 : Current flow between anode and cathode in a corrosion cell.

negative potential corrode significantly forming the anode sites, other locations of less negative potential do not corrode as much forming the cathode sites. The steel bar functions as an external conductor while the high humidity concrete functions as electrolyte [4].

The possibility of steel corrosion in a particular electrolyte can be determined by the energy relationship between the steel and the solution in contact. The pourbaix diagram of Fig. 1.3 shows the stability of iron as a function of the pH level and potential. Three different zones: corrosion, passivation and immunity can be seen in the diagram. The state of iron is determined by the solution potential and pH level. In the case of steel in concrete, the iron is normally in the passivation zone where a passive film of Fe_2O_3 and Fe_3O_4 is formed on the steel surface. The corrosion rate is small and only sufficient to maintain the passive film. Chloride ions disrupt the passive film. This initiates corrosion and induces a localized pH depletion, which further shifts the iron potential progressively towards a more electronegative potential. The reinforcing steel then starts corroding freely and becomes situated in the corrosion

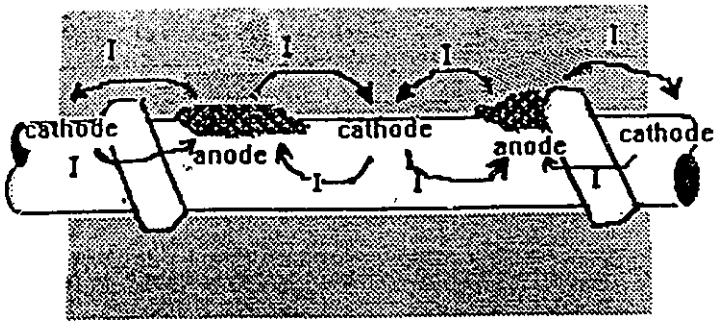

Figure 1.2 : Corrosion cell in reinforced concrete (Adopted from reference [4]).

zone shown in Fig. 1.3. When the cathodic protection is applied, the steel potential can be shifted into the immunity zone as discussed later [4].

In practice, the presence of oxide film, which provides a protective layer on the steel surface, is destroyed by intrusion of chloride ions which come from deicing salt. The reinforcing steel is subject to the galvanic corrosion process once the passive films are removed. Chloride ions can not be uniformly distributed within concrete as illustrated in Fig. 1.4. Portions of the steel reinforcement remain passive while the chloride ions remove the oxide film in other areas of the steel. Differences in chloride ion concentration establish differences in electrical potential. The concrete acts as an electrolyte. The conductor is provided by reinforcing ties and the main reinforcing bar. The volume of the rust product formed during corrosion is much greater than the original steel. The tensile stress caused by the corrosion products can be more intensive and exceed the tensile fracture limits of concrete, which cause cracks or delaminations and eventually result in spalling. Expansive stresses of 4700 psi have been measured at the concrete-steel interface [5].

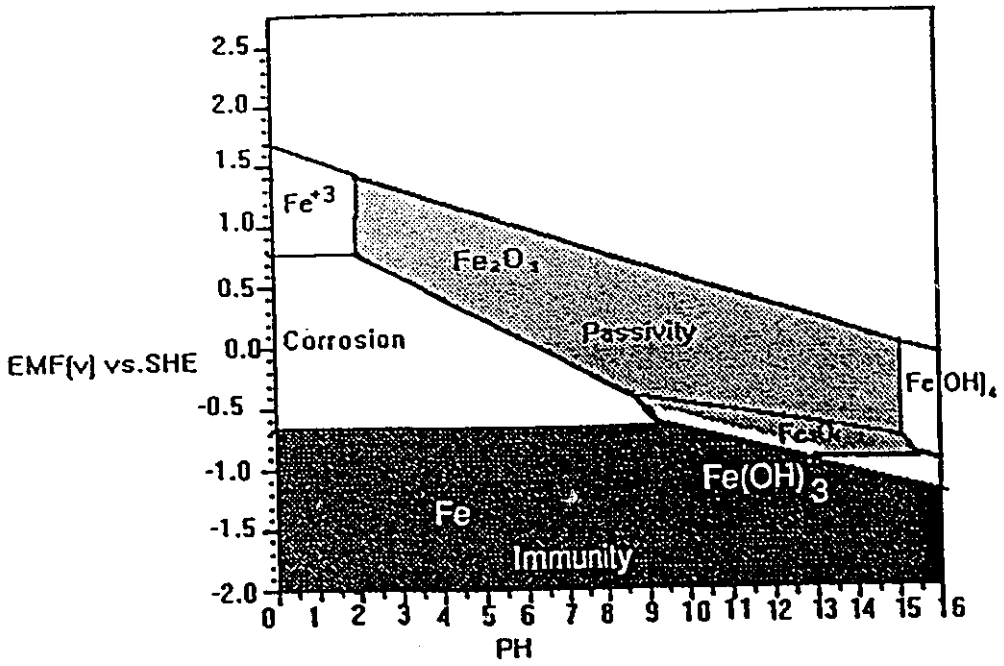

Figure 1.3 : Pourbaix diagram for iron at temperature of 298K (Adopted from reference [4]).

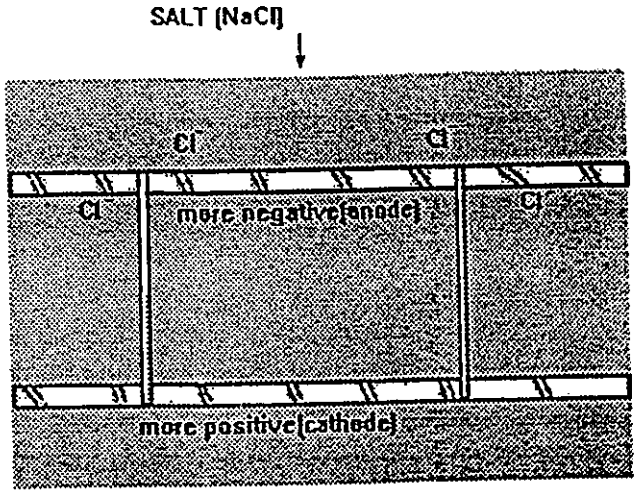

Figure 1.4 : A Chloride concentration gradient in a concrete deck can induce differences in electrical potential forming a macro corrosion cell (Adopted from reference [5]).

1.1.2 Possible Approaches to Mitigate Steel Reinforcement Corrosion

Waterproofing Membranes

Membranes can retard the intrusion of chloride ions into concrete but do not prevent corrosion when sufficient chloride ions have reached reinforcement. Two types of membranes are used in practice. The first type is applied in liquid form while the second type consists of prefabricated sheeting and bentonite panels.

Liquid elastomeric membrane systems are designed for specific methods of application, sold to licensed applicators. Prefabricated sheet membrane systems have better quality control. However, they must be installed carefully. The installation of a membrane system is different for new and existing structures. Waterproofing membrane is of great benefit on new structures. These membranes prevent, or at least retard, the intrusion of chloride ions to reinforcement. When the content of chloride in concrete equals or exceeds the corrosion rate, however, membranes can not significantly reduce corrosion. In heavily salt contaminated concrete, if membranes completely encapsulate the concrete, they could reduce corrosion rates and prevent any access of oxygen to steel reinforcement [6].

Patching

Patching refers to restoration of damaged concrete with relatively small areas. To repair such surface damage it is important to identify the cause of the damage since it may involve more than one factor. The objective of the repair can be provided by the identification of the cause [7].

The repair procedure involves:

1. Cut vertical patch edges;
2. Remove all salt contaminated concrete;
3. Clean reinforcing steel;

4. Apply cementitious bonding grout or epoxy coat on reinforcing steel and place epoxy bonding agent;

5. Place, finish and cure the patched area (see Fig. 1.5).

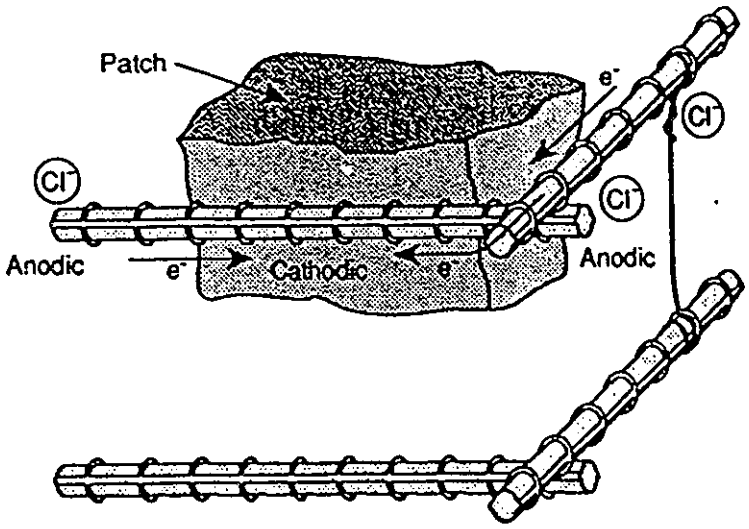

Figure 1.5 : A typical macro corrosion cell formed around a patched area (Adopted from reference [8]).

It is very important to replace the deteriorated concrete in order to provide a protective and durable environment for reinforcement. Impermeable, highly alkaline cement-based material with little shrinkage and excellent adhesion to parent concrete should be used to repair deteriorated concrete. The properties of repairing material should also be closely matched with the parent concrete. No matter what type of material is used, it must be worked well into the concrete surface. After the removal of salt-contaminated concrete, patching is one of the traditionally used treatment to rehabilitate corrosion-damaged structure. Unfortunately patch only repairs concrete surface and it does not always slow down corrosion to a desired level. In the patch repair work a galvanic cell is induced. Steel bar areas exposed to fresh concrete serve

as the cathode, while steel bars in salt-contaminated concrete around the patches serve as the anode and accelerate corrosion rates [7].

The structure should be adequately investigated to determine the cause, extent, and severity of deterioration before any patching and waterproofing are considered. This process has a significant effect on the selection of repair method.

1.1.3 Cathodic Protection

Cathodic protection (CP) is considered the only technique that can slow down corrosion to a negligible rate in salt contaminated concrete. This was demonstrated by experimental systems which were installed on reinforced concrete bridges in the early seventies. The first commercially available CP system appeared on the market in the early 1980's. In practice, the direct current source may be either a DC rectifier or any metal which is higher (more negative) in the electromotive series than the object to be protected. The first system is called impressed current cathodic protection, the latter, galvanic, or sacrificial cathodic protection.

The Principle of Cathodic Protection

The principal elements of a corrosion cell was discussed previously. It was also stated that a potential difference may exist in reinforced concrete producing a galvanic cell. The difference in potential is generally expressed in terms of electromotive force (E.M.F.). E.M.F. is usually measured relative to a reference potential. The potential between electrode and reference is called half cell. Two half cells give E.M.F. The internationally accepted primary reference is the standard hydrogen electrode (SHE), or normal hydrogen electrode (NHE). However, copper/copper sulphate ($Cu/CuSO_4$) is a reference electrode more suitable for reinforced concrete [9] (see Table 1.1).

Reactions of oxidation and reduction occur at different sites of the same steel surface as previously explained and illustrated in Fig. 1.2. The variation of potential with electrical current is usually expressed in the form of Evans diagram as shown in Fig. 1.6.

In Fig. 1.6 the relationships for anodic and cathodic reactions of an electrical cell

Table 1.1 : Potentials for standard references (Adopted from reference [9]).

Reference	E scale at 25 °C
Standard Hydrogen electrode (SHE)	0.00 v
Copper sulphite electrode (CSE)	+0.32 v
Saturated calomel electrode (SCE)	+0.25 v

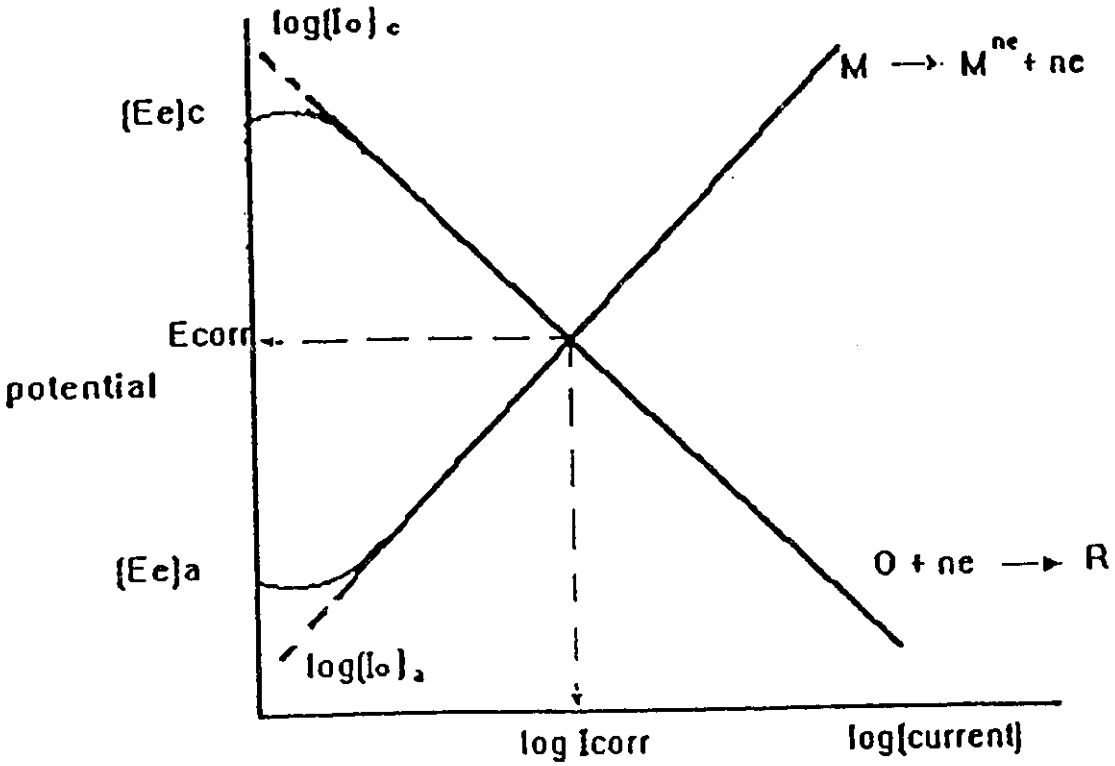

Figure 1.6 : Evans diagram for the corrosion process (Adopted from reference [10]).

intersect at a point where the mean anodic and cathodic current densities are equal to I_{corr}, which is called corrosion current density. The electrode potential of the couple at this point is called the corrosion potential E_{corr}. No significant corrosion occurs when the current density is close to the value of I_{corr}. When the current density is not close to the value of I_{corr} two possibilities exist:

1) Potential E decreases towards the negative direction, activating cathodic reaction. The steel is cathodically protected in this area.

2) Potential E increases towards the positive direction, activating anodic reaction. A metal (Zinc) is sacrificed while the steel is protected.

An electrode at which no charge transfer across the metal-solution interface occurs, regardless of the amount of potential imposed by an outside source of voltage, is called an ideal polarized electrode. Some electrodes approach ideal polarizability over certain limited potential ranges since no real electrode can behave as an ideal polarized electrode over the whole potential range in a solution. Fig. 1.7 illustrates two electrodes polarized at point $E_{(mixed)}$ potential for galvanic cathodic protection [11].

Cathode is the electrode where reduction occurs, and anode is the electrode where oxidation occurs. Electrons strip from anode and flow through conductor to cathode. They combine with oxygen and water to form hydroxide ions on the cathode surface. Extra electrons make oxidation of iron difficult at cathode. Therefore, cathodic protection is defined as reduction or elimination of corrosion by making the metal a cathode by introducing impressed direct current or attachment to a sacrificial anode (usually Magnesium, Aluminum, and Zinc). Most structures which have corroded will have both cathodic areas and anodic areas prior to the application of cathodic protection. If all anodic areas can be changed to cathodic areas by applying cathodic protection, the entire reinforcement becomes a cathode and no corrosion occurs [12].

The areas of delamination in a reinforced concrete structure are generally removed and repaired prior to the application of cathodic protection. However, some areas of concrete, which are not cracked or delaminated, may be near the tensile fracture

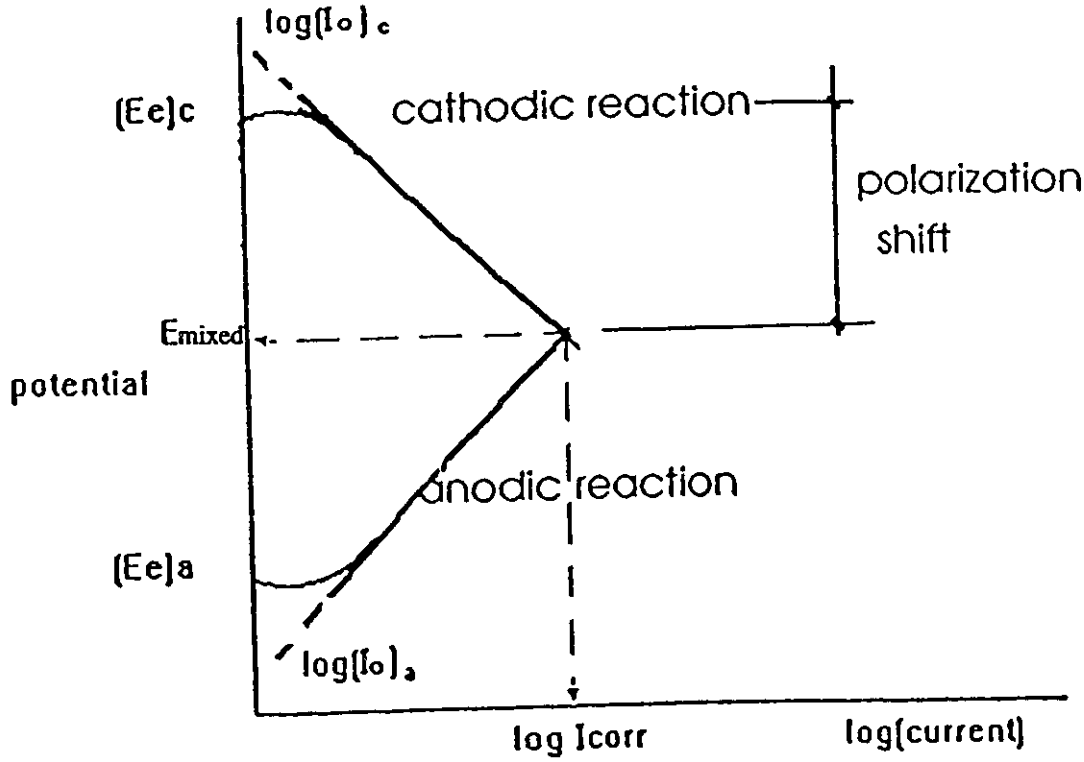

Figure 1.7 : Polarization diagram for a galvanic cathodic protection cell (Adopted from reference [11]).

strength of concrete because of the accumulated expansive forces caused by corrosion products of reinforcing steel. If the reduction in the rate of corrosion achieved by cathodic protection is not substantial, stresses from new corrosion products continue building up. The use of valid cathodic protection criteria is extremely important for long-term effectiveness to mitigate corrosion of reinforcing steel effectively. In the present study, the 100 mV polarization shift criterion is used for this purpose [13].

Impressed Current Anodes

The principle of impressed current cathodic protection is to apply sufficient current density to corroding metal by rectifier power source. Therefore, the rate of anode current discharged into the electrolyte is either stopped or reduced to an acceptable level. Power source will force a voltage difference between anode and steel bar. Fig. 1.8 illustrates schematically the cathodic protection mechanism under various amounts of cathodic protection current densities. As shown in the figure, the application of an external cathodic protection current to the corrosion cell increases the negative potential of cathode. This is because of sufficiently negative charged electrons on the steel surface [13].

Fig. 1.9 shows the principle of impressed current cathodic protection, which is explained using a polarization diagram under an ideal condition of charge transfer control. Once cathodic protection current is applied to a corroding steel, the corrosion current density decreases from I_{corr} to $I_{1.corr}$ along the anodic polarization curve. Potential decreases from $E_{(corr)}$ to $E_{(mixed)}$ which shows the polarization shifts. When the rate of anodic dissolution is exactly balanced by the rate of deposition at the exchange current density ($I_{o.a}$), or polarization of the cathode reaches the open-circuit potential of the anode ($E_{o.a}$), the net corrosion rate is zero [13].

It is important to provide anode materials that are consumed at relatively low rates to have long life expectancy [12]. There are a number of anode materials that are frequently used in practice. The titanium mesh with a concrete or shotcrete overlay is currently considered as the industry standard. It is frequently used on bridge decks, parking garages, docks and retaining walls. However, occasional delamination

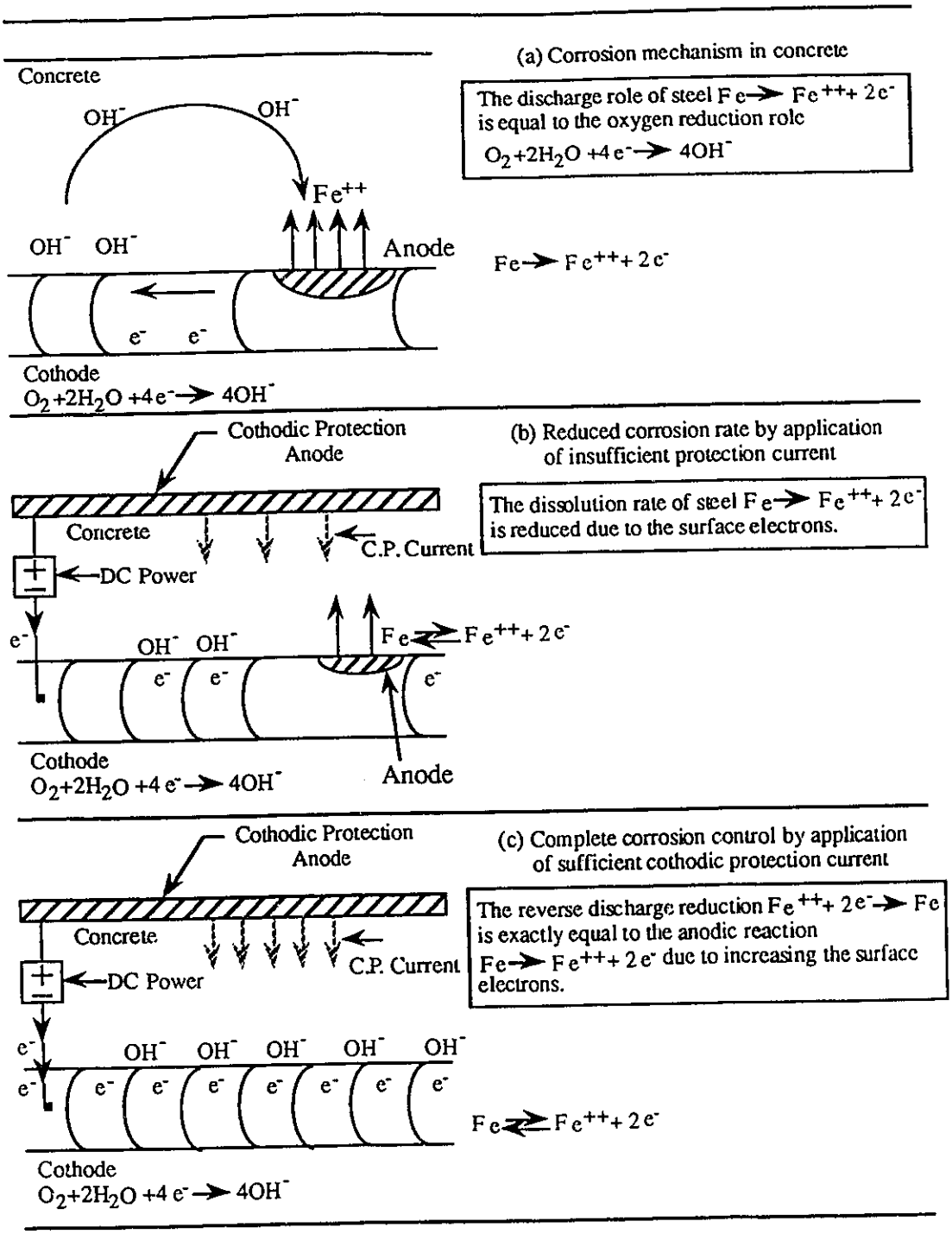

Figure 1.8 : Schematic representation of mechanism of steel corrosion in concrete and of the basic principles of Cathodic Protection (Adopted from reference [13]).

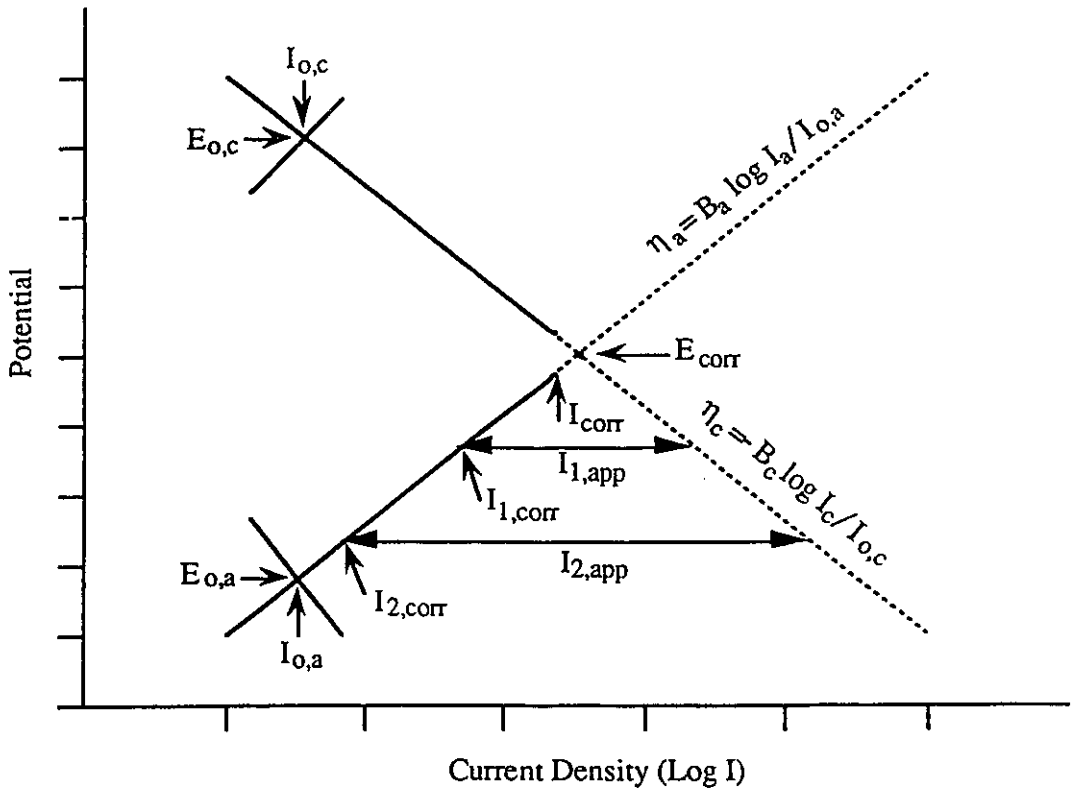

Figure 1.9 : Principle of cathodic in polarization diagram when cathodic protection current ($I_{1,app}$ or $I_{2,app}$) is applied to corroding steel, the corrosion current density decreases from I_{corr} to $I_{1,corr}$ or $I_{2,corr}$ respectively (Adopted from reference [13]).

of shotcrete overlay in columns and walls has been experienced, but overall this anode system is expected to have a superior service life [8].

The conductive coke breeze asphalt is another anode material used on bridge decks. This system has been successfully used by some ministries of transportation. However extra deadload is added to the structure by coke breeze asphalt layer. It is a relatively inexpensive system with a good performance record [8].

In recent year, a lot of attention have been paid on the use of metallized zinc material. This material is first melted by a flame or electric arc and then sprayed on concrete. The melted zinc is sprayed on concrete surface by an air gun having high velocity [8].

Impressed current cathodic protection systems require a rectifier, i.e. a power source which forces a voltage difference between the rebars and the anode. Example of application in practice of impressed current zinc cathodic protection system are listed below: [14]

1. Richmond-San Rafael Bridge on Route 17, California.
2. East Camino Bridge on U.S.Route 50.
3. Leslie Street Bridge, Toronto, Ontario, Canada.
4. Credit View Road Bridge, Highway 401, Mississauga Ontario, Canada.
5. Big Spring Bridge, west of Abilene Texas.
6. Willoughby Spit Bridge, in Norfork Virgina.
7. Cape Creek Bridge, Devils Elbow State Park, Oregon.
8. Yaquina Bay Bridge, Newport, Oregon.

These impressed current cathodic protection (CP) systems have produced good results. They do, however, require a rectifier and special maintenance over the entire service life of the system. Careful voltage adjustments of their output is an example of the type of maintenance required to ensure that the system delivers appropriate

protection to steels. they may not be applicable to parking garages although these CP systems have produced good results on bridges [15].

The concrete cover over steel reinforcement is much thinner in parking garages than in bridges. The thin cover accentuates corrosion induced by chlorides, and makes rectifier impossible to impose a potential difference due to electrical shorting between the anode and the steel. One solution to this problems, which is currently being studied, is to use galvanic cathodic protection [14].

Galvanic Cathodic Protection

Galvanic cathodic protection is powered by the difference in electromotive forces (EMF) between two dissimilar metals. Here zinc, acting as a sacrificial anode, is put in direct electrical contact with the steel at few locations. The flow of current is induced by the difference in the electromotive force (EMF) between the zinc and the steel (Fig. 1.10). From previous studies, galvanic cathodic protection can only work for concrete with sufficiently high conductivity (i.e..concrete is moist enough). In other words the moist concrete should be able to serve as the electrolyte.

A practical galvanic anode material should satisfy certain requirements: [12].

1. It must provide enough potential difference between the anode and corroding steel of the structure. This different potential is able to overcome the anode-cathode cells in the corroding structure and deliver the protective current through the concrete.

2. The quantity of anode material must be sufficient to permit reasonably long life with sufficient electrical current.

3. The efficiency of content of electrical energy from the anode must be available for useful output of cathodic protection current.

Suitable materials used as galvanic anodes include aluminum, magnesium, and zinc [12]..

The current needed to protect a given buried metal may vary over a wide range, depending on the nature of the environment and coating. If the current required per

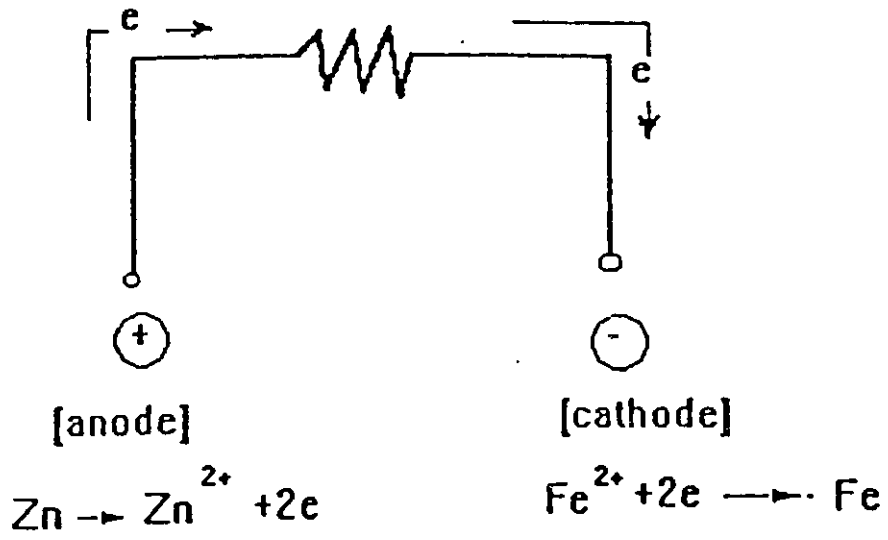

Figure 1.10 : Schematic representation of a galvanic cell (Adopted from reference [11]).

cathodic protection installation is up to 1.5 or 2.0 amps, galvanic anodes may be the best choice. Working potential for zinc anode with respect to a copper/copper sulfate electrode is in the order of -1.10 volts. Working potential for aluminum anodes is about the same as that for zinc. High temperature and moisture environment will make corrosion worse. To achieve galvanic cathodic protection, the minimum polarization shift of the potential for steel is 100 mV.

Development of Cathodic Protection Methods

A 1988-1989 survey conducted by Battelle indicated that more than 275 bridge structures in the United States and Canada have been cathodically protected. About 99 percent of the protected area is on bridge decks, with the remainder on piers, caps and beams. About 90 percent of the protected structures are located in deicing salt regions and 10 percent are in marine environment. The first cathodic protection system for bridge deck was developed by the California Department of Transportation. In 1973 they placed a cathodic protection system on the Sly Park Road bridge on US Highway 50 near Sacramento, California. The coke-asphalt system used proved

to be an effective cathodic protection anode. However, it resulted in additional dead load that could not be permitted for most structural application. The second generation anode system, first used in 1979, eliminated the dead load problem of the coke-asphalt system by placing a thin wire anode in saw cut slots on the bridge deck. Tests indicated that this system met 100 mV depolarization criteria [16].

In 1981, FHWA researchers began to consider a mounted grid of platinized wire and carbon strand anode cathodic protection system in conjunction with latex modified and conventional concrete overlays. The use of cathodic protection under rigid overlays was completed on one bridge in 1983 and five others in 1984. An alternative conductive coating for concrete members was developed in 1983 by California Department of Transportation researchers. This material, flamed-sprayed zinc, functions as anode covering the entire concrete surface [16].

In 1981, the Ontario Ministry of Transportation and Communications initiated a program aimed at developing a cathodic protection method for bridge substructures. Eleven experimental systems with different anode materials, at two sites, were designed, installed, and monitored over the period between 1982 and 1986. The main conclusion drawn from this application was that cathodic protection of bridge substructure components was feasible using an impressed current system. The current density was in the range of 10 to 15 mA/m^2 of concrete surface. It was concluded that better distribution of current was achieved in systems with mesh anodes or continuous coatings, than those with discrete anodes. It was also concluded that there was little spread of protective current to steel beyond the limits of the protection system. There was insufficient current output from the galvanic system to provide adequate protection to the embedded steel [17].

The Galvanic cathodic protection was first used for concrete bridges by the California Department of Transportation [18]. FDOT employed this method to stop corrosion of reinforcement in the piers of Seven Mile Bridge where the resistivity due to continuous exposure to salt water, and warm and humid environment was maintained. FDOT reported current flow of 1 milliampere per square foot of concrete for this protection system, which is a typical value for impressed current systems. Similar galvanic cathodic protection systems have been employed since then on Causeway

Bridge at Cape Kennedy and on oil pumping platforms for Shell Offshore Inc. off the Louisiana coast.

1.2 Research Needs

Cathodic protection has been used for many years to protect a variety of metallic structures. It becomes obvious from the previous discussion that the basic principle of cathodic protection is quite simple. However, some questions remain to be answered for effective applications of the method in practice. These include how much minimum current is needed to protect a given structure, how much potential is required, how do temperature and moisture influence corrosion. Furthermore, much of the work on cathodic protection of reinforcement in concrete structures has centered on the use of impressed current systems because it has been tacitly assumed that the relatively high resistivity of concrete would preclude the use of low driving voltage of sacrificial systems. The use of sacrificial systems deserves further study because there is little positive evidence to support the assumption that the high resistance of concrete will prevent their application to reinforced concrete structures. In areas where AC current is not available, where periodic maintenance of control rectifiers is costly, or where down-time due to rectifier malfunctions or vandalism is to be expected, a system based on sacrificial anodes may be preferable. Research on use of metallized zinc coating as sacrificial anode is particularly scarce in the literature. Therefore an experimental investigation has been undertaken in this thesis to investigate various aspects of metallized zinc coatings on reinforced concrete structures for cathodic protection.

1.3 Objective

The overall objective of this research project is to develop a metallized zinc coating suitable for long-term galvanic cathodic protection of steel reinforcement in reinforced concrete structures. The objective for the experiments conducted is to determine a suitable anode material and to establish how much current density and depolarization shift values are achieved with the use of different anode materials and different

concrete cover thicknesses in different environments.

1.4 Scope

The following forms the scope of the investigation:

- Review of previous research on cathodic protection of reinforcing steel in concrete.
- Experiments in solutions to select the most suitable anode. Four different anode materials are considered in 16 experiments.
- Experiments on reinforced concrete specimens with salt uncontaminated concrete. Test parameters include concrete cover, anode material, temperature and humidity. A total of 48 specimens are tested.
- Experiments on reinforced concrete specimens with salt contaminated concrete. Test parameters include concrete cover, anode material, temperature and humidity. A total of 42 specimens are tested.
- Analysis of test data in terms of current density and depolarization.
- Evaluation of the effects of test parameters and assessment of the significance of each parameter.
- Recommendation to be used in practice.
- Presentation of results and conclusion.

1.5 Previous Research

Previous research on galvanic cathodic protection of steel reinforcement is scarce in the literature. The electrochemical behavior of pure zinc galvanized steel in concrete environment and in simulated concrete pore solution has been discussed in the literature titled electrochemical behavior of galvanized Al-Zn coatings in saturated $Ca(OH)_2$ solution [19]-[28]. Research by Macias and Andrade [24]-[27] elucidated

that the concentration of Ca^{2-} ion in the alkaline solution and its pH value are two of the most important factors controlling passivation of galvanized steels in alkaline solution. In recent years, two newly developed hot-dip galvanized Al-Zn coating systems, namely, 5% Al-Zn and 55% Al-1.5% Si-Zn, have been successfully used to enhance the atmospheric corrosion resistance of steel plates in urban and industrial areas [28]. Cheng investigated the electrochemical behavior of hot-dip galvanized 5% Al-Zn and 55% Al-Zn coatings. Experimental results show that these two Al-containing coatings have more negative open-circuit potentials than the pure zinc galvanized coating. The corrosion potential is negatively decreased with increasing Al content in galvanic coatings. The passive current density was found to increase as the Al content of galvanic coatings increased. In other words, the Al-containing coatings passivate less readily than the pure zinc coating in such a highly alkaline solution. From the viewpoint of cathodic protection, Al-Zn coatings can provide a much greater degree of galvanic protection for steel than pure zinc coatings. [29]

Little work has been done, however, to evaluate the behavior of galvanic cathodic protection in real concrete environment. A comprehensive research program was undertaken by the National Cooperative Highway Research Program. The research program includes two cathodic protection systems. The first consists of commercially available ribbon zinc anodes while the second consists of perforated zinc anode sheets. The result showed that both ribbon and zinc sheet anode design afforded significant shift of half-cell (CSE) potentials into the cathodic range. In warm, moist periods, steel on ribbon anode showed polarized potentials ranging from 400 to 650 mV negative to CSE, while the zinc sheet showed from 600 to 700 mV negative to CSE. The perforated zinc sheets system met the 100 mV criteria. In dry seasons polarization of steel was very small. Current flow from the ribbon anodes to steel was around 43 mA/m^2 for the first year, which, progressively decreased in later years. The current flow from the zinc sheet was around 27 to 37 mA/m^2. The results indicate that sacrificial anodes can be applied for cathodic protection of reinforced concrete structure provided that the concrete cover is small. The effectiveness of these systems in maintaining long-term protection cannot be judged at this time because the result is achieved under moist and warm condition. The perforated sheet is preferred because

it offers more uniform protective potentials and more rapid installation. Generally, the cost of zinc sheet systems is approximately 50 percent higher than that of ribbon anode systems since they have to be custom fabricated [30].

The application of a low-cost galvanic anode system for use in reinforced concrete marine substructures was investigated by Rodney G. Powers in several Florida bridges and by means of laboratory experiments. The results indicated that levels of protection meeting the 100 mV depolarization criterion were observed in the field, and in laboratory specimens where direct wetting of the anode existed, or where expected current density was low. However, depolarization in higher humidity laboratory tests was much smaller than that in lower humidity. In lower humidity laboratory tests depolarization was moderate, suggesting that only partial protection was being achieved [31].

A strategic highway research program was conducted in 1991 by Rodney G. Powers. The results in slabs showed that appreciable protection current was being delivered in all test conditions. Depolarization in dryer environments typically exceeded 100 mV. However, in humid environments depolarization peaked near 50 mV after about one day. After 80 days, the current delivery increased and resistance decreased with increasing humidity and conductivity. The depolarization shifts were over 100 mV for both dry and room air specimens. It appeared that humidity was not an important factor for galvanic cathodic protection in this research program. This controversial conclusion needs further study [32].

According to the National Association of corrosion Engineers a minimum negative potential shift of 100 mV is adequate and the amount of voltage shift necessary to control bridge deck spalling may be even less than 100 mV. Another research program carried out by John L. Saner of the State of Illinois, Department of Transportation described a field investigation of the use of sacrificial zinc ribbon anode to cathodically protect the reinforcing steel in a bridge deck. The results indicated that the 100 mV shift was achieved only up to a concrete depth of 3 inches (75 mm) from the anode. Salt could reduce the resistivity of concrete. The resistivity of both the backfill mortar and deck concrete could have been reduced by placing a porous open graded asphalt wearing surface over them thus increasing their moisture content [33].

Chapter 2

Experiments in Solutions

2.1 General

The first phase of experimental research included tests in electrolyte solution. The objective of the first phase tests was to determine the most suitable anode material for cathodic protection. Four different anode materials were considered for this purpose. The test for each anode material was repeated four times for improved reliability of results. The test set up, test procedure and the results are discussed in the following section.

2.2 Test Set Up

The test set-up for Phase 1 experiments involved plastic containers with 4.4- liter electrolyte solution, as shown in Fig. 2.1. The electrolyte solution was made of $Ca(OH)_2$ saturated +0.05 mole $NaCl$.

The cathode was made of steel wire. Anode materials varied for each test and consisted of pure zinc, zinc-aluminum (98:2), zinc-aluminum(85:15), pure aluminum wire. Since the potential of aluminum is more negative than zinc, the use of these four materials as anode would permit comparisons of current densities and depolarization values. Both cathode and anode wires were 3 mm in diameter and 147 mm in length, resulting in a surface area of 1393 mm^2. The anode and cathode were connected with electrical wire. This completed the electrochemical cell.

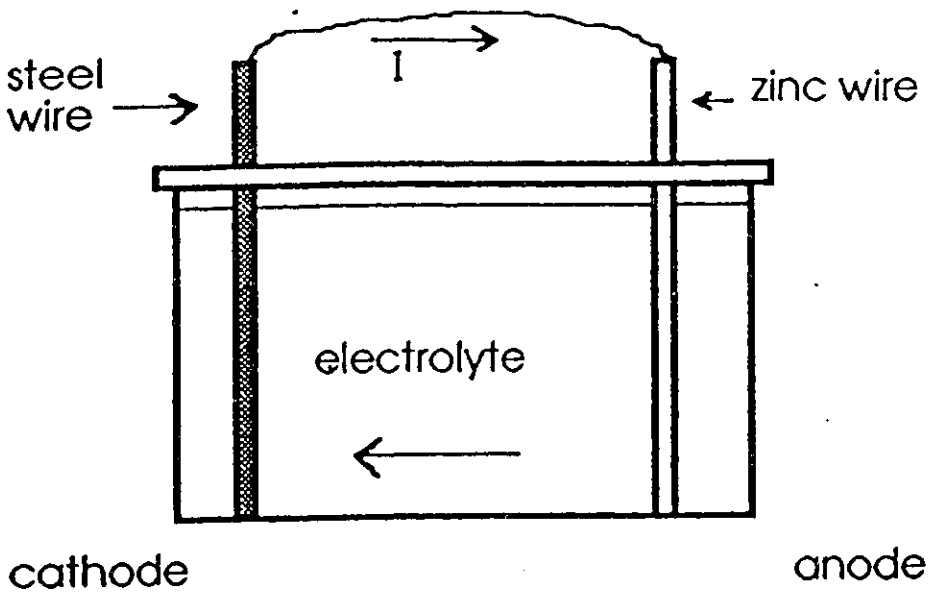

Figure 2.1 : Schematic diagram of the electrochemical cell used in Phase 1 experiments

2.3 Test Procedure

The test procedure involved measurements of current flow and depolarization shifts on each sample. The current flow and depolarization shifts were measured by means of a multimeter. The electrodes were polarized because of the wires connected. Therefore, the electrical wires were disconnected during the test.

The experiments were started on March 5, 1992. The current flow measurements were taken three times a week until the end of March, 1992. Additional measurements were also taken at a later date. Variation of depolarization shifts with time on each solution sample was monitored up to 1.5 hours. Calomel reference electrode was used to take the measurements. The experiments with different anode materials were repeated four times, and the average values of current densities and depolarizations obtained from the four tests were used and reported in the next section.

2.4 Test Results

The experimental data recorded are presented in Tables 2.1 and 2.2 in terms of current density and depolarization of steel. The values tabulated represent the average of four readings taken on four companion samples. The data are plotted in Figs. 2.2 and 2.3 for current density and depolarization, respectively. As the aluminum content in the anode material is increased the data show more fluctuations, as opposed to the other anode materials which show stable behavior. The results also show that zinc-aluminum (85:15) produced the highest current flow and depolarization, indicating that this anode material is the best candidate to perform galvanic cathodic protection in the solution environment. Pure aluminum also show a reasonably good potential for use in galvanic cathodic protection. The remaining two materials, namely pure zinc and zinc-aluminum (98:2) show the lowest current density and depolarization.

The observed trend in Phase 1 tests was later verified using concrete specimens. The details of tests on concrete specimens are discussed in Chapter 3.

Table 2.1 : The Current Density of Steel in the Four Anode Materials Considered.

Date	Time (Hour)	Average Current Density of Four Tests in mA/m^2			
		Zinc	Zinc-Al(98:2)	Zinc-Al(85:15)	Aluminum
March 5, 1992	48	6.751	15.368	46.105	1039.740
March 6, 1992	72	4.955	13.501	46.608	466.078
March 10, 1992	168	2.894	12.532	75.406	120.793
March 12, 1992	216	2.585	10.700	60.468	599.259
March 13, 1992	240	2.298	9.839	57.308	313.615
March 17, 1992	336	1.889	9.982	76.986	83.987
March 19, 1992	384	1.996	8.833	64.921	59.086
March 20, 1992	408	1.975	7.864	63.987	49.786
March 24, 1992	504	1.759	8.654	40.001	29.444
March 26, 1992	552	2.119	10.270	70.235	29.552
March 27, 1992	576	1.724	10.054	52.317	27.254
June 30, 1992	2112	1.781	44.992	65.190	21.616

Table 2.2 : Depolarization of Steel in the Four Anode Materials Considered.

Time (Hour)	Average Depolarization of Four Tests in V			
	Zinc	Zinc-Al(98:2)	Zinc-Al(85:15)	Aluminum
48	0.099	0.143	0.214	0.190
72	0.112	0.141	0.234	0.586
216	0.111	0.201	0.231	0.252
240	0.103	0.188	0.354	0.514
384	0.112	0.182	0.225	0.349
408	0.108	0.165	0.371	0.520
552	0.108	0.186	0.433	0.368

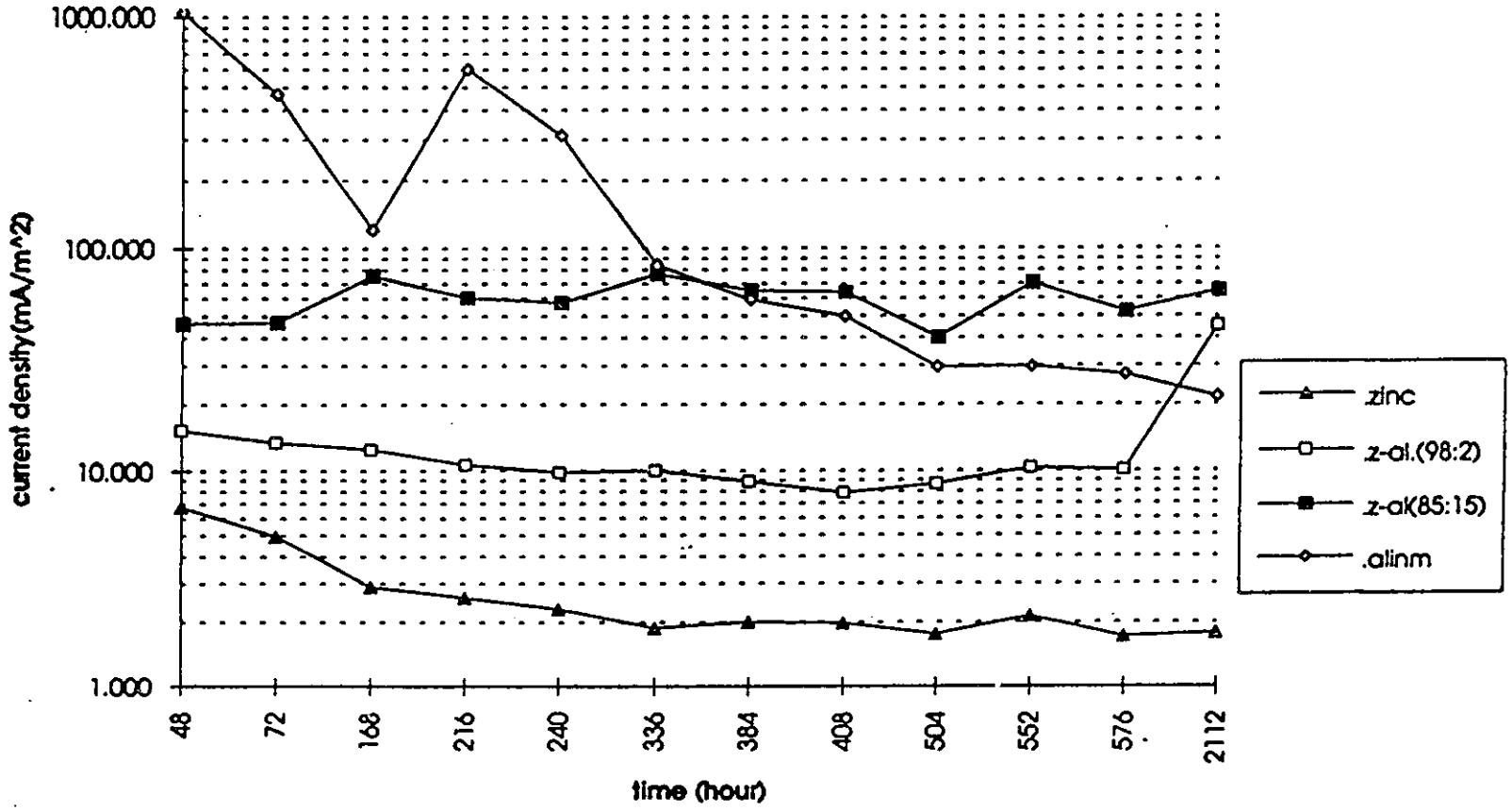

Figure 2.2 : The variation of average current density in steel with four anode materials.

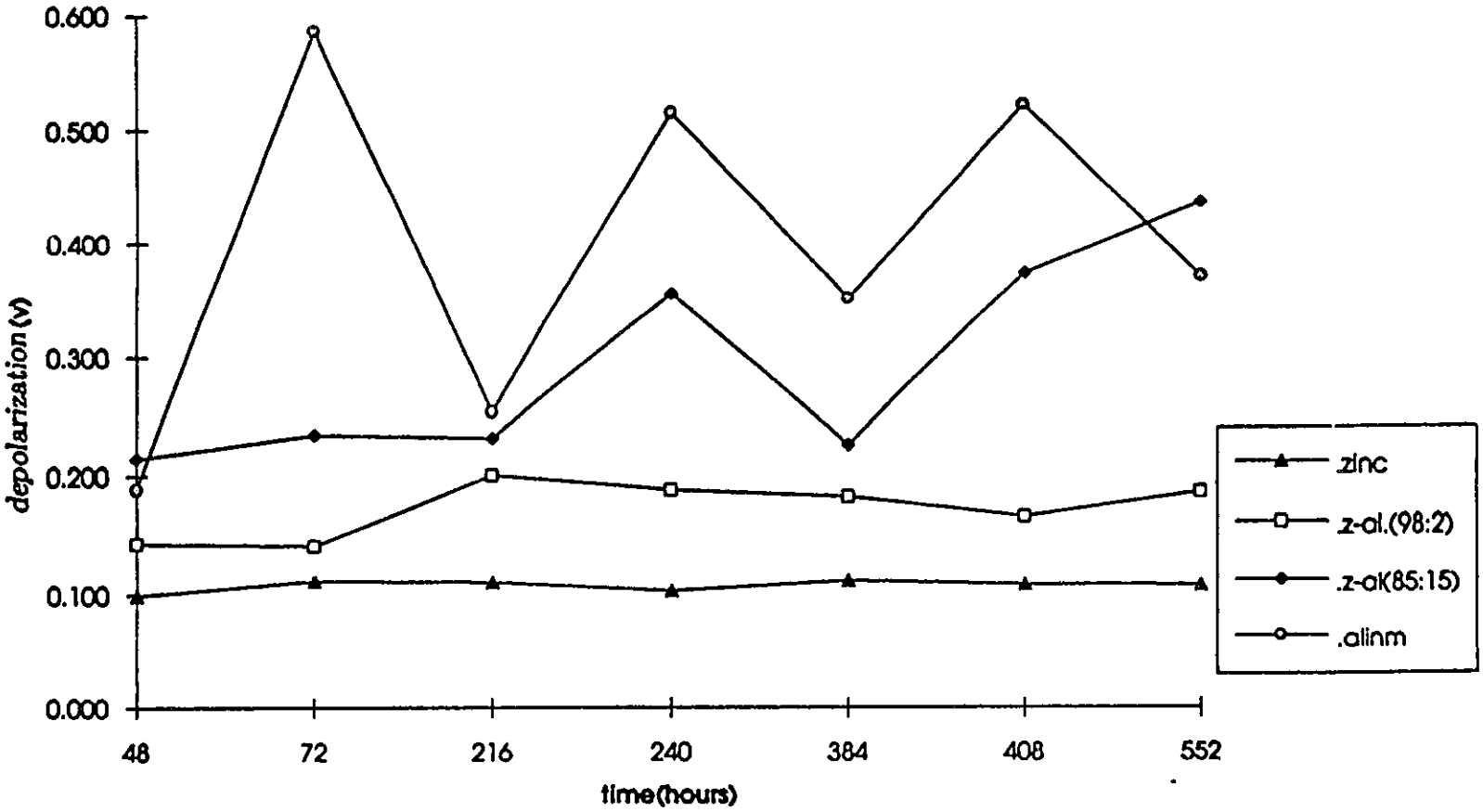

Figure 2.3 : The variation of steel depolarization shifts measured for 1.5 hours on samples immersed in solution.

Chapter 3

Experiments on Reinforced Concrete Specimens

3.1 General

Experiments were carried out using reinforced concrete specimens with selected galvanic systems and different geometric and ambient conditions. Reinforcing steel was used as cathode, and metallized zinc or zinc-aluminum sprayed on the surface was used as anode. The surface area of cathode was 0.04 m^2 and the area of anode was 0.025 m^2. Test parameters included concrete cover, temperature and humidity of the environment, and presence of salt. The electrochemical process was monitored for an extended time period to assess long term performance of samples.

Experiments on reinforced concrete samples were conducted in two stages. The first stage involved specimens without salt, except when salt was used as a test parameter. These experiments are labeled as Phase 2 tests, following the Phase 1 tests conducted in solution, and reported earlier in Chapter 2. The second stage of experiments on reinforced concrete samples involved concrete samples all contaminated with salt. The same test variables were considered in this stage, and the experiments are referred to as Phase 3 tests. The details of both Phase 2 and Phase 3 tests are reported in this Chapter.

3.2 Phase 2 Experiments

3.2.1 Test Specimens and Parameters

A total of 48 reinforced concrete specimens were tested in Phase 2. Three levels of concrete cover were considered in the test program. This led to the use of three different sample sizes. Fig. 3.1 illustrates geometric details of all test specimens. Samples with 20 mm cover were 70×150×300 mm in cross-section. Samples with 50 mm and 130 mm cover had cross-sectional dimensions of 100×150×300 mm and 180×150×300 mm, respectively. All samples contained two No. 20 bars (19.5 mm diameter) and were of 300 mm length. Each had a graphite reference rod positioned as illustrated in Fig. 3.1.

Table 3.1 : Test parameters.

	100% humidity		50% humidity		
	Anode material		Anode material		
concrete cover	Zn	Zn-Al (85:15)	Zn	Zn-Al (85:15)	salt contain
20 mm	3	3	3	3	No
50 mm	3	3	3	3	No
130 mm	3	3	3	3	No
50 mm	3	3	3	3	Yes

Note: Salt water was added to all specimens after 1 month from the start.
Salt water was removed 2 months after the start.

Two different environmental conditions were considered in the test program. One half of the samples were tested in 100% humidity and 32°C temperature. The remaining samples were tested in 50% humidity and laboratory room temperature, which was approximately 20°C. Twelve samples were contaminated with salt prior to testing. The others were tested without salt. However, salt water was added to all the specimens after a month from the start of the experiments to increase the electric current. Upon the addition of the salt water, those specimens subjected to 100% humidity showed quick consumption of anode due to high chloride ratio. Therefore, the experiments in 100% humidity chamber were disconnected, while those in 50% humidity continued with salt water removed after approximately one month. Table 3.1

includes test parameters considered in Phase 2.

3.2.2 Preparation of Concrete

Air entrained concrete, with water cement ratio of 0.5 was used for concrete mix design. Air entraining agent was used to obtain 5 - 7% air. Washed stone and sand were used as coarse and fine aggregates. The results of sieve analysis for the aggregates are included in Table 3.2. Superplasticizer was added to the mix during the last 3 minutes of mixing. Salt, in the form of $NaCl$, was added for those samples where salt was a test parameter. The resulting concrete mix produced a slump of 75 - 95 mm.

Once the concrete mix was ready, it was placed in molds which contained steel reinforcement and graphite (reference) bar. The molds were sprayed with a silicone releasing agent as a bond breaker prior to casting. The samples were placed in 100% humidity curing room where they were cured for a minimum of 28 days before being moved into the appropriate environmental conditions for testing [29].

Table 3.2 : Sieve Analysis of Coarse and Fine Aggregates (From reference [29]).

Sieve analysis of coarse		sieve analysis of fine (sand)	
> 3/4"	0%	> 4	2.1%
3/4" - 1/2"	12.7%	4 - 8	6.9%
1/2" - 1/4"	80.4%	8 -16	11.8%
(fines) < 1/4"	6.9%	30 - 50	28.6%
		50 - 100	36.5%
		(fines) < 100	2.9%

3.2.3 Spraying Metallized Anode

The top surface of each specimen was sprayed with metallized zinc or zinc-aluminum (85:15) to act as anode. This was done after curing of concrete and preparation of the surface. The samples were first stored in a 50% relative humidity tent for at least one month. The surface of each sample was then gritblasted and preheated to 50°C immediately prior to the metallizing. This was done to increase the adhesion of zinc and zinc-aluminum (85:15) coatings [30].

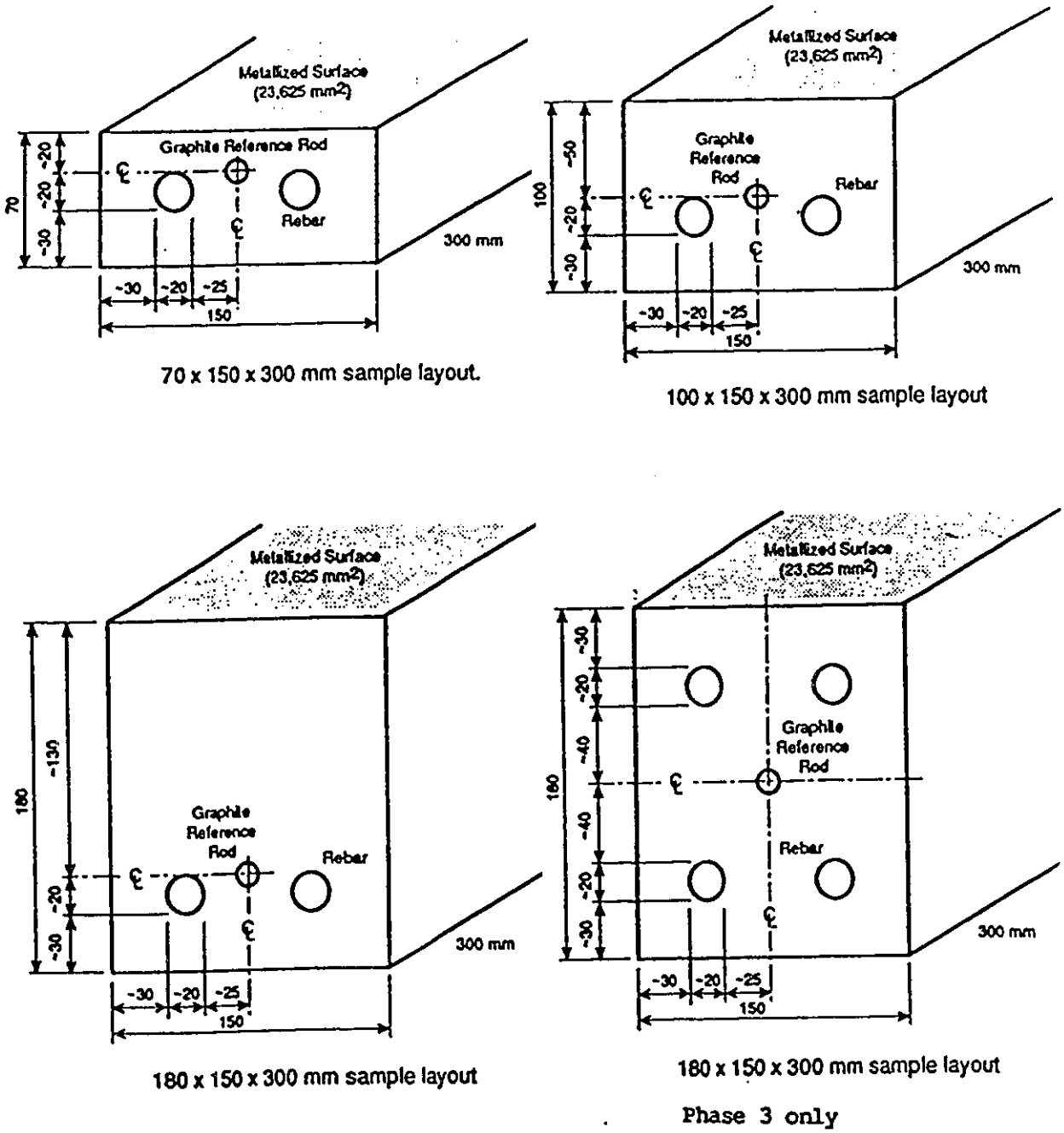

Figure 3.1 : Reinforced concrete specimens. *(Adopted from reference [29]).*

Thermal spraying was performed using a thermal gun at IMI in Bouchorville, Quebec. Spraying was performed with either pure zinc or a zinc-aluminum alloy (85:15). The metals were sprayed to have a thickness of 0.4 mm (see Fig. 3.1), covering a surface area of 34000 mm^2.

3.2.4 Wire Connection

The anode and cathode in each sample must be connected by an electric wire to form a galvanic cell. The cathode was cast in concrete in the form of steel bar. The reference bar (graphite) was also embedded in concrete, while the anode was sprayed on the surface of concrete. Since the voltage measurements were done relative to the reference bar, an electric wire connection was needed between the reinforcing steel, reference bar and the surface anode, as shown in Fig. 3.2. A 3 mm diameter wire was used to provide the required connection.

Once the connection was completed as discussed above, the samples were placed in two different chambers, depending on the environmental conditions of the test. The wires were then connected to a panel outside the chambers for convenience in data recording. The 100% humidity chamber remained closed at all times to maintain the inside humidity.

3.2.5 Test Procedure

The following test procedure was followed in all experiments:

1. The voltage between reference graphite and reference copper/copper sulphate electrode (CSE) was measured prior to wire connection. All data recorded were normalized relative to CSE, as this reference electrode was known to be stable.

2. After connecting the wire, the current flow between zinc or zinc-aluminum (85:15) anode and steel cathode was measured once a day except weekends.

3. The depolarization of cathode and anode was measured.

The level of cathodic protection delivered to the steel by sacrificial zinc coatings was monitored with time through routine measurements of depolarization and current

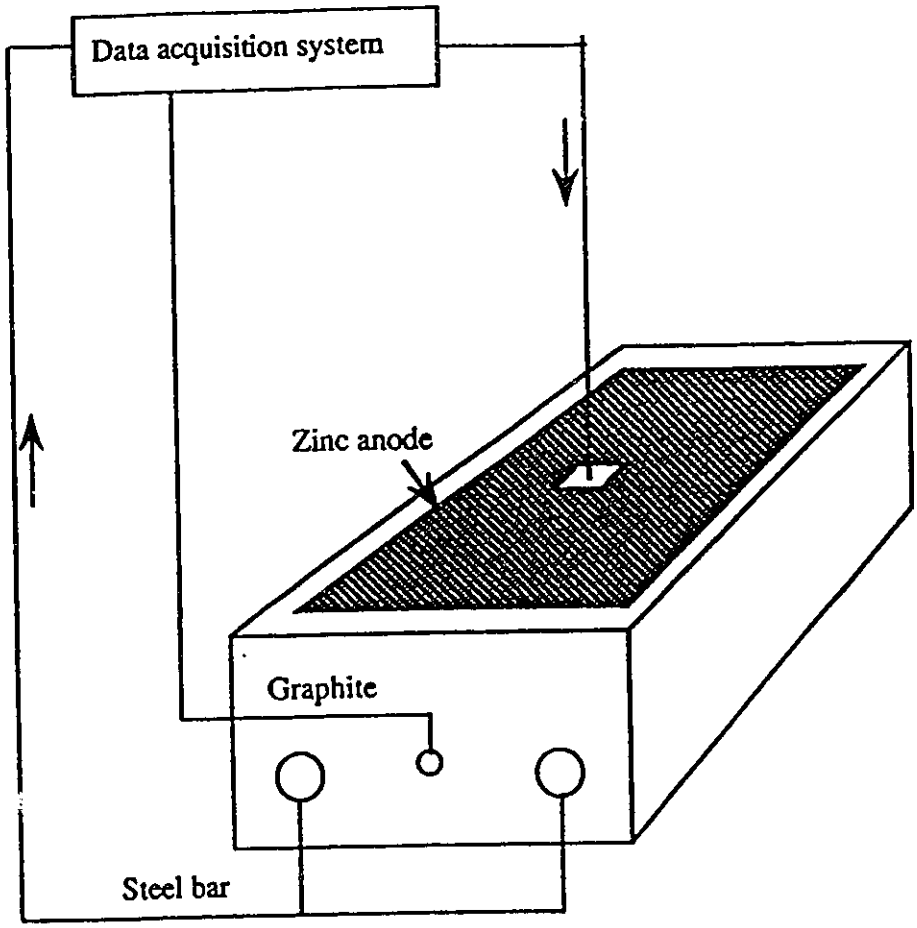

Figure 3.2 : Metallized reinforced concrete samples under tests along with the wiring of the data acquisition system.

passing through the system.

The first series of test started on May 19,1992. Salt water was added to all samples one month later. Depolarization method was utilized to measure the polarization of steel which indicated the amount of cathodic protection. The anode and cathode were polarized because they were connected to each other before the measurement. They were disconnected during the measurement, and current reading was taken first, followed by depolarization readings. The depolarization voltage between the anode and reference, and the voltage between steel cathode and reference were recorded through two different channels simultaneously up to four hours.

A multimeter was used to record the measurements before Nov. 1992. Then a computerized data acquisition system was used to record the current and depolarization values simultaneously for 24 specimens. Current readings were taken five times a week during the initial three months. Subsequently the frequency of readings were reduced to once a week. Depolarization measurements were taken once a month. To measure the depolarization of the steel potential, the galvanic current is interrupted and the polarized potential of the steel is measured against the reference electrode.

3.2.6 Test Results

The current density data recorded are presented in Tables 3.3 and 3.4 for samples in 50% and 100% relative humidity environments, respectively. The tables include average current densities and depolarizations for each type of specimen, having a specific concrete cover and anode material. Since three identical samples were tested for each parameter, the average values indicate the average of three readings recorded on three identical test samples having the same properties. The current density readings cover the time period between May 28, 1992 and August 26, 1993 for tests conducted in 50% humidity. Tests in 100% humidity were discontinued shortly after the salt water was removed, as discussed previously. The current density readings for these tests cover the time period between May 19, 1992 and January 4, 1993.

Table 3.3 : The average current density (mA/m^2) of two steel bars in 50% humidity. Z: Zn, ZA: Zn-Al. The number following Z and ZA represents the thickness of concrete cover in mm. (continued on next page)

The area of two steel bars = 0.032 m^2.

Date	Time (Hour)	Average Z130	Average Z50	Average Z20	Average Z50 s	Average ZA130	Average ZA50	Average ZA20	Average ZA50 s
5/28/92	24	0.154	0.179	0.126	0.521	0.305	0.278	0.342	0.479
6/1/92	120	0.059	0.064	0.050	0.338	0.142	0.142	0.175	0.314
6/2/92	144	0.027	0.029	0.021	0.248	0.095	0.094	0.122	0.235
6/4/92	192	0.024	0.026	0.017	0.197	0.083	0.082	0.105	0.190
6/8/92	288	0.029	0.034	0.018	0.290	0.074	0.073	0.096	0.218
6/9/92	312	0.020	0.018	0.014	0.193	0.068	0.065	0.083	0.160
6/11/92	360	0.018	0.020	0.016	0.155	0.060	0.063	0.096	0.157
6/15/92	456	0.020	0.017	0.013	0.149	0.059	0.057	0.076	0.184
6/16/92	480	0.019	0.025	0.016	0.192	0.061	0.060	0.079	0.175
6/18/92	528	0.019	0.022	0.018	0.184	0.054	0.054	0.071	0.163
6/22/92	624	0.011	0.015	0.010	0.151	0.056	0.045	0.053	0.134
6/23/92	648	0.014	0.010	0.008	0.106	0.042	0.044	0.053	0.094
6/25/92	696	0.018	0.016	0.014	0.174	0.053	0.047	0.056	0.123
7/9/92	1032	18.693	48.605	59.618	51.266	19.986	29.130	54.777	44.697
7/10/92	1056	18.826	47.101	58.381	50.528	19.913	28.658	53.218	43.216
7/13/92	1128	18.296	42.893	53.775	45.130	19.002	26.980	48.499	39.598
7/14/92	1152	18.249	42.361	53.343	44.702	18.954	27.054	47.990	39.190
7/15/92	1176	17.854	41.252	51.819	43.661	18.574	26.488	46.621	38.207
7/16/92	1200	17.754	40.521	51.707	44.180	18.532	26.254	46.175	37.736
7/17/92	1224	18.070	40.524	51.117	43.243	18.432	26.290	45.929	37.638
7/20/92	1296	17.328	39.036	51.189	43.403	17.856	25.449	43.834	36.335
7/21/92	1320	19.460	38.429	49.219	42.831	17.585	25.508	42.808	35.659
7/22/92	1344	19.445	38.420	49.547	42.002	17.540	25.193	42.985	36.467
7/23/92	1368	18.934	37.675	48.901	40.731	16.930	24.368	41.125	34.549
7/24/92	1392	18.853	37.571	47.776	41.149	17.191	24.253	40.721	34.381
7/27/92	1464	17.957	35.895	45.293	39.670	16.216	22.924	39.596	32.318
7/28/92	1488	17.893	37.142	44.977	39.148	16.116	22.675	38.146	32.074
7/29/92	1512	17.544	35.346	44.482	38.283	16.152	22.158	37.154	31.290
7/30/92	1536	17.328	34.830	43.791	37.797	15.728	22.156	32.074	31.661
7/31/92	1560	17.003	34.184	42.820	36.933	15.411	21.681	31.232	30.199
8/12/92	1848	15.119	30.690	38.533	35.300	14.024	19.342	31.461	27.714
8/13/92	1872	14.845	30.300	37.982	33.245	13.710	18.996	30.931	27.198
8/17/92	1968	14.245	29.388	36.699	32.128	13.757	18.443	29.905	26.327
8/19/92	2016	14.067	29.008	36.185	31.597	13.169	18.213	29.402	25.870
8/21/92	2064	13.736	28.251	35.368	31.155	12.828	17.758	28.410	25.124
8/24/92	2136	13.601	28.169	35.133	32.199	12.741	17.735	28.548	25.023

Table3.3: (Cont'd)

Date	Time (Hour)	Average Z130	Average Z50	Average Z20	Average Z50 s	Average ZA130	Average ZA50	Average ZA20	Average ZA50 s
8/27/92	2208	14.164	29.684	37.081	32.564	13.352	18.923	30.264	26.551
9/23/92	2832	10.011	23.657	27.741	22.161	7.109	13.078	20.541	11.364
10/7/92	3168	8.899	21.419	24.248	19.729	6.432	13.479	18.858	11.481
10/16/92	3384	8.467	20.233	22.659	18.169	7.465	12.610	18.381	13.992
11/5/92	3864:	6.615	16.740	17.146	9.469	5.646	9.719	13.031	10.698
11/7/92	3912:	7.531	18.010	18.583	10.281	6.625	10.729	14.094	11.813
11/27/92	4392:	6.208	14.448	14.208	8.406	5.552	8.604	10.792	9.469
12/1/92	4488:	6.521	15.260	14.906	8.719	5.802	8.813	11.198	9.719
12/7/92	4632:	5.854	13.740	13.021	11.375	5.188	7.531	9.719	8.344
12/22/92	4992:	4.833	10.896	9.615	9.016	4.271	5.594	7.219	6.156
1/4/93	5304:	4.125	9.302	7.792	7.719	3.667	4.688	5.896	5.198
4/6/93	7512:	2.385	5.604	4.979	3.677	2.604	2.438	4.583	3.760
4/15/93	7728:	2.438	5.188	4.781	4.375	2.500	2.250	4.271	3.406
4/22/93	7896:	1.875	5.240	6.000	5.948	3.198	2.750	5.698	4.979
4/27/93	8016	2.344	5.188	6.563	5.406	2.854	2.490	5.135	4.333
5/4/93	8184	2.031	5.292	7.229	5.594	2.948	2.479	5.240	4.385
5/11/93	8352	2.750	5.083	6.979	4.938	2.813	2.438	4.979	4.177
5/17/93	8496	1.979	5.031	6.719	4.688	2.656	2.344	4.833	3.969
5/26/93	8712	1.979	4.885	6.313	4.938	2.656	2.292	4.740	3.865
6/2/93	8880	1.875	4.781	6.052	4.281	2.552	2.198	2.854	3.708
6/8/93	9024	2.135	4.427	5.500	4.219	2.396	2.135	4.177	3.448
6/14/93	9168	1.271	3.969	5.146	4.271	1.927	1.583	4.063	3.302
6/23/93	9384	2.646	4.635	5.792	4.729	2.500	2.333	7.177	3.969
6/30/93	9552	0.750	1.010	1.010	0.906	0.854	0.958	0.958	0.906
7/2/93	9600	1.979	4.885	6.000	4.375	2.604	1.531	4.260	4.073
7/8/93	9744	2.135	4.990	6.365	5.438	2.802	2.146	5.802	4.677
7/15/93	9912	1.979	4.938	6.156	4.740	2.656	2.031	5.333	4.323
7/22/93	10080	1.927	4.781	5.844	5.844	2.604	1.927	5.188	4.073
7/29/93	10248	1.938	4.729	5.802	5.094	2.552	1.990	5.229	4.125
8/5/93	10416	1.979	4.635	5.698	4.781	2.552	2.031	5.250	3.969
8/12/93	10584	1.875	4.635	5.646	4.573	2.500	1.833	5.198	4.021
8/19/93	10752	1.979	4.677	5.802	5.146	2.604	1.990	5.135	4.177
8/26/93	10920	1.979	4.323	5.542	4.833	2.708	1.573	4.896	3.813

Table 3.4 : The average current density (mA/m^2) of two steel bars in 100% humidity. Z: Zn, ZA: Zn-Al. The number following Z and ZA represents the thickness of concrete cover in mm. (continued on next page)

The area of two steel bars = 0.032 m^2.

Date	Time (Hour)	Average Z130	Average Z50	Average Z20	Average Z50 s	Average ZA130	Average ZA50	Average ZA20	Average ZA50 s
5/19/92	4	0.247	0.469	0.678	4.754	0.356	0.406	0.307	3.331
5/21/92	48	0.256	0.224	0.160	3.240	0.282	0.322	0.220	2.428
5/25/92	144	0.207	0.178	0.111	2.311	0.219	0.248	0.152	2.141
5/26/92	168	0.136	0.123	0.079	2.100	0.133	0.182	0.308	1.506
5/28/92	216	0.110	0.124	0.083	2.267	0.121	0.167	0.241	2.341
6/1/92	312	0.077	0.065	0.041	1.032	0.116	0.144	0.238	0.699
6/2/92	336	0.255	0.060	0.033	1.252	0.115	0.149	0.288	0.743
6/4/92	384	0.184	0.220	0.281	2.016	0.167	0.195	0.248	1.079
6/8/92	480	0.165	0.173	0.255	2.105	0.144	0.175	0.198	1.356
6/9/92	504	0.664	0.567	0.736	2.961	0.440	0.500	0.533	3.458
6/11/92	552	0.497	0.122	0.105	1.611	0.138	0.153	0.188	0.821
6/15/92	648	0.129	0.133	0.175	1.817	0.110	0.124	0.141	1.543
6/16/92	672	0.040	0.027	0.035	0.567	0.074	0.092	0.117	0.369
6/18/92	720	0.107	0.119	0.114	1.409	0.110	0.131	0.163	0.680
6/22/92	816	0.043	0.036	0.039	0.594	0.078	0.096	0.133	0.463
6/23/92	840	0.110	0.118	0.097	1.266	0.101	0.117	0.130	0.660
6/30/92	1008	38.132	53.167	96.377	78.759	19.201	51.586	78.640	68.471
7/2/92	1056	33.247	49.504	96.267	78.782	19.343	48.080	75.682	71.665
7/3/92	1080	29.582	43.104	82.692	68.426	17.275	42.481	64.723	62.199
7/6/92	1152	29.596	44.973	83.402	70.316	17.899	41.234	62.091	63.389
7/7/92	1176	36.188	53.928	98.194	77.320	21.300	46.713	69.818	71.664
7/8/92	1200	43.020	63.295	107.541	85.084	23.307	49.540	78.085	65.770
7/9/92	1224	42.317	59.854	105.106	90.165	23.900	49.755	74.252	74.559

Table3.4: (Cont'd)

Date	Time (hour)	Average Z130	Average Z50	Average Z20	Average Z50 s	Average ZA130	Average ZA50	Average ZA20	Average ZA50 s
7/10/92	1248	39.447	57.988	103.660	81.136	22.986	46.315	70.472	71.350
7/13/92	1320	38.386	53.092	88.788	73.532	21.668	41.046	59.733	56.220
7/14/92	1368	42.039	58.458	96.516	83.526	24.033	44.570	68.951	69.479
7/15/92	1392	35.077	50.738	82.920	70.067	20.844	36.740	54.453	52.642
7/16/92	1416	44.076	64.895	106.401	89.780	26.718	46.965	72.279	69.729
7/17/92	1440	40.004	59.160	96.128	84.350	24.989	43.030	69.026	68.206
7/20/92	1512	42.441	60.728	93.506	80.551	25.254	41.247	63.723	58.401
7/21/92	1536	41.570	62.375	97.542	89.726	27.279	44.152	72.772	70.603
7/28/92	1704	46.298	63.044	92.830	95.301	28.871	43.001	70.790	66.753
8/11/92	2040	68.392	74.705	105.031	129.280	41.327	58.661	100.265	95.574
8/17/92	2168	67.705	74.550	101.991	144.803	46.540	68.279	107.378	112.029
8/19/92	2216	62.064	68.374	92.381	131.065	43.328	62.920	97.370	102.369
8/21/92	2264	61.396	66.393	89.351	124.494	43.891	64.120	96.121	99.008
8/24/92	2336	61.539	65.305	85.990	117.979	45.020	65.633	93.816	98.944
8/27/92	2408	61.064	63.535	82.308	115.058	45.784	66.668	91.229	96.206
10/7/92	3392	34.543	24.575	19.956	60.510	26.031	39.327	27.205	57.419
10/16/92	3608	42.840	27.556	24.533	69.776	36.706	43.550	34.096	31.218
11/7/92	4136	47.729	26.760	27.635	48.354	37.406	46.760	36.583	31.250
11/27/92	4616	32.010	15.927	16.229	44.125	19.542	31.500	16.646	21.625
11/30/92	4688	35.417	17.198	17.656	49.615	28.750	35.063	18.833	21.375
12/7/92	4856	24.875	10.646	11.146	37.052	19.490	21.927	16.427	17.354
12/22/92	5216	28.146	11.354	12.927	28.250	22.135	24.063	18.375	18.573
1/4/93	5528	29.521	11.656	13.635	36.177	23.875	22.083	20.958	23.615

The current density data are plotted in Figures 3.3 and 3.4. The depolarization readings were recorded monthly and cover the time period between June, 1992 and August, 1993 for tests conducted in 50% humidity. The depolarization readings for 100% humidity cover the time period between June, 1992 and January, 1993. The data are plotted in Figures 3.5 and 3.6.

Current density decreases with time as the materials are sacrificed. When the anode is fully sacrificed, the current flow stops and the cathodic protection ends. So long as the anode material is available, the magnitude of initial current is a good indicator of the duration of protection. Hence, one may conclude that the higher the initial current, the longer the protection. The best anode material is the one with the highest value of current density at initial connection. The results indicate that zinc anode has higher current density than zinc-aluminum (85:15), signifying that zinc is a better anode than zinc-aluminum (85:15). The results further indicate that reduction in concrete cover produces higher current flow. Therefore, samples with smaller concrete cover show better cathodic protection. The data have been further analyzed to assess the significance of test parameters, and are discussed in detail in Chapter 4.

Examination of the current density plots shown in Fig. 3.3 indicates that the average current flow varies between 0.014 and 0.174 mA/m^2 for samples tested in 50% relative humidity during the initial one month period. This range of values indicates low current flow when compared with the average current flow of 0.097 to 1.266 mA/m^2 shown in Fig. 3.4 for samples tested in 100% relative humidity. When all the samples were immersed in salt water a drastic increase in current flow was observed as shown in Fig. 3.3 and 3.4. The current density values approached, and in some cases exceeded 100 mA/m^2. This increased current flow resulted in partial consumption of the anode material in the 100% humidity samples, which could be visibly noticeable on the surface of the samples. Furthermore, the protruding part of the steel bars were badly corroded, reducing the quality of wire connection. Therefore, these tests were discontinued when the readings dropped to the range between 11.656 and 36.177 mA/m^2.

The current density values for the 50% humidity samples show a steady decrease

with time, as expected. The removal of salt at 2208 hrs increased the rate of drop noticeably as can be observed in Fig. 3.3. The presentation of readings was discontinued when the current density readings dropped to approximately 1.573 to 5.542 mA/m^2 even though the experiments continued.

Depolarization data are presented in Tables 3.5 and 3.6 for specimens in 50% and 100% humidity, respectively. Examination of the depolarization plots shown in Fig. 3.5 indicates that the monthly average depolarization values vary between 11.65 and 42.55 mV for samples tested in 50% relative humidity during the initial one month period. This range of values indicates low depolarization when compared with the monthly average depolarization values of 37.944 to 137.190 mV shown in Fig. 3.6 for samples tested in 100% relative humidity. When all the samples were immersed in salt water a drastic increase in depolarization is observed as shown in Figs 3.5 and 3.6. The tests were discontinued when the readings ranged between 144 and 349.333 mV. The depolarization values showed a steady decrease with time especially for the 50% humidity samples.

Additional data in the form of EMF readings and On-potential readings are included in Appendix C.

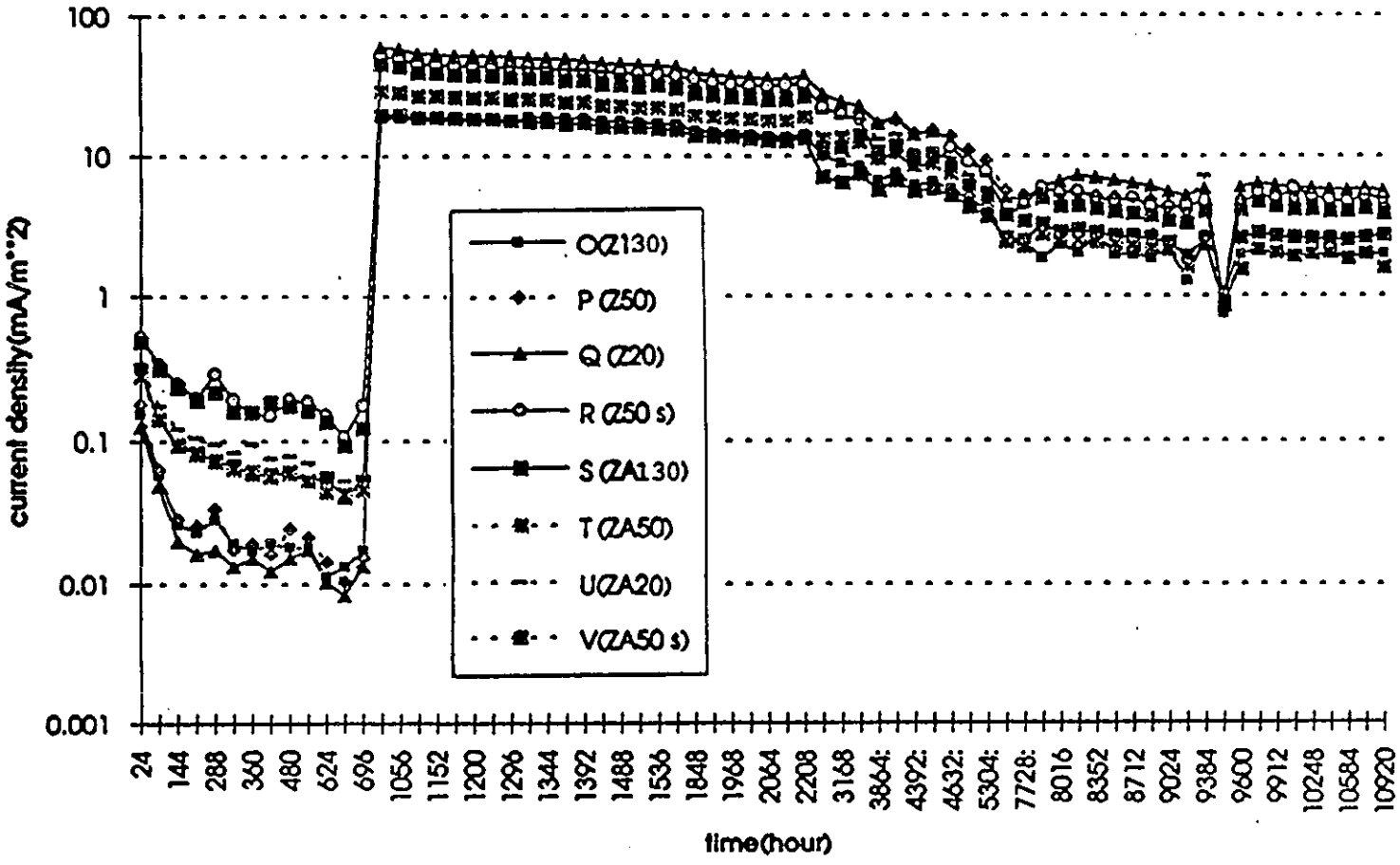

Figure 3.3 : The average current density (mA/m^2) of two steel bars in 50% humidity.

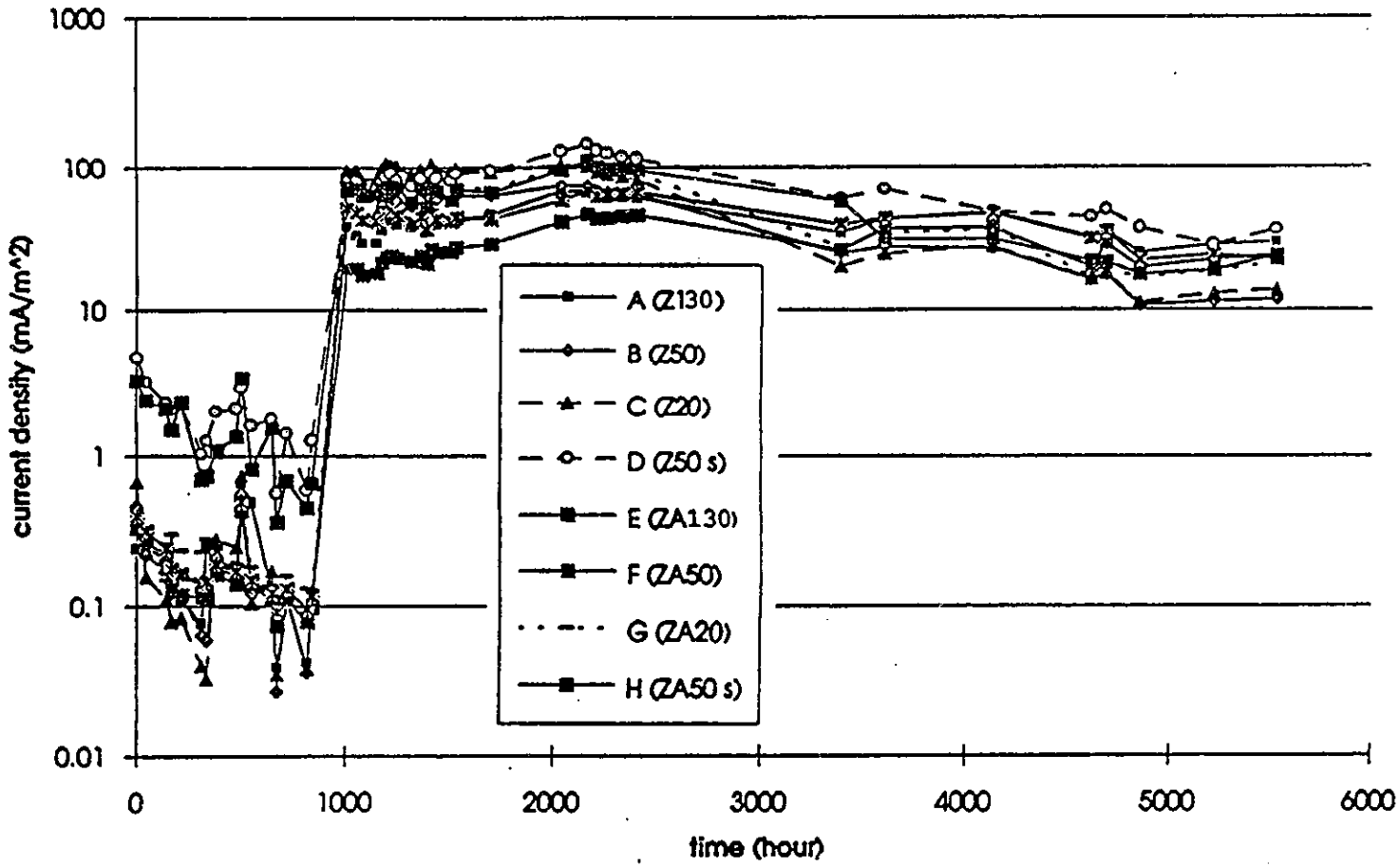

Figure 3.4 : The average current density (mA/m^2) of two steel bars in 100% humidity.

Table 3.5 : The monthly average depolarization shifts (mV) of two steel bars up to 4 hours in 50% humidity. Z: Zn, ZA: Zn-Al. The number following Z and ZA represents the thickness of concrete cover in mm.

Steel -Reference (mv)								
Time	**Z130**	**Z50**	**Z20**	**Z50 s**	**ZA130**	**ZA50**	**ZA20**	**ZA50 s**
June,92	11.65	22.50	19.62	21.01	24.56	37.47	42.55	31.91
July,92	**316.846**	**378.109**	**414.544**	**389.176**	**285.365**	**336.02867**	**389.056**	**403.87**
Dec.92	**301.67**	**374.67**	**391.67**	**310.67**	**249.67**	**325.00**	**348.00**	**347.00**
Jan.93	**262.00**	**338.67**	**348.33**	**225.67**	**207.67**	**289.67**	**254.00**	**294.33**
Apr.93	**275.33**	**317.67**	**336.00**	**304.67**	**246.00**	**280.67**	**295.67**	**304.33**
May.93	**181.670**	**312.670**	**341.670**	**307.000**	**258.330**	**201.330**	**306.670**	**316.000**
Jun.93	**230.000**	**303.330**	**340.330**	**277.330**	**248.000**	**189.670**	**295.000**	**305.330**
Jul.93	**215.000**	**311.330**	**351.330**	**280.330**	**255.670**	**172.670**	**316.670**	**320.000**
Aug.93	**178.330**	**305.330**	**342.000**	**280.670**	**244.000**	**181.670**	**300.670**	**308.000**

Table 3.6 : The monthly average depolarization shifts (mV) of two steel bars up to 4 hours in 100% humidity. Z: Zn, ZA: Zn-Al. The number following Z and ZA represents the thickness of concrete cover in mm.

Steel -Reference (mv)								
Time	**Z130**	**Z50**	**Z20**	**Z50 s**	**ZA130**	**ZA50**	**ZA20**	**ZA50 s**
June,92	**52.239**	**37.944**	**67.635**	**137.190**	**39.224**	**44.965**	**40.381**	**101.087**
July,92	**338.682**	**362.665**	**444.441**	**298.967**	**287.471**	**282.106**	**395.348**	**385.210**
Nov.92	**308.667**	**233.667**	**269.667**	**342.000**	**259.667**	**324.667**	**264.667**	**171.000**
Jan.93	**336.667**	**248.000**	**295.667**	**114.000**	**318.000**	**292.333**	**349.333**	**242.000**

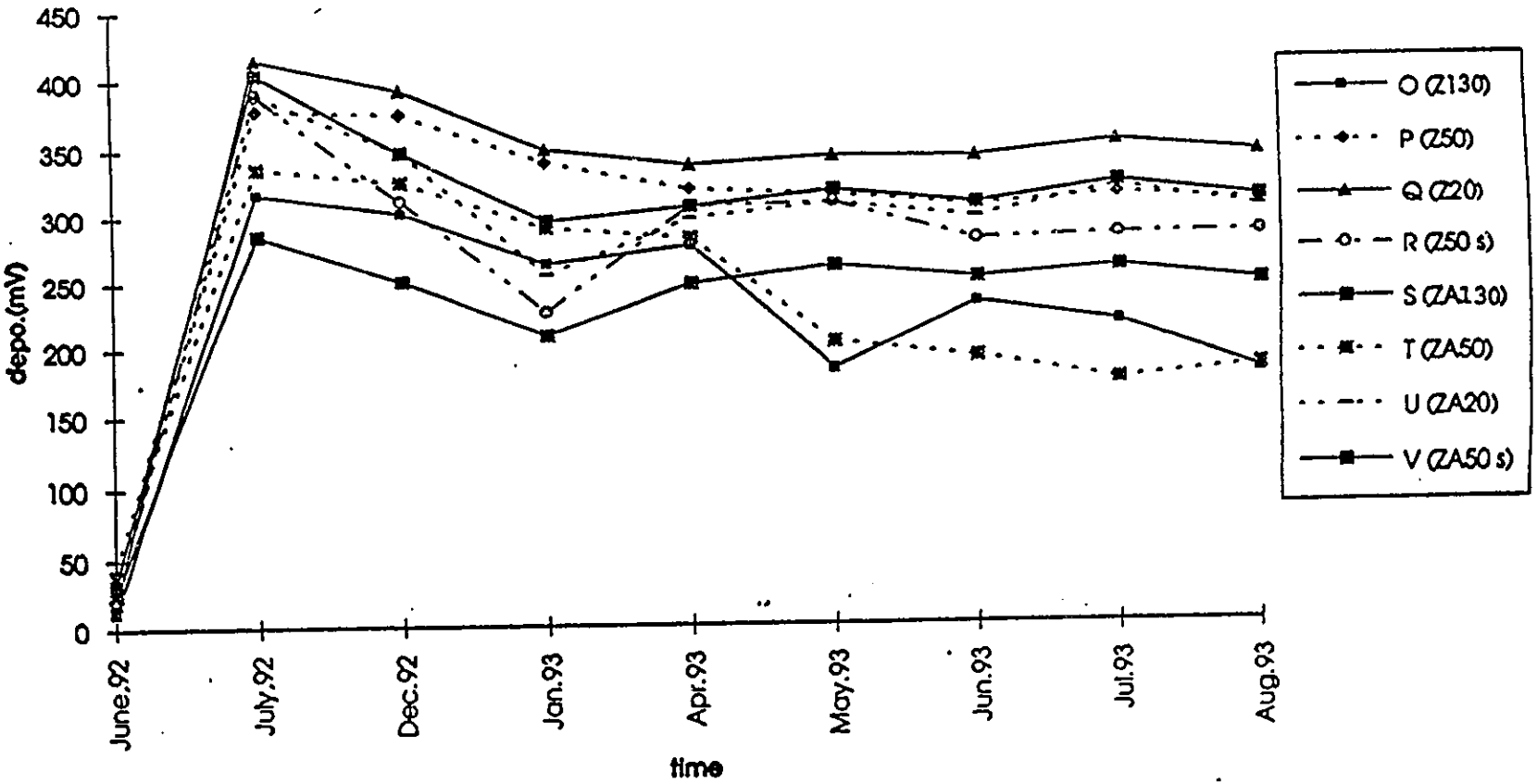

Figure 3.5: Variation of monthly average depolarization shifts (mV) of two steel bars up to 4 hours in 50% humidity.

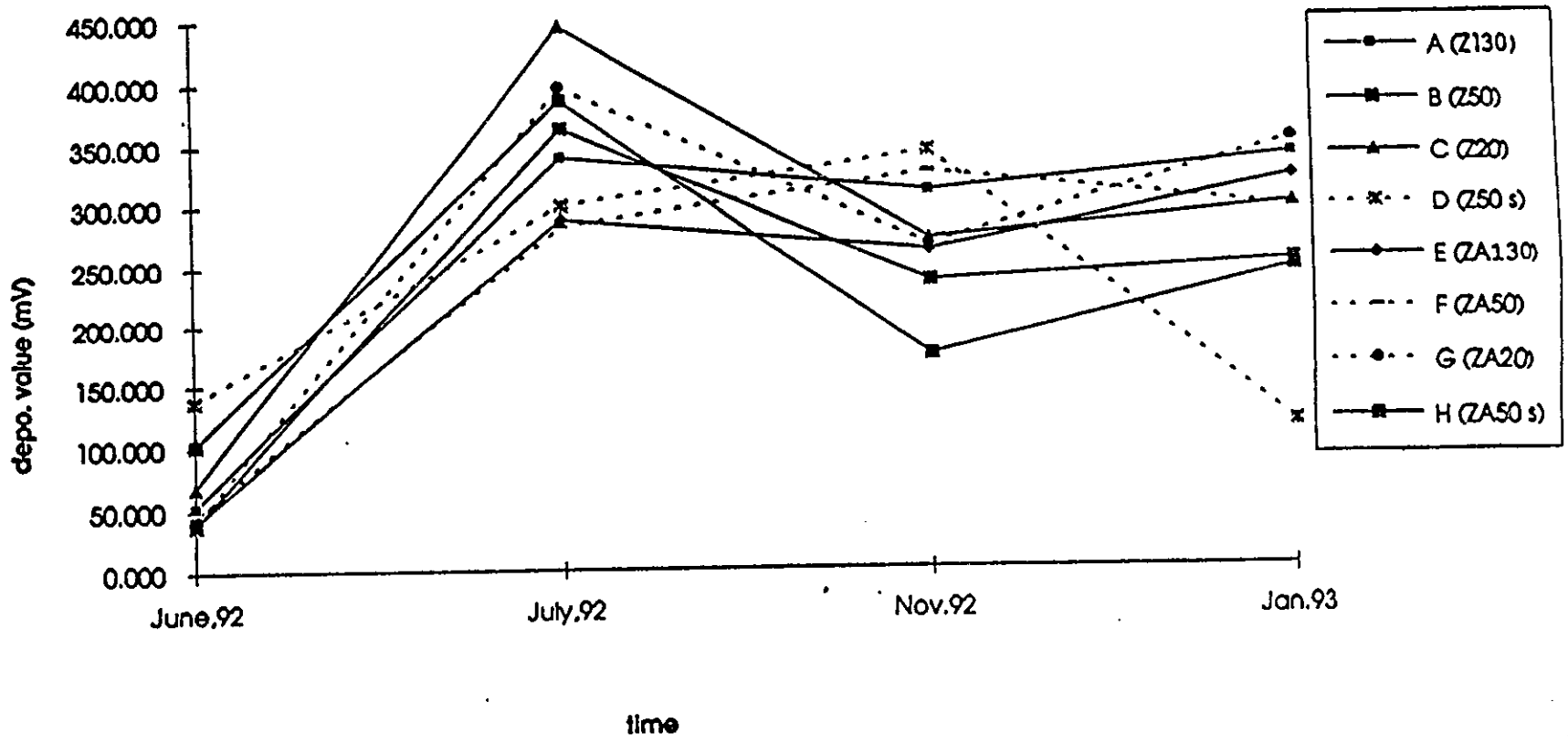

Figure 3.6 : Variation of monthly average depolarization shifts (mV) of two steel bars up to 4 hours in 100% humidity.

3.3 Phase 3 Experiments

3.3.1 Test Specimens and Parameters

A total of 42 reinforced concrete specimens were tested in Phase 3. Four levels of concrete cover and two arrangements of reinforcement layout were considered in the test program. This led to the use of four different sample sizes. Fig. 3.1 illustrates geometric details of all test specimens. Samples with 20 mm cover were 70×150×300 mm in cross-section. Samples with 50 mm and 130 mm cover had cross-sectional dimensions of 100×150×300 mm and 180×150×300 mm, respectively. Some of the samples with 130 mm cover also contained a second layer of reinforcement closer to the surface with 30 mm clear cover. All samples contained two No. 20 bars (19.5 mm diameter) except those with four bars, which had two additional No. 20 bars placed closer to the surface. All samples were of 300 mm length and each had a graphite reference rod positioned as illustrated in Fig. 3.1.

Two different environmental condition were considered in the test program. One half of the samples were tested in 100% humidity and 32°C temperature. The remaining samples were tested under 50% humidity and laboratory room temperature, which was approximately 20°C. All samples were contaminated with salt prior to testing. Table 3.7 includes test parameters considered in Phase 3.

Table 3.7 : quantities of specimen

	100% humidity		50% humidity		
	Anode material		Anode material		
concrete cover	Zn	Zn-Al (78:22)	Zn	Zn-Al (78:22)	salt contain
20 mm	3	3	3	3	yes
50 mm	3	3	3	3	yes
130 mm	3	3	3	3	yes
130 mm double layer of steel bar	2	1	2	1	yes

3.3.2 Preparation of Specimens

The procedures for preparation of concrete, spraying metallized anode, and wire connection were the same as those used in Phase 2. However, salt in the form of NaCl was added to all the Phase 3 samples at mixing. The zinc-aluminum sprayed had 78:22 ratio. The wire was connected to a data acquisition system, and a software called depol., issued by SCIEMETRIC INSTUMENTS INC. was used to record current and depolarization values.

3.3.3 Test Procedure

The following test procedure was followed in all experiments:

1. The voltage between reference graphite and reference copper/copper sulphite electrode (CSE) was measured prior to wire connection. All data recorded were normalized relative to CSE, as this reference electrode was known to be stable.
2. E_{corr} and I_{corr} measurements were taken.
3. Concrete impedance between anode and steel was measured.
4. After connecting the wire, the current flow between zinc or zinc-aluminum (78:22) anode and steel cathode was measured once a day except weekends.
5. The depolarization of cathode and anode was measured.

The first current reading was recorded on March 29, 1993.

3.3.4 Test Results

The current density data recorded are presented in Tables 3.8 and 3.9 for samples in 50% and 100% relative humidity environments, respectively. The tables include average current densities and depolarizations for each type of specimen, having specific concrete cover and anode material. The average values indicate the average of three readings recorded on three identical test samples, except for samples containing four steel bars.

Table 3.8 : The average current density (mA/m^2) of two steel bars in 50% humidity. Z: Zn, ZA: Zn-Al. The number following Z and ZA represents the thickness of concrete cover in mm. dt: top steel layer in double steel layers samples, db: bottom steel layer in double steel layers samples. (continued on next page)

The area of two steel bars = 0.04 m^2.

Date	Time (Hour)	Average Z20	Average ZA20	Average Z50	Average ZA50	Average Z130	Average ZA130	Average Z130dt	Average Z130db	Average ZA130dt	Average ZA130db
3/29/93	0	4.108	2.242	3.950	1.950	2.775	2.850	2.438	1.775	1.350	1.600
3/30/93	22	9.650	6.758	8.633	6.758	7.367	8.183	5.075	2.875	3.050	3.175
3/31/93	46	8.475	5.042	7.408	5.533	5.975	6.025	3.788	2.313	3.675	3.900
4/1/93	68	8.550	5.500	7.283	6.958	6.958	8.267	4.150	2.688	4.650	4.525
4/2/93	97	7.783	4.758	6.392	4.717	5.167	5.458	3.113	2.075	3.675	3.775
4/5/93	122	14.450	26.575	11.850	24.675	10.133	14.733	6.413	3.725	17.225	10.750
4/6/93	140	7.083	5.817	5.625	5.950	5.000	5.950	2.813	1.713	4.275	4.400
4/7/93	166	5.900	3.708	4.767	3.792	4.192	3.783	2.138	1.525	2.675	2.925
4/8/93	188	5.500	4.150	4.683	4.567	4.392	4.033	2.075	1.525	2.925	3.175
4/13/93	308	2.967	1.667	2.692	1.833	2.325	1.750	1.288	1.100	1.350	1.700
4/14/93	338	2.525	1.392	2.275	1.467	1.992	1.383	1.288	0.788	1.225	1.700
4/15/93	356	2.325	1.267	2.158	1.225	1.867	1.350	0.913	0.663	0.725	1.475
4/16/93	388	2.608	1.958	2.400	2.075	2.325	1.992	1.163	0.850	0.850	1.475
4/19/93	407	1.992	1.183	1.792	1.142	1.633	1.350	1.038	0.725	0.850	1.350
4/20/93	431	2.967	2.842	2.733	3.258	2.567	3.050	1.288	0.975	2.200	2.675
4/21/93	455	3.383	5.050	3.292	6.842	3.458	5.975	1.950	1.350	5.375	5.625
4/22/93	477	3.217	4.967	3.167	7.333	3.500	6.800	1.588	1.350	4.150	4.275
4/23/93	503	2.725	3.625	2.567	5.050	2.767	4.967	1.475	1.163	3.675	3.775
4/24/93	528	2.483	3.008	2.317	4.475	2.408	4.033	1.288	0.975	2.675	3.175
4/26/93	577	1.950	1.625	1.800	2.158	1.867	2.117	0.975	0.913	1.825	1.825
5/3/93	745	1.675	1.225	1.467	1.592	1.392	1.592	0.850	0.850	0.975	1.350
5/4/93	769	1.592	1.225	1.467	1.425	1.433	1.433	0.850	1.038	0.850	1.475
5/5/93	793	1.592	1.142	1.392	1.392	1.308	1.350	0.913	0.850	0.850	1.225
5/6/93	817	1.592	1.142	1.392	1.433	1.267	1.433	0.850	0.913	1.100	1.100
5/7/93	841	1.425	1.017	1.308	1.308	1.225	1.183	0.788	0.850	0.975	1.475
5/10/93	913	1.342	0.933	1.183	1.100	1.058	1.100	0.788	0.850	0.975	0.975
5/11/93	937	1.267	0.892	1.183	1.100	1.100	1.058	0.613	0.788	0.975	1.350
5/12/93	961	1.225	0.850	1.058	1.017	0.975	1.058	0.725	0.788	0.850	1.225
5/13/93	985	1.225	0.892	1.142	1.058	1.017	1.142	0.788	0.613	0.975	1.225
5/17/93	1081	1.100	0.808	1.017	0.933	0.933	0.975	0.663	0.725	0.850	0.975
5/20/93	1153	1.058	0.850	0.975	0.850	0.975	1.017	0.738	0.850	0.975	0.725
5/26/93	1297	0.975	0.767	0.892	0.892	0.808	0.850	0.725	0.600	0.850	1.100
5/27/93	1321	0.933	0.767	0.892	0.850	0.808	0.892	0.725	0.663	0.725	0.850
6/1/93	1441	0.933	0.767	0.892	0.892	0.808	0.808	0.600	0.675	0.975	0.725
6/2/93	1465	0.975	0.850	0.975	0.892	0.892	1.017	0.663	0.725	0.850	0.975
6/3/93	1489	0.975	0.850	0.892	0.808	0.850	0.892	0.850	0.663	0.725	0.850

Table3.8: (Cont'd)

Date	Time (Hour)	Average Z20	Average ZA20	Average Z50	Average ZA50	Average Z130	Average ZA130	Average Z130dt	Average Z130db	Average ZA130dt	Average ZA130db
6/7/93	1585	0.933	0.525	0.850	0.850	0.725	0.850	0.663	0.663	0.725	0.850
6/8/93	1609	0.808	0.725	0.808	0.808	0.692	0.767	0.663	0.600	0.600	0.725
6/10/93	1657	0.850	0.850	0.808	0.892	0.767	0.892	0.725	0.663	0.725	0.850
6/14/93	1753	0.850	0.808	0.767	0.808	0.794	0.767	0.613	0.788	0.725	0.975
6/15/93	1777	0.892	0.767	0.767	0.850	0.794	0.892	0.663	0.600	0.725	0.850
6/16/93	1801	0.808	0.767	0.767	0.808	0.781	0.892	0.663	0.663	0.600	0.975
6/17/93	1824	0.808	0.725	0.767	0.767	0.753	0.767	0.725	0.600	0.725	0.725
6/23/93	1968	0.767	0.725	0.767	0.767	0.753	0.767	0.725	0.663	0.725	0.725
6/24/93	1992	0.808	0.725	0.767	0.767	0.753	0.808	0.600	0.663	0.725	0.850
6/25/93	2019	0.767	0.725	0.725	0.733	0.728	0.808	0.613	0.550	0.600	0.600
6/28/93	2090	0.808	0.767	0.767	0.892	0.808	0.808	0.663	0.663	0.850	0.975
6/30/93	2116	0.808	0.725	0.767	0.808	0.767	0.808	0.600	0.663	0.725	0.850
7/2/93	2162	0.725	0.683	0.725	0.767	0.725	0.725	0.600	0.600	0.725	0.725
7/8/93	2306	0.850	0.767	0.767	0.892	0.808	0.767	0.613	0.425	0.975	1.100
7/15/93	2474	0.767	0.767	0.767	0.808	0.781	0.767	0.725	0.600	0.725	0.850
7/22/93	2642	0.725	0.725	0.683	0.767	0.725	0.767	0.600	0.600	0.600	0.850
7/29/93	2810	0.725	0.725	0.683	0.725	0.711	0.767	0.600	0.600	0.500	0.850
8/5/93	2978	0.767	0.725	0.725	0.767	0.725	0.767	0.600	0.725	0.500	0.975
8/12/93	3146	0.808	0.725	0.767	0.767	0.725	0.767	0.663	0.663	0.500	0.975
8/19/93	3314	0.767	0.725	0.767	0.767	0.725	0.808	0.663	0.663	0.600	0.975
8/26/93	3482	0.767	0.725	0.767	0.767	0.725	0.767	0.600	0.663	0.500	0.975

Table 3.9 : The average current density (mA/m^2) of two steel bars in 100% humidity. Z: Zn, ZA: Zn-Al. The number following Z and ZA represents the thickness of concrete cover in mm. dt: top steel layer in double steel layers samples, db: bottom steel layer in double steel layers samples. (continued on next page)

The area of two steel bars = 0.04 m^2.

Date	Time (Hour)	Average Z20	Average ZA20	Average Z50	Average ZA50	Average Z125	Average ZA130	Average Z130dt	Average Z130db	Average ZA130dt	Average ZA130db
3/29/93	0	4.075	5.375	4.183	7.492	4.808	7.125	3.363	3.425	4.875	4.875
3/30/93	20	4.925	7.125	6.717	8.875	5.458	7.608	4.088	4.525	4.875	5.000
3/31/93	45	4.567	6.475	5.983	7.692	4.842	7.167	3.725	3.900	4.775	4.875
4/1/93	66	10.383	10.258	10.342	8.467	6.342	9.567	7.938	6.650	5.850	5.375
4/2/93	95	4.067	4.483	5.983	6.108	6.717	6.550	4.400	4.888	3.425	4.400
4/5/93	116	4.683	5.458	9.400	9.733	8.508	9.325	6.838	8.238	5.375	7.450
4/6/93	140	4.517	6.067	8.867	8.675	7.892	8.958	5.438	7.025	4.775	7.200
4/7/93	166	3.542	5.217	5.700	7.608	6.017	7.733	3.538	4.575	4.400	6.100
4/8/93	188	3.417	5.008	4.958	7.525	5.417	7.492	3.300	4.038	4.400	5.850
4/13/93	308	3.542	4.608	5.617	6.758	5.542	7.000	4.100	5.375	4.525	5.625
4/14/93	338	2.975	4.242	4.400	6.350	4.483	6.392	3.050	3.975	4.025	5.250
4/15/93	356	2.850	4.117	3.908	5.950	4.025	6.067	2.688	3.538	4.025	4.875
4/16/93	388	3.092	4.192	3.983	6.067	3.983	5.942	2.925	3.663	4.025	4.875
4/19/93	407	2.725	3.908	3.375	5.867	3.542	5.542	2.513	2.988	3.675	4.525
4/20/93	431	5.008	4.967	11.567	7.567	7.125	7.167	5.013	5.913	4.525	5.625
4/21/93	455	5.050	5.000	12.783	8.917	9.650	8.633	6.900	7.638	4.875	6.100
4/22/93	477	4.392	4.150	10.017	8.383	8.717	8.142	4.888	6.713	4.400	5.750
4/23/93	503	2.975	3.467	7.817	7.158	6.233	8.008	3.363	4.763	4.150	5.375
4/24/93	527	3.375	3.500	9.400	7.700	7.733	7.975	4.088	5.800	4.275	5.625
4/26/93	575	2.367	3.500	4.850	6.392	4.800	6.875	2.675	3.600	3.775	4.775
5/3/93	743	2.125	3.383	4.192	6.308	4.075	6.433	2.388	3.175	3.425	4.275
5/4/93	767	2.167	3.417	3.783	6.058	3.783	6.233	2.325	2.938	3.425	4.150
5/5/93	791	2.083	3.500	3.500	7.125	3.542	6.108	2.200	2.813	3.425	4.150
5/6/93	815	2.125	3.333	3.300	5.775	3.417	5.942	2.075	2.625	3.300	4.025
5/7/93	839	5.292	4.225	8.875	8.142	6.967	8.142	4.463	5.000	4.275	4.875
5/10/93	911	2.083	2.975	3.825	5.692	2.650	5.783	2.325	3.413	3.425	4.275
5/11/93	935	4.233	3.867	7.942	7.208	6.108	6.842	4.163	5.188	4.025	4.650
5/12/93	959	2.158	2.933	4.967	5.333	4.558	5.492	2.938	4.400	2.800	3.900
5/13/93	983	2.967	2.850	8.667	6.075	6.392	7.083	4.275	5.750	3.900	4.875
5/17/93	1079	2.042	3.008	3.375	5.258	3.417	5.208	2.325	3.238	3.175	3.900
5/20/93	1151	1.958	2.933	3.583	3.300	3.092	5.208	2.013	2.625	2.925	3.775
5/26/93	1295	3.825	3.667	9.767	5.867	5.950	7.492	6.650	7.338	4.875	5.625
6/1/93	1439	2.567	2.367	8.708	5.850	7.367	7.325	5.625	8.250	5.625	7.450
6/2/93	1463	1.458	1.625	3.375	4.758	4.275	4.358	2.138	3.425	1.600	2.800
6/3/93	1487	3.175	3.133	6.392	3.983	4.842	5.133	5.075	6.838	5.125	6.225

Table3.9: (cont'd)

Date	Time (Hour)	Average Z20	Average ZA20	Average Z50	Average ZA50	Average Z125	Average ZA130	Average Z130dt	Average Z130db	Average ZA130dt	Average ZA130db
6/7/93	1583	2.692	2.933	8.017	6.150	5.700	6.475	5.913	7.200	5.250	7.450
6/8/93	1607	1.875	1.875	3.783	2.683	3.908	3.950	4.038	5.438	3.050	4.525
6/10/93	1655	2.117	2.400	8.750	3.658	8.058	8.875	4.463	8.250	4.650	7.575
6/14/93	1753	1.258	2.442	4.108	4.517	4.642	7.292	2.438	3.113	3.550	5.500
6/15/93	1777	1.217	2.400	3.825	6.183	4.400	7.125	2.313	2.813	3.175	5.375
6/16/93	1801	1.300	2.392	3.383	5.658	3.700	6.067	2.200	2.375	2.800	4.525
6/17/93	1824	1.258	2.350	3.300	5.458	3.450	5.775	2.138	2.263	2.675	4.525
6/23/93	1968	1.300	2.358	2.808	4.725	2.858	5.050	1.888	1.950	2.675	4.025
6/24/93	1992	1.383	2.275	2.725	4.683	2.858	5.050	1.825	1.950	2.800	3.775
6/25/93	2019	1.308	2.358	2.642	4.475	2.900	4.883	1.713	1.950	2.450	3.775
6/28/93	2091	1.425	2.567	2.517	4.317	2.767	4.808	1.700	1.888	2.450	3.675
6/30/93	2139	0.933	1.750	2.042	3.908	2.317	4.275	1.225	1.350	2.075	3.175
7/8/93	2331	1.350	1.958	2.358	4.033	2.683	4.275	1.650	1.700	2.325	3.300
7/15/93	2499	1.342	1.992	2.158	3.750	2.892	3.992	1.413	1.825	2.200	3.050
7/22/93	2667	1.425	1.917	2.358	3.542	2.975	3.783	1.650	1.775	1.950	3.050
7/29/93	2835	1.350	1.667	2.283	3.583	2.975	3.867	1.475	1.950	2.075	3.050
8/5/93	3003	1.342	2.233	2.117	3.375	2.892	3.783	1.600	1.825	1.825	2.800
8/12/93	3171	1.342	1.583	2.283	3.375	3.008	3.667	1.538	1.950	1.950	2.800
8/19/93	3339	1.300	1.458	2.125	3.258	2.967	3.550	1.475	1.900	1.950	2.800
8/26/93	3507	1.142	1.175	2.325	3.050	2.925	3.792	1.475	1.900	1.950	2.800

For samples with 130 mm cover with double layer reinforcement and zinc anode, the average value indicates the average of two readings, as only two samples were tested in this group. There was only one sample with 130 mm cover, double layer reinforcement, and zinc-aluminum (78:22) anode. The current density readings cover the time period between March 29, 1993 and August 26, 1993 for tests conducted in 50% and 100% humidity.

The current density data are plotted in Figures 3.7 and 3.8. These figures indicate that the current density decreases with time as the material is sacrificed. The results of 50% humidity samples indicate that zinc anode has higher current density than zinc-aluminum (78:22), signifying that zinc is a better anode than zinc-aluminum (78:22). The results further indicate that reduction in concrete cover produces higher current flow. Therefore, samples with smaller concrete cover show better cathodic protection. The results of 100% humidity samples indicate that zinc-aluminum (78:22) anode has higher current density than zinc, and the samples with smaller concrete cover do not show higher current flow. The data has been further analyzed to assess the significance of test parameters, and discussed in detail in Chapter 4.

Examination of the current density plots shown in Fig. 3.7 indicates that the average current flow varies between 1.35 and 4.108 mA/m^2 for samples tested in 50% relative humidity during the initial period. This range of values, compared with those between 3.363 and 7.42 mA/m^2 shown in Fig. 3.8 for samples tested in 100% relative humidity, indicates low current flow. The current density values approach each other during the last period of readings.

Depolarization data recorded are included in Tables 3.10 and 3.11 for samples in 50% and 100% relative humidity, respectively. These readings were taken weekly, and cover the same time period as current density readings. The data are plotted in Figures 3.9 and 3.10 and show the variation with time. Examination of the depolarization plots shown in Fig. 3.9 indicates that weekly average depolarization varies between 0.132 and 0.238 V for samples tested in 50% relative humidity during the initial period. This range of values indicates higher depolarization when compared with weekly average depolarization values of 0.114 to 0.225 V shown in Fig. 3.10 for samples tested in 100% relative humidity. The depolarization values are lower in

50% humidity during the last period of readings, when compared with those of 100% humidity for the same time period.

Additional data in the form of half cell potential, E_{corr} and I_{corr} for each metal used, impedance of concrete between anode and steel bar and EMF, On-potential are included in Appendix C.

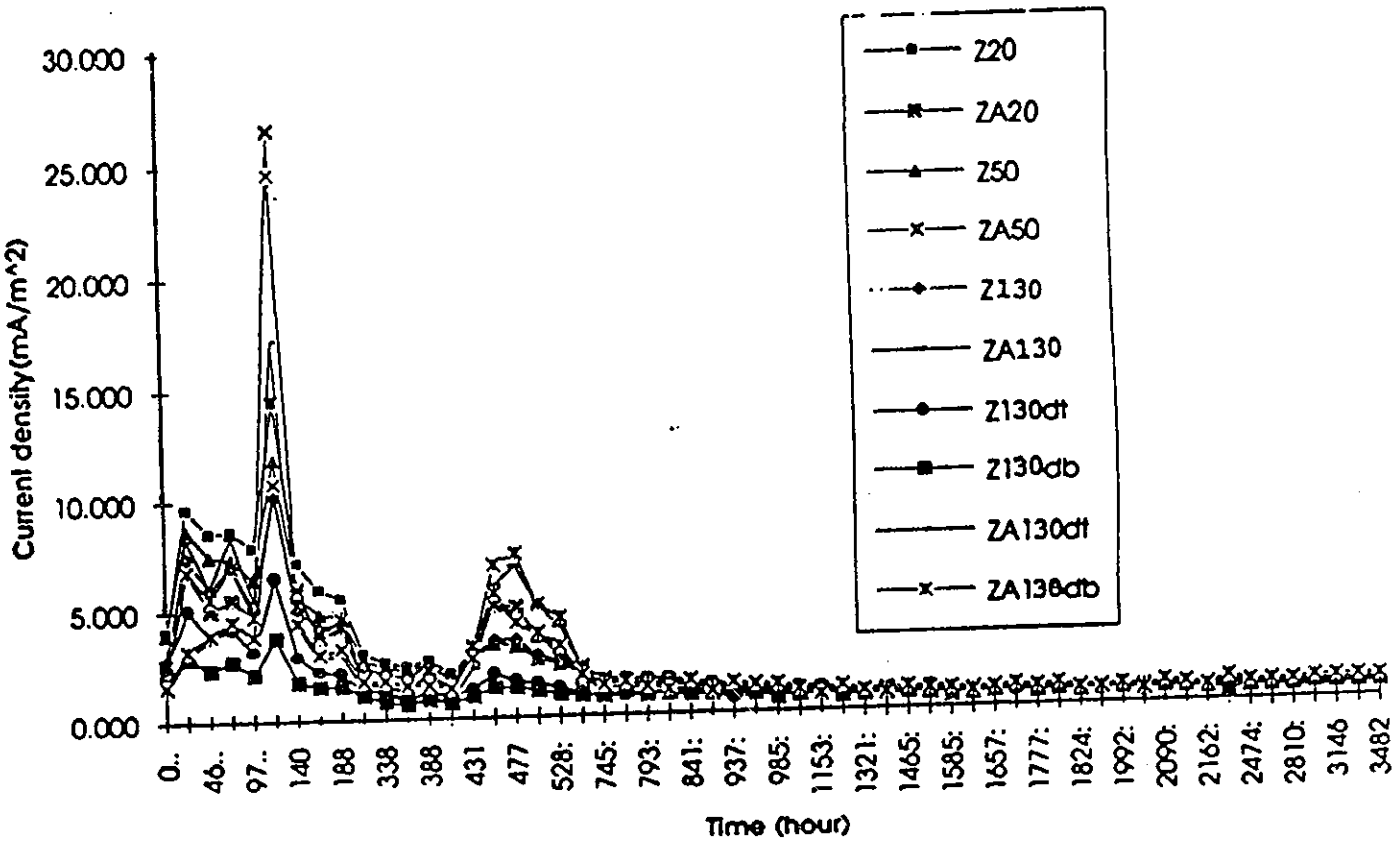

Figure 3.7: The average current density (mA/m^2) of two steel bars in 50% humidity.

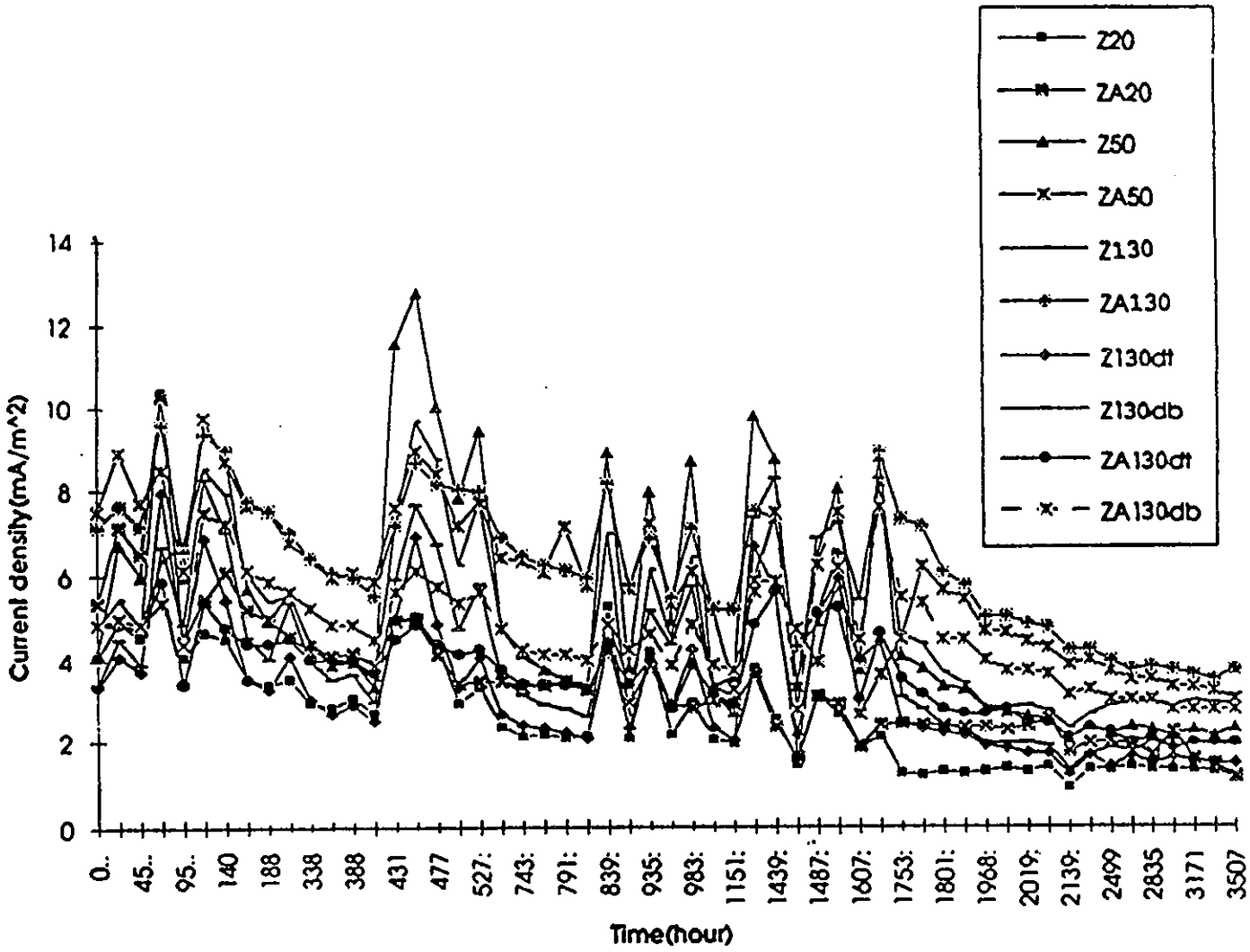

Figure 3.8: The average current density (mA/m^2) of two steel bars in 100% humidity.

Table 3.10 : The monthly average depolarization shifts (V) of two steel bars up to 4 hours in 50% humidity. Z: Zn, ZA: Zn-Al. The number following Z and ZA represents the thickness of concrete cover in mm. dt: top steel layer in double steel layers samples, db: bottom steel layer in double steel layers samples.

	Time	Z20	ZA20	Z50	ZA50	Z130	ZA130	Z130dt	Z130db	ZA130dt	ZA130db
4hours depo.	3 days	0.238	0.197	0.205	0.174	0.189	0.200	0.162	0.150	0.142	0.132
4hours depo.	1st week	0.212	0.186	0.181	0.155	0.165	0.155	0.117	0.117	0.115	0.124
4hours depo.	2nd week	0.157	0.105	0.130	0.082	0.109	0.083	0.074	0.086	0.051	0.079
4hours depo.	3rd week	0.180	0.207	0.159	0.206	0.157	0.201	0.104	0.114	0.161	0.169
4hours depo.	4th week	0.162	0.165	0.130	0.172	0.124	0.166	0.074	0.090	0.107	0.132
4hours depo.	5th week	0.129	0.100	0.105	0.095	0.090	0.091	0.060	0.077	0.051	0.093
4hours depo.	6th week	0.113	0.082	0.092	0.079	0.077	0.075	0.053	0.072	0.040	0.073
4hours depo.	7th week	0.104	0.080	0.087	0.077	0.070	0.073	0.050	0.068	0.036	0.070
4hours depo.	8th week	0.098	0.078	0.082	0.075	0.064	0.071	0.048	0.064	0.037	0.066
4hours depo.	9th week	0.097	0.078	0.083	0.076	0.064	0.075	0.050	0.068	0.041	0.078
4hours depo.	10th week	0.094	0.092	0.078	0.086	0.068	0.080	0.049	0.066	0.041	0.076
4hours depo.	11th week	0.090	0.082	0.075	0.076	0.064	0.072	0.090	0.026	0.137	0.071
4hours depo.	12th week	0.091	0.079	0.073	0.076	0.064	0.073	0.046	0.061	0.042	0.049
4hours depo.	13th week	0.089	0.079	0.074	0.077	0.063	0.073	0.036	0.062	0.037	0.069
4hours depo.	14th week	0.091	0.086	0.077	0.083	0.065	0.079	0.048	0.061	0.039	0.074
4hours depo.	18th week	0.083	0.070	0.069	0.069	0.057	0.065	0.039	0.054	-0.024	0.101

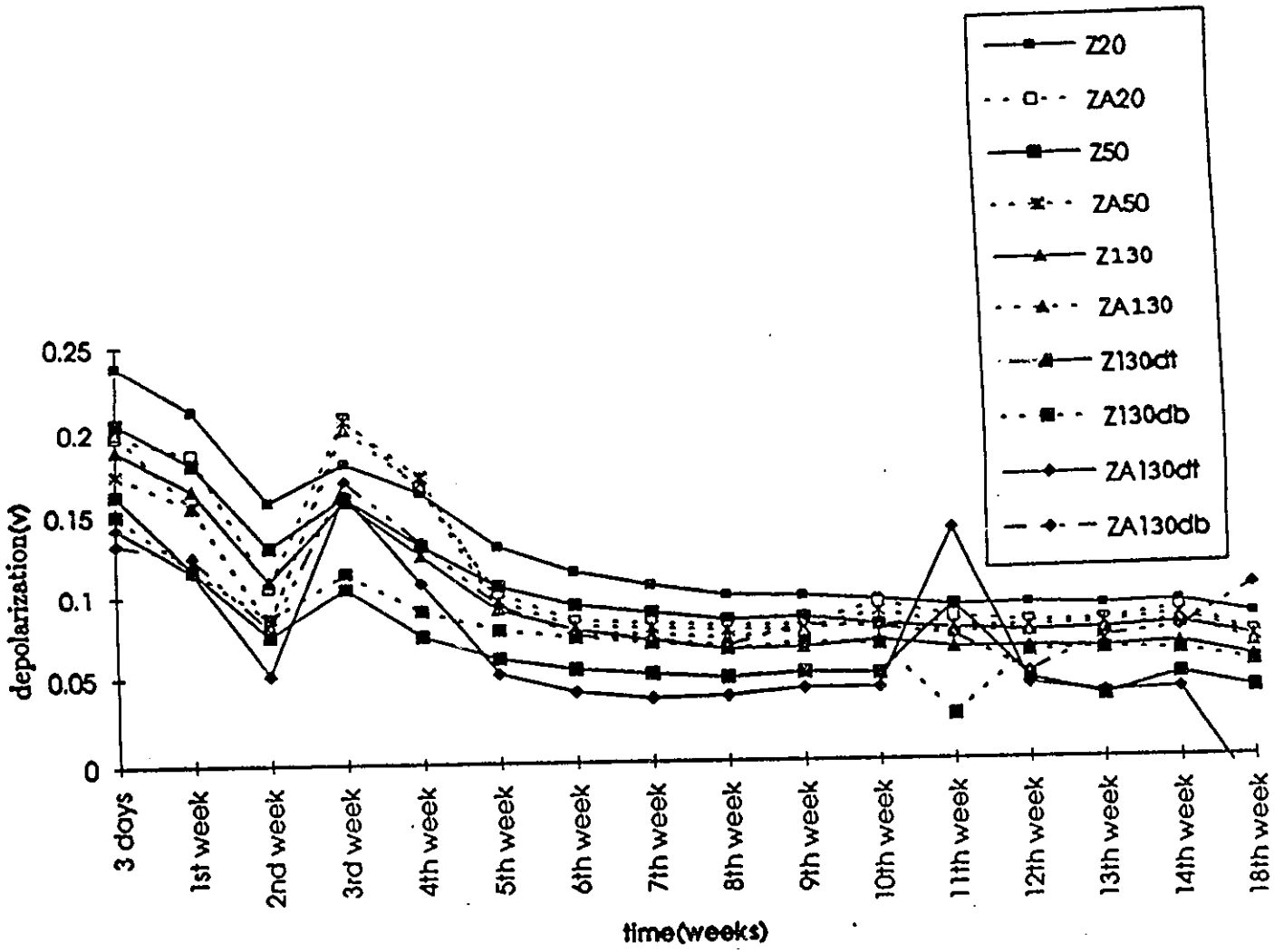

Figure 3.9 : Variation of monthly average depolarization shifts (V) of two steel bars up to 4 hours in 50% humidity.

Table 3.11 : The monthly average depolarization shifts (V) of two steel bars up to 4 hours in 100% humidity. Z: Zn, ZA: Zn-Al. The number following Z and ZA represents the thickness of concrete cover in mm. dt: top steel layer in double steel layers samples, db: bottom steel layer in double steel layers samples.

	Time	Z20	ZA20	Z50	ZA50	Z130	ZA130	Z130dt	Z130db	ZA130dt	ZA130db
4hours depo.	1st week	0.212	0.210	0.188	0.196	0.114	0.225	0.193	0.127	0.188	0.196
4hours depo.	2nd week	0.208	0.198	0.177	0.181	0.099	0.209	0.187	0.126	0.185	0.186
4hours depo.	3rd week	0.303	0.228	0.324	0.239	0.147	0.242	0.248	0.165	0.195	0.203
4hours depo.	4th week	0.254	0.237	0.280	0.225	0.135	0.233	0.210	0.133	0.186	0.188
4hours depo.	5th week	0.179	0.181	0.161	0.192	0.094	0.209	0.165	0.107	0.174	0.178
4hours depo.	6th week	0.295	0.232	0.255	0.210	0.142	0.232	0.229	0.165	0.195	0.193
4hours depo.	7th week	0.184	0.179	0.169	0.167	0.095	0.205	0.169	0.110	0.169	0.171
4hours depo.	8th week	0.314	0.262	0.268	0.181	0.136	0.249	0.263	0.210	0.227	0.213
4hours depo.	9th week	0.234	0.191	0.227	0.147	0.134	0.219	0.246	0.187	0.210	0.212
4hours depo.	10th week	0.208	0.160	0.295	0.136	0.158	0.274	0.238	0.193	0.205	0.205
4hours depo.	11th week	0.124	0.169	0.145	0.173	0.099	0.194	0.156	0.086	0.180	0.193
4hours depo.	12th week	0.138	0.150	0.134	0.169	0.087	0.194	0.154	0.081	0.176	0.183
4hours depo.	13th week	0.131	0.154	0.110	0.153	0.076	0.186	0.145	0.080	0.164	0.176
4hours depo.	14th week	0.151	0.151	0.134	0.169	0.089	0.186	0.146	0.078	0.162	0.173
4hours depo.	18th week	0.143	0.150	0.130	0.160	0.097	0.179	0.142	0.081	0.149	0.169

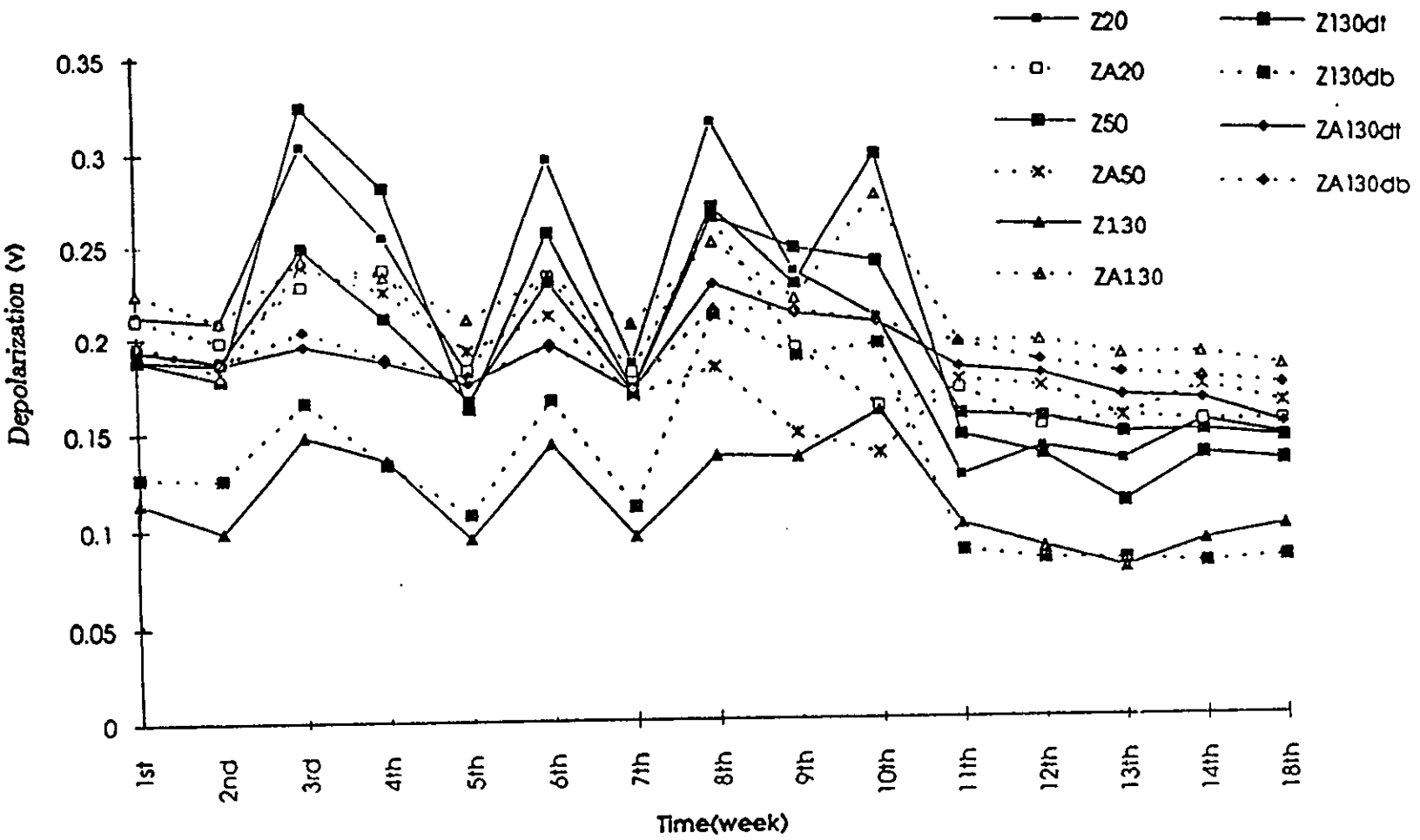

Figure 3.10: Variation of monthly average depolarization shifts (V) of two steel bars up to 4 hours in 100% humidity.

Chapter 4

Analysis of Test Data

4.1 General

This chapter contains analysis of test data and evaluation of test parameters. Both experiments in solutions and tests of reinforced concrete samples are considered. Current density and depolarization shifts are used as indicators of cathodic protection. The test parameters evaluated include anode material, concrete cover, salt contamination, humidity condition, and the number of layers of reinforcement. Details of the experimental program, including material and geometric properties, are presented in Chapters 2 and 3.

4.2 Effects of Test Parameters on Cathodic Protection

4.2.1 Effects of Anode Material

The suitability of selected anode materials for galvanic cathodic protection has been investigated both in electrolyte solution and concrete samples. The results of Phase 1 tests, obtained from tests in solutions, indicate that zinc-aluminum (85:15) produced stable and high current density, implying that this anode material is the best candidate in the solution environment. The other zinc-aluminum solution considered, i.e., zinc-aluminum (98:2) also showed improved current density values with time after a slow start. Fig. 4.1 shows performance of selected anode materials in terms of current

density variation with time. The figure indicates that aluminum and zinc showed poor performance. Nevertheless, zinc was investigated as a potential anode material in concrete samples since it is commonly used in practice for impressed current systems.

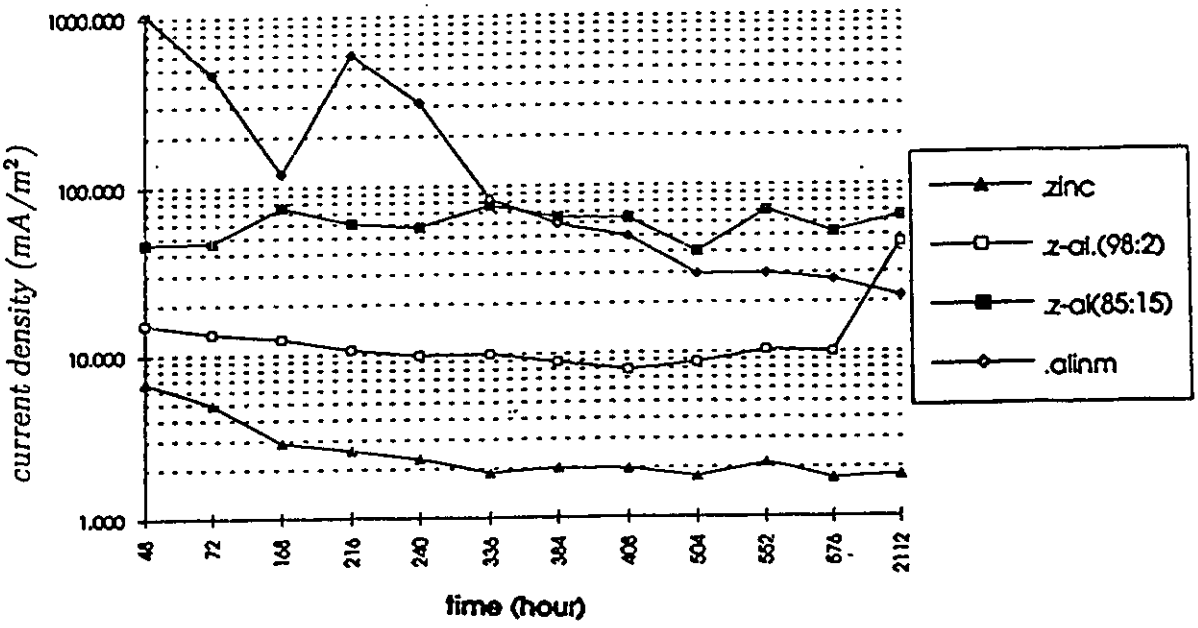

Figure 4.1 : The average current density (mA/in^2) for four anode materials in solution.

Zinc and zinc-aluminum (85:15) were used as anode materials sprayed on concrete in Phase 2. Variation of current density is shown in Figs. 4.2 through 4.4 for samples with different concrete cover and salt contamination, tested in 50% relative humidity. The results indicate that the samples with zinc-aluminum (85:15) anode showed higher current density initially until the samples were sprayed with salt water, at which time there was a drastic jump in the current density values. Beyond this time the performance of the two anode materials did not show significant variation and samples with both anode materials showed very high current density values. The samples that did not originally contain salt showed slightly higher values for zinc anode when the concrete cover was 50 mm.

Zinc and zinc-aluminum (78:22) were used in Phase 3 on concrete samples. How-

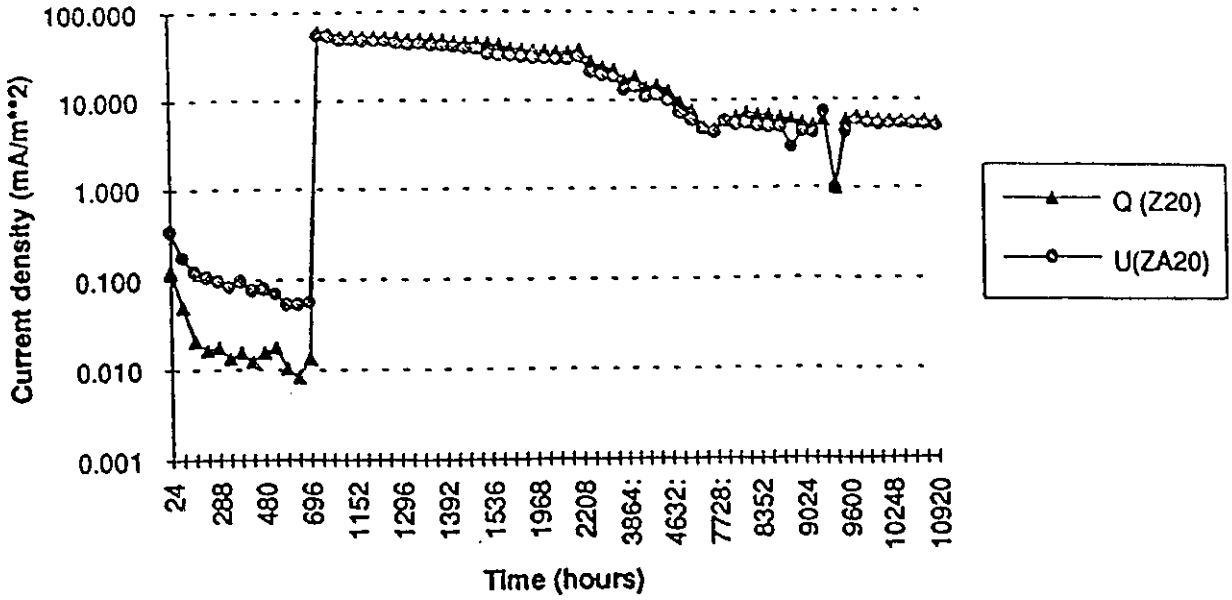

Figure 4.2 : The average current density (mA/m^2) for samples in 50% humidity with 20 mm concrete cover.

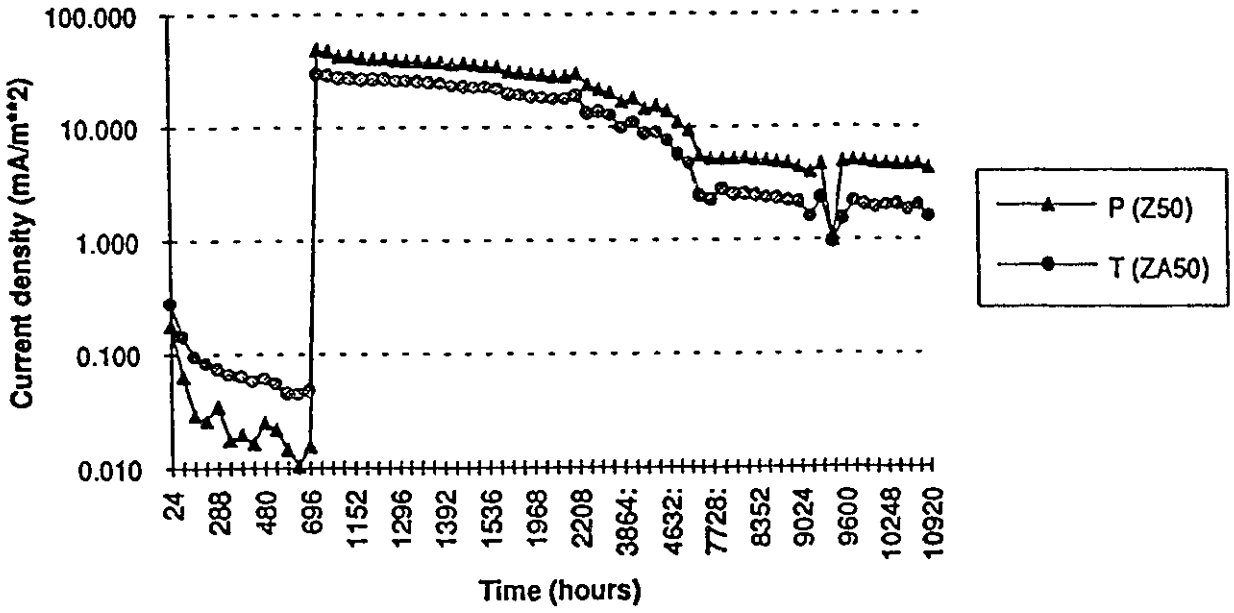

Figure 4.3 : The average current density (mA/m^2) for samples in 50% humidity with 50 mm concrete cover.

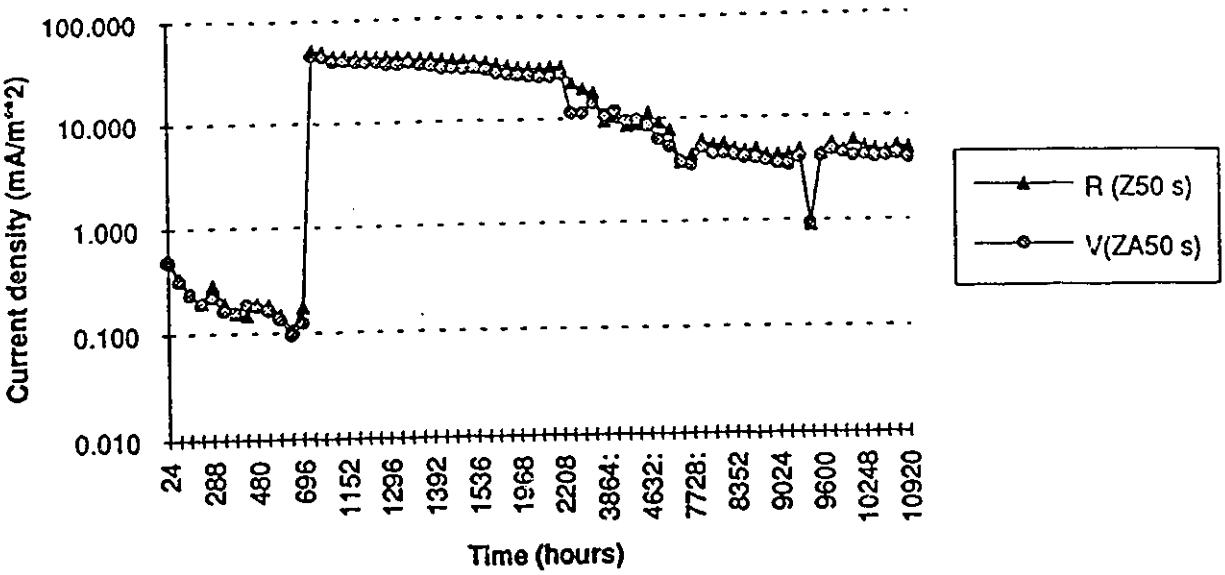

Figure 4.4 : The average current density (mA/m^2) for samples in 50% humidity with 50 mm concrete cover and salt contamination.

ever, this time zinc-aluminum (78:22) was used instead of zinc-aluminum (85:15) because of the availability of the material and the relatively close performance of the two materials observed in Phase 1. The average current density values are plotted in Figs. 4.5 through 4.7 for samples with 20 mm, 50 mm and 130 mm concrete cover, tested in 100% humidity. The results indicate that, although some fluctuations were observed at early ages, zinc-aluminum (78:22) consistently showed higher values when compared with pure zinc. The results also indicate that the variation between the performance of each material was not substantial.

It may be concluded from the foregoing discussion that both zinc and zinc-aluminum can be used for galvanic cathodic protection, although zinc-aluminum shows marginally better performance characteristics.

4.2.2 Effect of Concrete Cover

Effects of concrete cover thickness on current density have been investigated in Phase 2 and Phase 3. Figs. 4.8 and 4.9 illustrate comparisons of samples with different

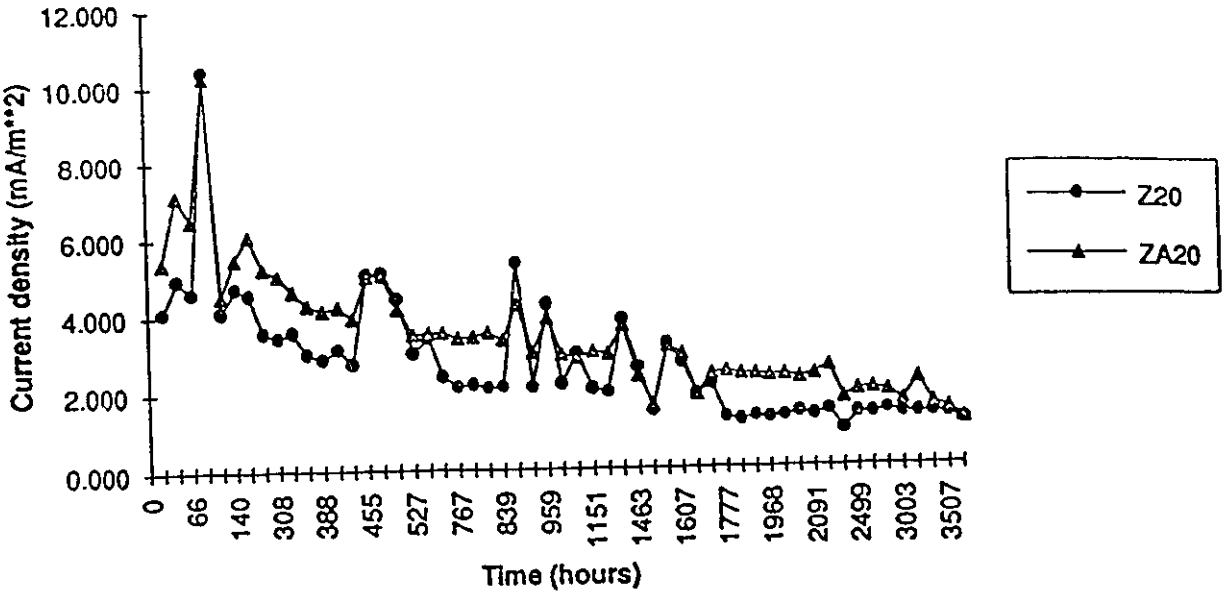

Figure 4.5 : The average current density (mA/m^2) for samples in 100% humidity with 20 mm concrete cover.

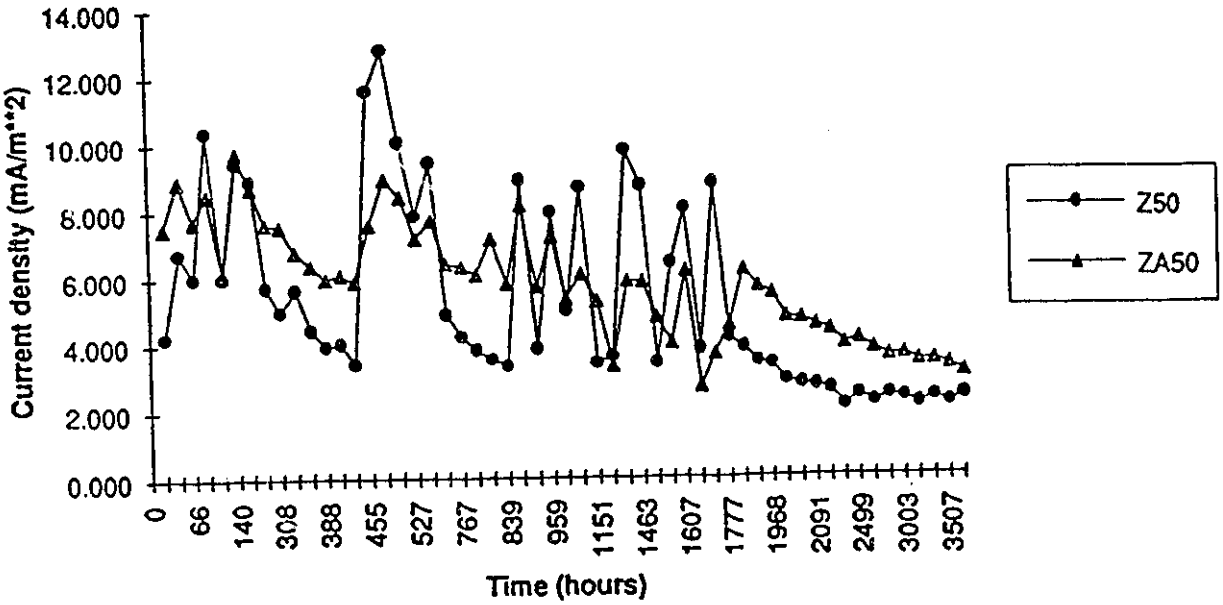

Figure 4.6 : The average current density (mA/m^2) for samples in 100% humidity with 50 mm concrete cover.

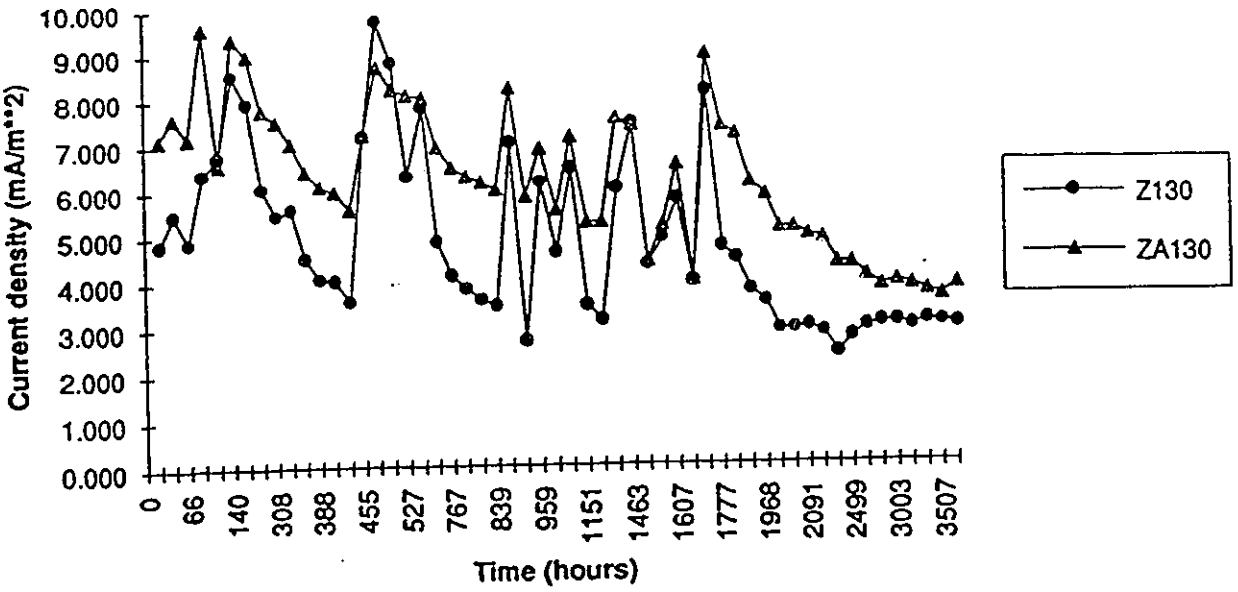

Figure 4.7 : The average current density (mA/m^2) for samples in 100% humidity with 130 mm concrete cover

concrete cover, obtained from Phase 2. The results indicate that concrete samples with zinc or zinc-aluminum (85:15) both showed high current density when the cover thickness was small. The samples with 20 mm concrete cover consistently developed highest current densities than those with 50 mm and 130 mm. However, this observed trend changed in Phase 3 where salt contaminated concrete was tested. Fig. 4.10 and 4.11 show variation of current density with time for samples tested in Phase 3. The results indicate that in this series of tests, increased concrete cover resulted in higher current density. Samples with 130 mm cover developed higher current density than those with 50 mm and 20 mm. The results also indicate that although increase in cover resulted in increased current density, the increase obtained beyond a cover of 50 mm was not very significant. It appears that there is an optimum concrete cover, beyond which further increase in cover does not result in significantly higher current density.

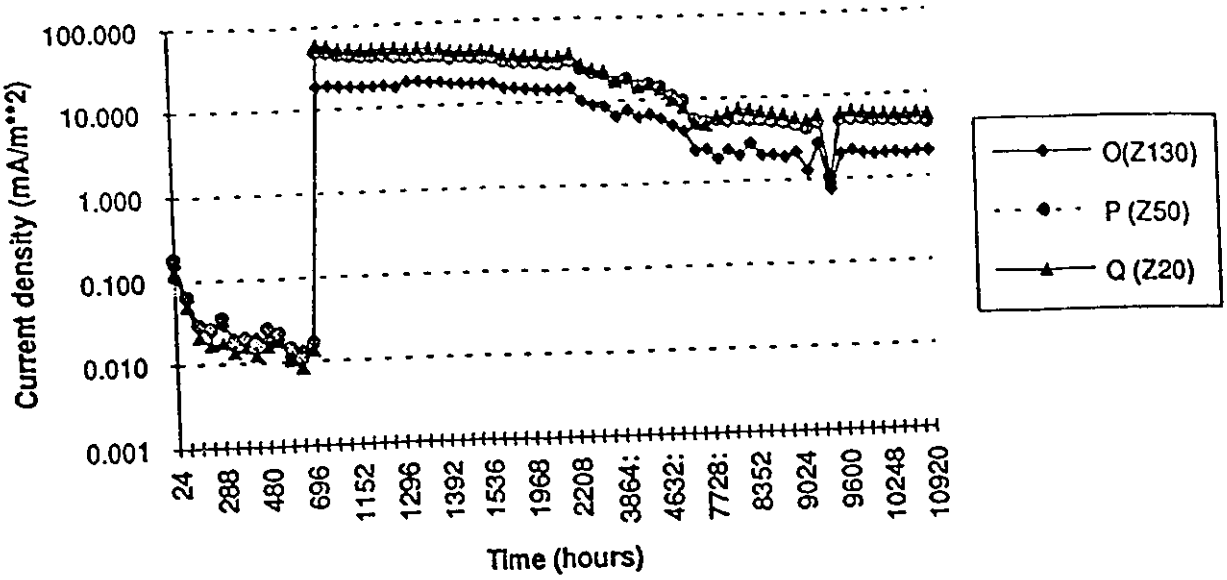

Figure 4.8 : The average current density (mA/m^2) for samples in 50% humidity with different concrete cover and zinc anode.

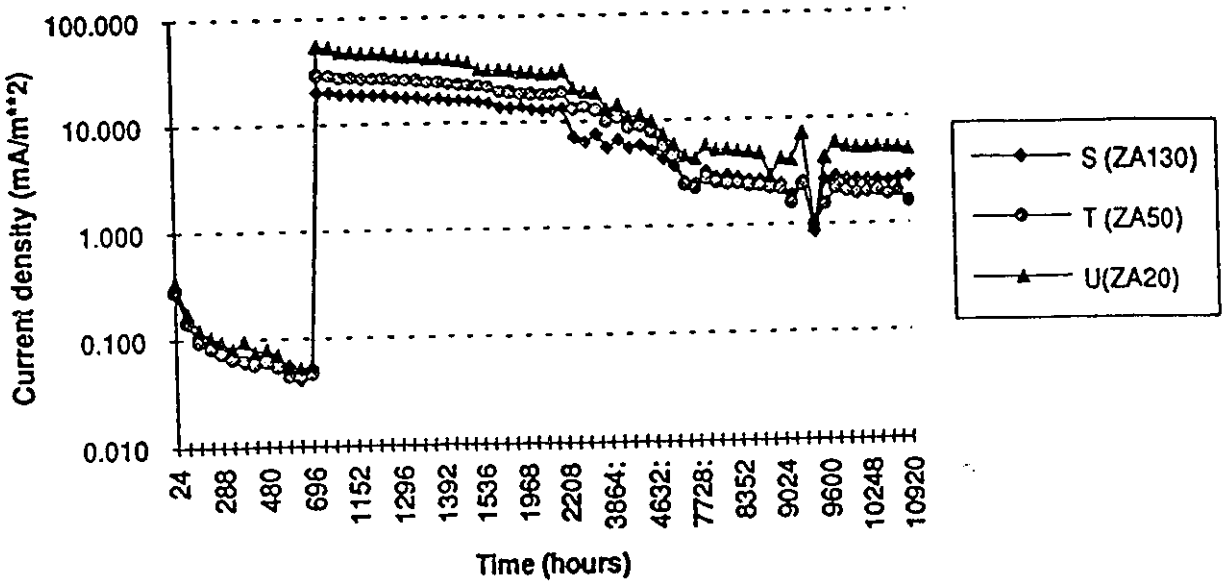

Figure 4.9 : The average current density (mA/m^2) for samples in 50% humidity with different concrete cover and zinc-aluminum (85:15) anode.

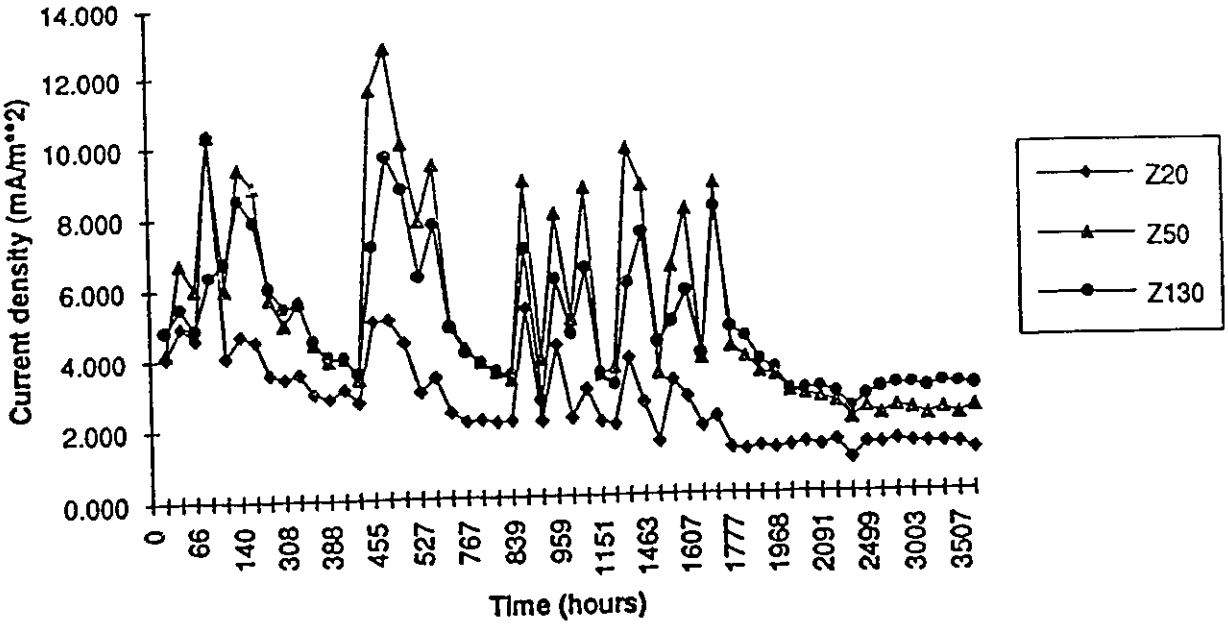

Figure 4.10 : The average current density (mA/m^2) for samples in 100% humidity with three different concrete cover and zinc anode.

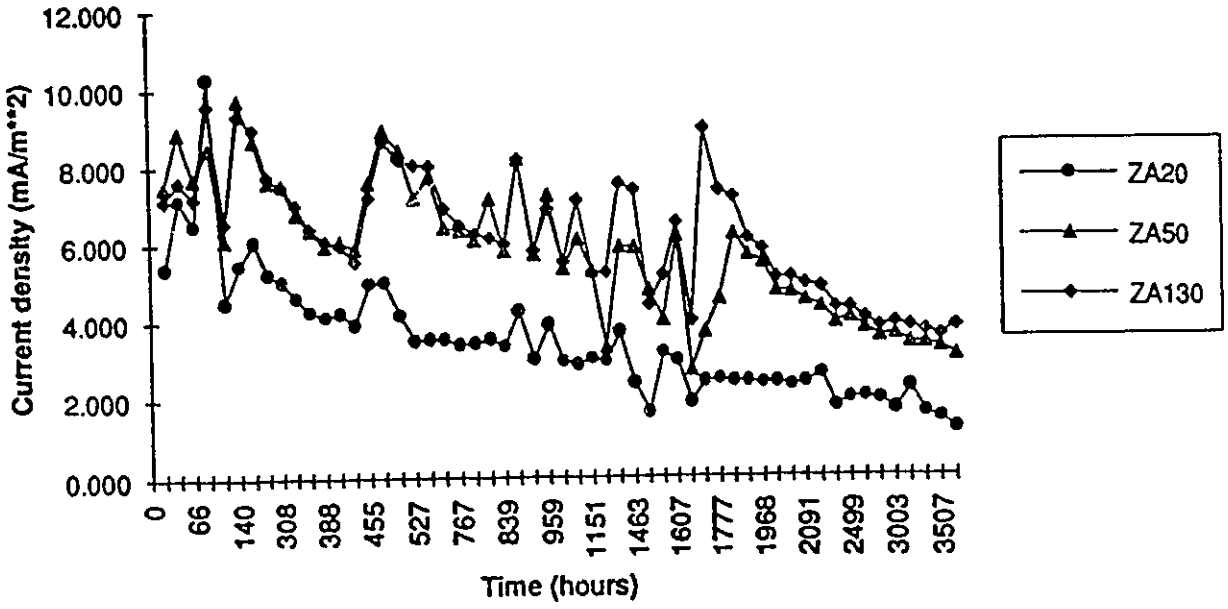

Figure 4.11 : The average current density (mA/m^2) for samples in 100% humidity with three different concrete cover and zinc-aluminum (78:22) anode.

4.2.3 Effect of Humidity

Effects of humidity have been investigated by testing samples in 50% and 100% relative humidity. The comparisons of current densities can be made in Figs. 4.12 and 4.13, for samples tested in Phase 2 and Phase 3. In both cases the samples in 100% humidity produced higher values of current density than those in 50% humidity, indicating increased galvanic cathodic protection in higher moisture environment.

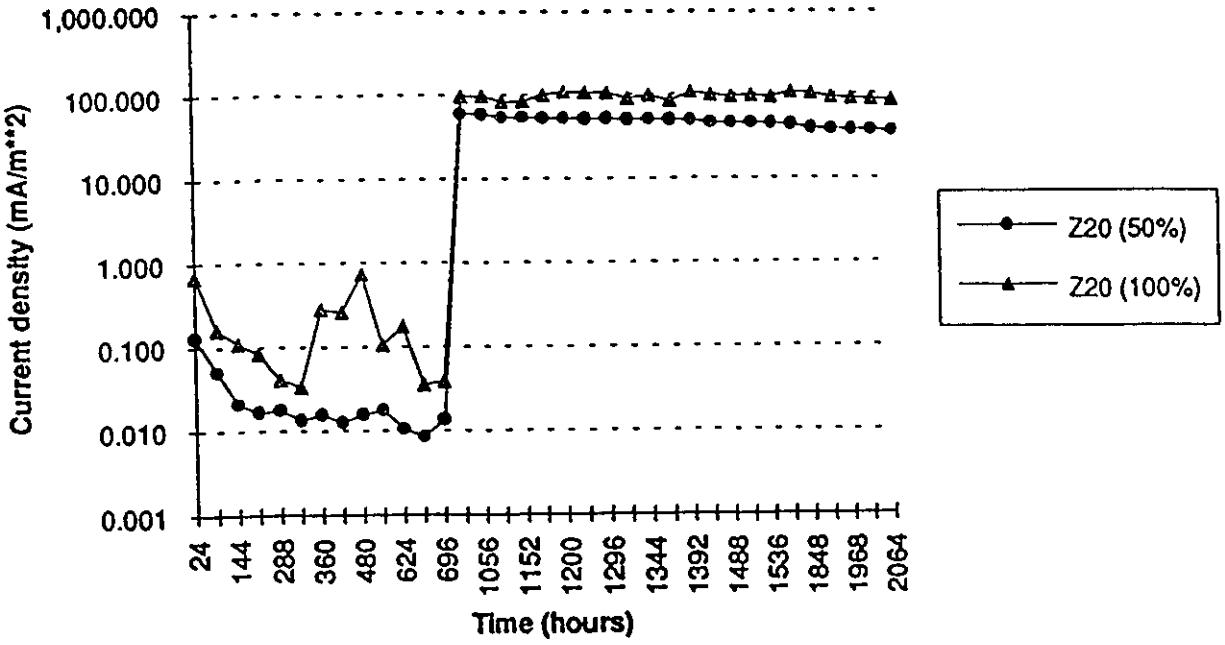

Figure 4.12 : The average current density (mA/m^2) for samples with 20 mm concrete cover and zinc anode in 50% and 100% humidity.

4.2.4 Effect of Salt

The effects of salt on cathodic protection have been investigated in two steps. First, samples were prepared with and without salt added to concrete prior to testing, as a contaminant. Secondly, both clean and contaminated samples in Phase 2 were sprayed with salt water, after a month of testing. Fig. 4.14 shows a comparison of current densities measured on samples with and without salt. The results indicate that the presence of salt in samples increased current density. The addition of salt

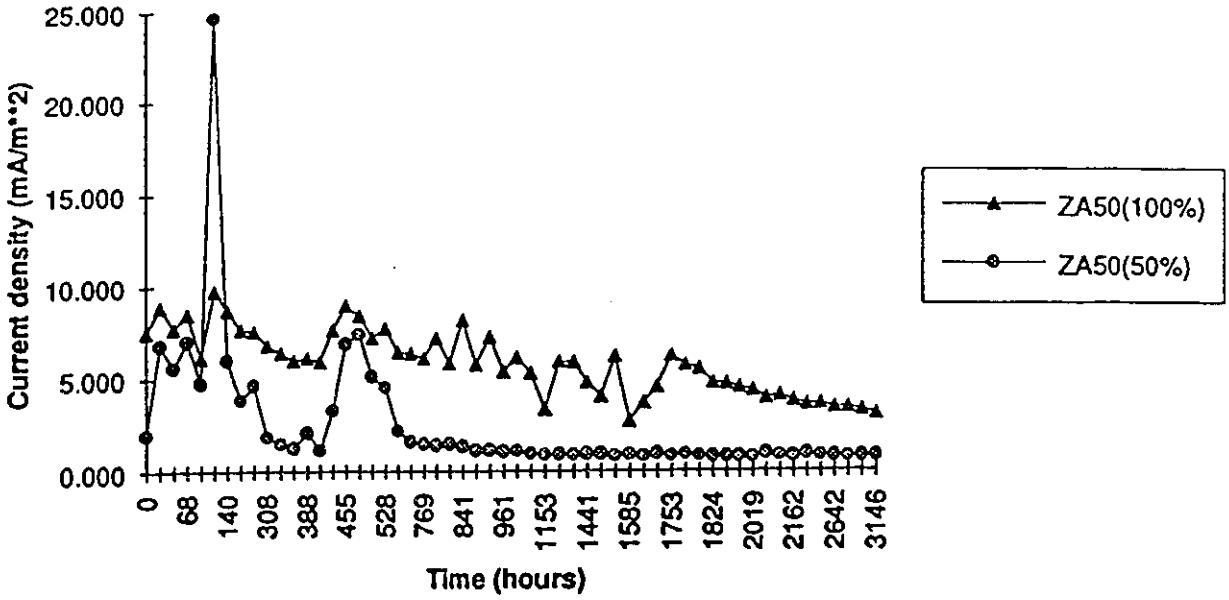

Figure 4.13 : The average current density (mA/m^2) for samples with 50 mm concrete cover and zinc-aluminum (78:22) anode in 50% and 100% humidity.

water after 696 hours of testing drastically increased the current density. Beyond this rather substantial increase the difference in behavior between the originally clean and contaminated specimens diminished, and the specimens developed approximately the same current densities. One may conclude from these tests that cathodic protection is more effective in presence of salt.

4.2.5 Effect of Double Layer Reinforcement

Double layer reinforcement was used in a group of specimens in Phase 3 to investigate cathodic protection of top and bottom layers of reinforcement. Current densities measured on top and bottom reinforcement are compared in Fig. 4.15 and 4.16. The results indicate that the current density measurement for the bottom reinforcement is higher than that for top steel. This is consistent with previous observations made relative to the effect of concrete cover. The effect of cover for Phase 3 specimens was such that samples with large concrete cover developed higher current density. Since the bottom reinforcement had higher concrete cover, it was expected to develop higher

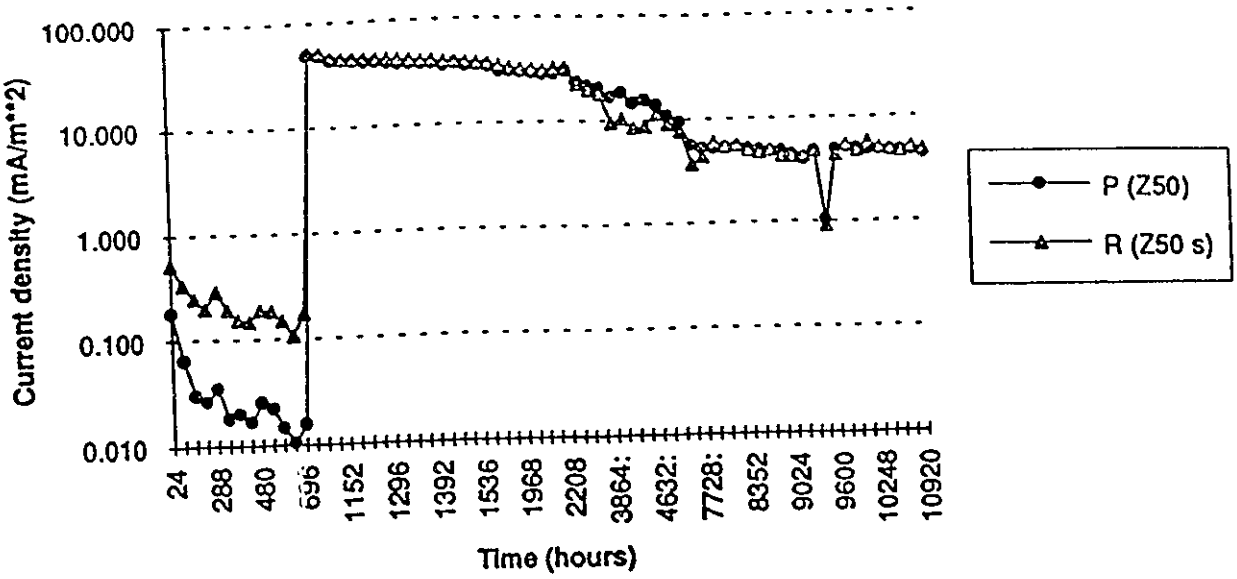

Figure 4.14 : The average current density (mA/m^2) for samples with 50 concrete cover, without salt prior to tests, and zinc anode in 50% humidity.

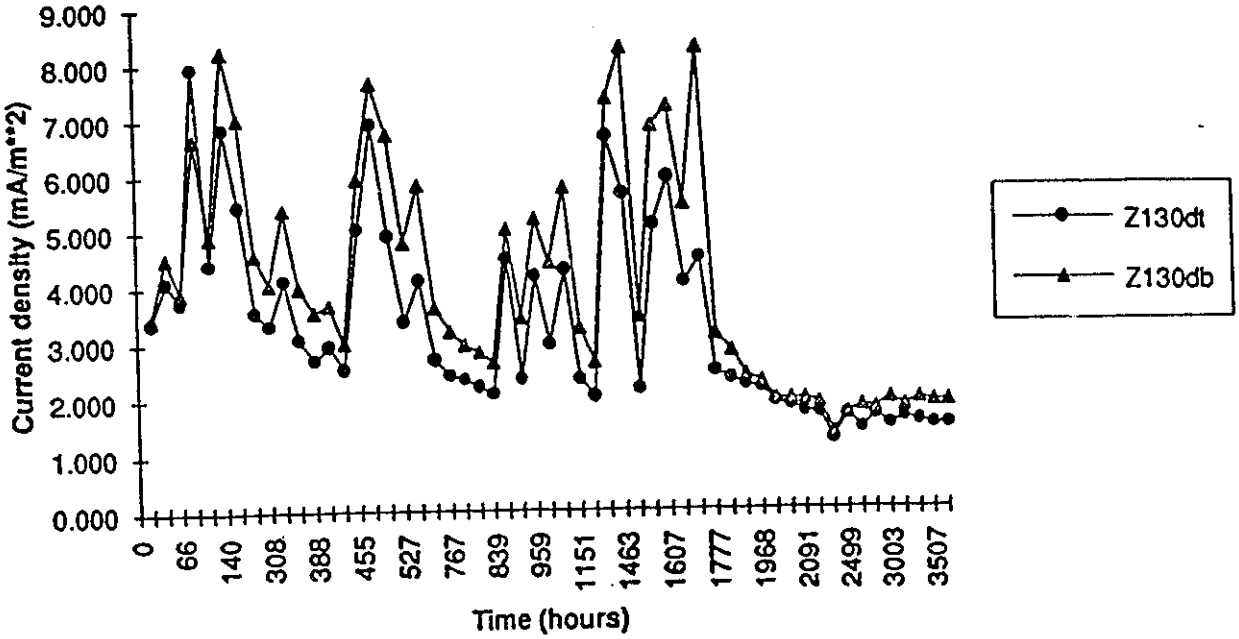

Figure 4.15 : The average current density (mA/m^2) for samples with 130 mm concrete cover, double layer reinforcement, and zinc anode in 100% humidity.

current density than that for the top layer. This observation implies that in reinforced concrete elements contaminated with salt, the second layer of reinforcement may benefit from cathodic protection more than the first layer, although this observation is limited to the cover range considered in the current test program.

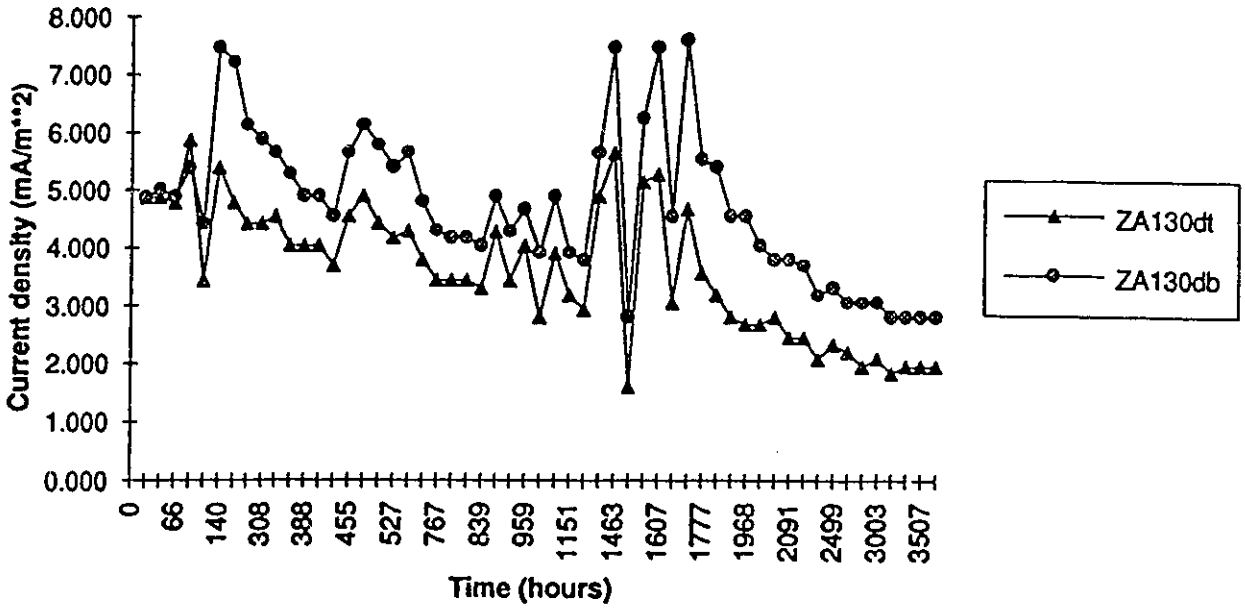

Figure 4.16 : The average current density (mA/m^2) for samples with 130 mm concrete cover, double layer reinforcement, and zinc-aluminum (78:22) anode in 100% humidity.

Chapter 5

Conclusions

5.1 Summary

The performance of galvanic cathodic protection was investigated experimentally. The experiments were conducted in three phases, either in electrolyte solution, or on concrete samples. A large number of samples were tested to assess feasibility of galvanic cathodic protection under different test conditions. The test parameters included anode material, concrete cover, humidity conditions and salt contamination. The progress of cathodic protection was monitored through current density and depolarization readings.

5.2 Conclusions

The following conclusions can be drawn from this experimental investigation:

- From the results, galvanic cathodic protection appears to be an effective method to slow down corrosion of reinforcement in concrete.
- All the anode materials considered in Phase 1 tests (in solutions), i.e., Zinc, Zinc-Aluminum (98:2), Zinc-Aluminum (85:15), and Aluminum developed depolarization values in excess of 100 mV, indicating that they all form suitable anode materials for galvanic cathodic protection. The data also shows that among the materials considered, Zinc-Aluminum (85:15) showed more stable

and higher current density values, indicating potentially superior cathodic protection characteristics.

- The anode materials investigated in Phase 2 and 3 indicated that zinc-aluminum anode consistently showed higher cathodic protection when compared with pure zinc anode.

- Cathodic protection increases in salt contaminated environment mainly because salt contamination lowers the resistivity of concrete. Concrete samples with and without the presence of salt indicate that the current density values are significantly higher in presence of salt. Salt spraying on clean concrete samples drastically increases current density values, resulting in approximately 50 to 100 times more cathodic protection activity. All salt contaminated samples were able to develop depolarization values in excess of 100 mV, especially in 100% humidity.

- Cathodic protection increases with decreasing concrete cover in clean concrete samples. Samples with 20 mm concrete cover showed higher current density and depolarization values than those with 50 mm and 130 mm covers. However, a reversed trend is observed in salt contaminated concrete used in Phase 3. In these specimens the cathodic protection was higher in concrete with 130 mm cover than those with 50 mm and 20 mm covers. Samples with salt contaminated concrete containing two layers of reinforcement, one with 30 mm and the other with 130 mm cover showed the same trend, with increased cathodic protection in the bottom bar with 130 mm cover.

- Higher humidity increases conductivity of concrete and improves cathodic protection. Samples in 100% humidity consistently showed higher cathodic protection than those in 50% humidity.

5.3 Significance of Research Findings on Practice

The experiments carried out in this investigation indicates that galvanic cathodic protection is an effective method to slow down corrosion of reinforcing steel in concrete. This method is especially suitable for parking garages and other similar reinforced concrete structures where the concrete cover is relatively thin, typically ranging between 40 to 50 mm, making impressed current systems difficult to apply. The method includes direct connection between the anode and cathode without the need for rectifier, and has sufficient polarization values to protect reinforcing steel. Furthermore, it involves a simple procedure of spraying metallized zinc or zinc-aluminum coat on the surface of the structural element. This coat of metal can be replenished as needed when the anode material is consumed away. Therefore, it is an economical method which would minimize cost associated with repairing corroded structure periodically, and hence offers a tremendous potential for use in practice.

5.4 Recommendations for Further Research

Although the research program reported in this thesis produced a large volume of test data, many aspects of galvanic cathodic protection require further study. Among those are the following:

- Long term feasibility of galvanic cathodic protection should be investigated.
- The superiority of zinc-aluminum as an anode material needs further study, especially in concrete environment, where the pH value is high.
- The effect of concrete cover and its relationship with salt contamination need further study.
- Feasibility of replenishing consumed anode material and related technology should be investigated.
- The efficiency of galvanic cathodic protection in moderate environments, and its relationship with salt contamination needs further study.

Appendix A

The Data of Depolarization

Appendix A contains additional experimental data that are not included in the main body of the thesis.

Table A.1 : EMF (mV) measured in Phase 2 samples between anode and cathode in 50% humidity. Z: Zn, ZA: Zn-Al. The number following Z and ZA represents the thickness of concrete cover in mm.

time	Z125	Z50	Z20	Z50s	ZA125	ZA50	ZA20	ZA50s
Jun.92	132.61	158.47	123.10	196.71	208.77	209.02	193.05	203.50
Jul.92	880.86	880.44	872.84	870.56	860.75	859.32	840.30	841.11
Dec.92	737.83	728.83	693.67	627.67	707.83	705.34	683.33	695.00
Jan.93	690.83	689.67	659.33	592.67	688.17	674.33	649.67	654.00
Apr.93	663.67	699.67	685.00	623.67	675.00	657.34	653.00	652.00
May.93	612.33	681.66	684.00	630.00	684.66	739.66	670.67	683.00
Jun.93	639.33	670.67	677.67	629.33	663.00	592.67	646.00	653.67
Jul.93	680.67	675.00	685.66	664.33	682.33	605.67	669.00	675.00
Aug.93	667.67	659.66	667.67	637.34	657.00	564.33	644.33	651.33

Table A.2 : EMF (mV) measured in Phase 2 samples between anode and cathode in 100% humidity. Z: Zn, ZA: Zn-Al. The number following Z and ZA represents the thickness of concrete cover in mm.

time	Z125	Z50	Z20	Z50s	ZA125	ZA50	ZA20	ZA50s
Jun.92	218.927	223.755	240.976	283.727	284.971	228.498	363.942	320.1793
Jul.92	903.652	869.808	867.128	872.619	857.584	848.242	840.211	844.162
Nov.92	688	250.17	317.83	540.5	600	697.5	469.3	398.83
Jan.93	740.5	352.33	495.33	577.33	580.83	714.33	778.3	487.17

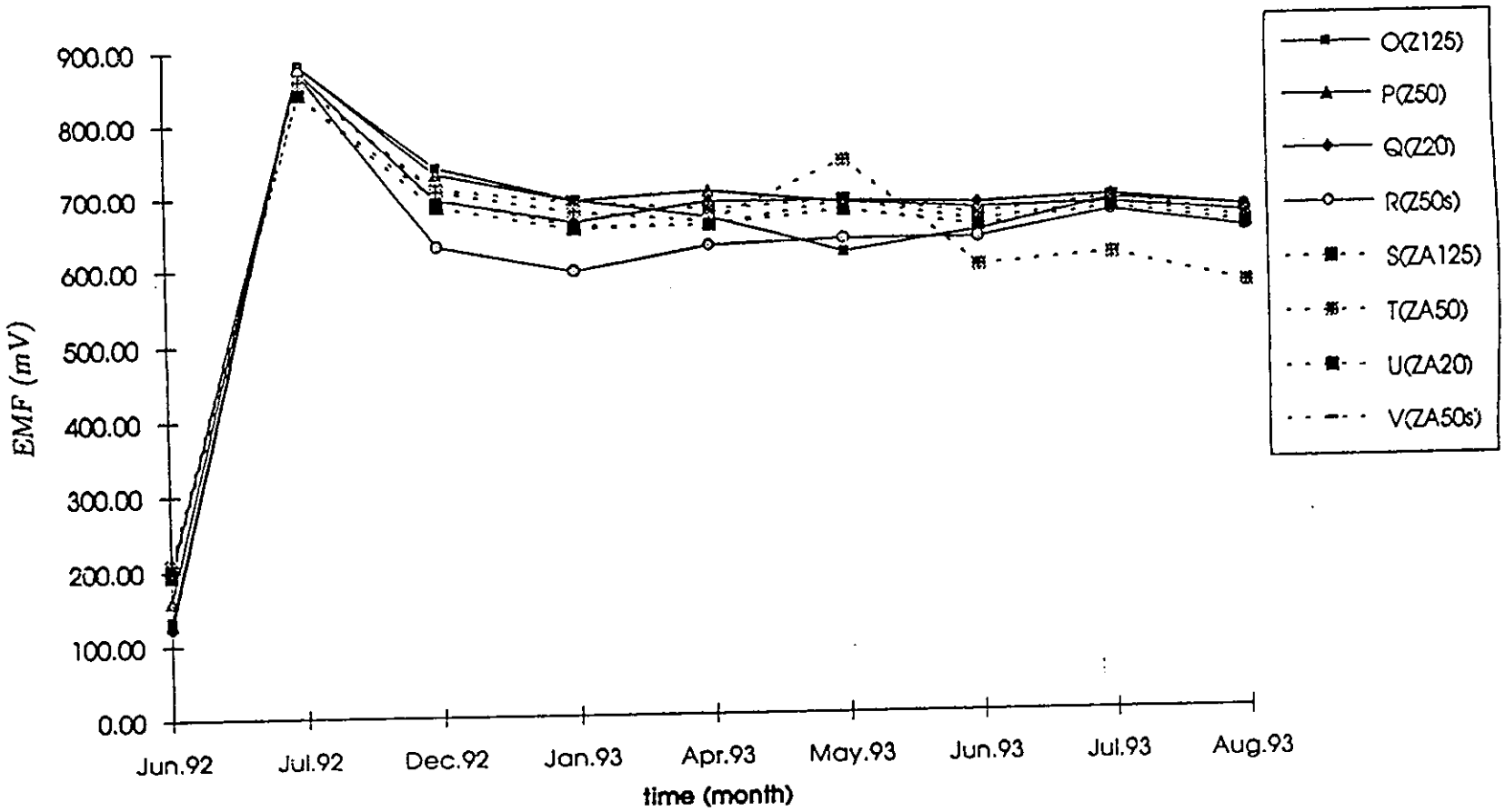

Figure A.1 : EMF (mV) vs. time measured in Phase 2 samples in 50% humidity.

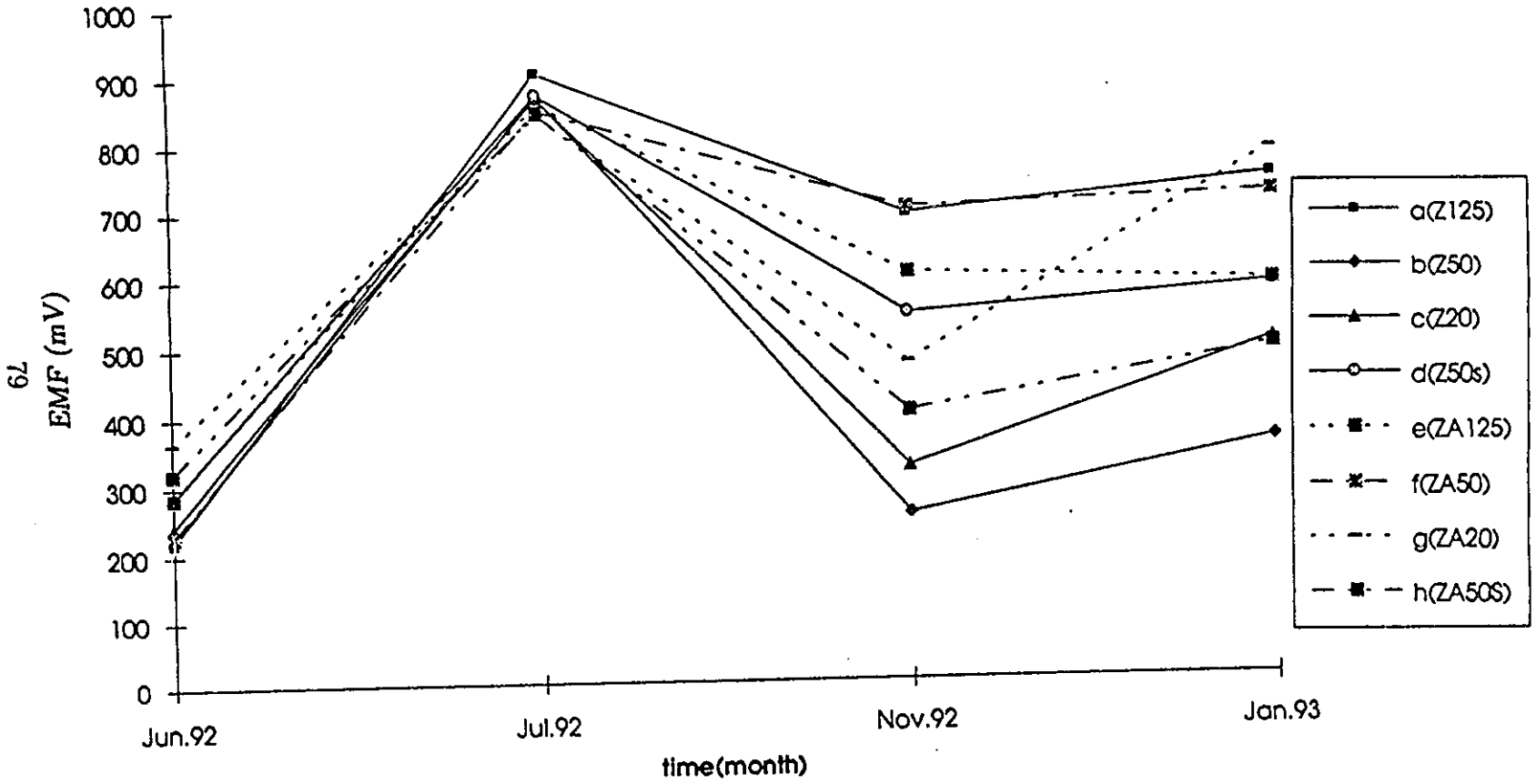

Figure A.2 : EMF (mV) vs. time measured in Phase 2 samples in 100% humidity.

Table A.3 : On-potential (mV) of two steel bars vs. $Cu/CuSO_4$ measured in Phase 2 samples in 50% humidity. Z: Zn, ZA: Zn-Al. The number following Z and ZA represents the thickness of concrete cover in mm.

time	Z125	Z50	Z20	Z50s	ZA125	ZA50)	ZA20	ZA50s
Jun.92	-23.95	-92.87	-40.46	-124.14	-77.19	-77.63	-104.37	-93.07
Jul.92	-492.08	-657.87	-800.60	-663.38	-498.32	-575.16	-804.70	-640.66
Dec.92	-380.00	-610.00	-697.33	-519.33	-414.67	-517.00	-663.33	-591.67
Jan.93	-374.33	-576.00	-674.67	-476.67	-422.00	-481.00	-590.00	-483.00
Apr.93	-464.33	-567.67	-711.67	-543.67	-419.34	-385.34	-650.33	-533.67
May.93	-379.33	-576.67	-696.00	-542.67	-457.00	-386.34	-683.00	-559.33
Jun.93	-413.67	-563.67	-702.33	-495.67	-442.00	-373.00	-660.00	-537.67
Jul.93	-389.00	-582.34	-722.33	-517.67	-454.34	-355.34	-703.33	-570.00
Aug.93	-342.67	-570.00	-710.33	-542.33	-444.00	-361.67	-669.00	-543.67

Table A.4 : On-potential (mV) of two steel bars vs. $Cu/CuSO_4$ measured in Phase 2 samples In 100% humidity. Z: Zn, ZA: Zn-Al. The number following Z and ZA represents the thickness of concrete cover in mm.

tiime	Z125	Z50	Z20	Z50s	ZA125	ZA50	ZA20	ZA50s
Jun.92	-223.74	-197.72	-189.99	-408.38	-254.33	-236.61	-256.75	-457.94
Jul.92	-706.81	-767.08	-910.79	-648.63	-639.40	-781.73	-919.89	-888.97
Nov.92	-683.00	-483.34	-510.66	-674.00	-345.33	-580.33	-470.00	-720.00
Jan.93	-680.33	-387.34	-472.00	-696.00	-679.00	-551.33	-455.67	-800.67

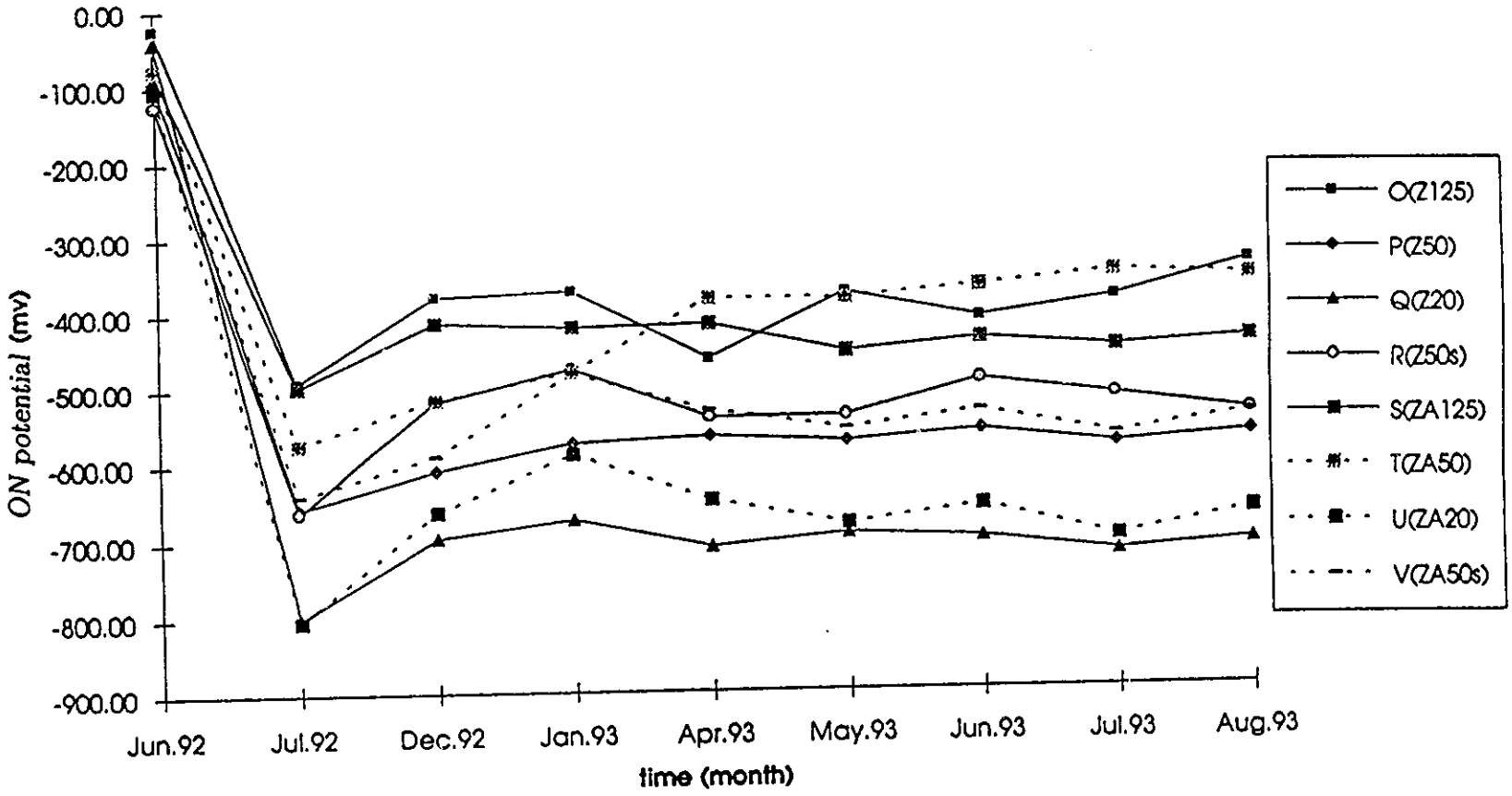

Figure A.3 : On-potential of steel-Cu/$CuSO_4$ vs. time measured in Phase 2 samples in 50% humidity.

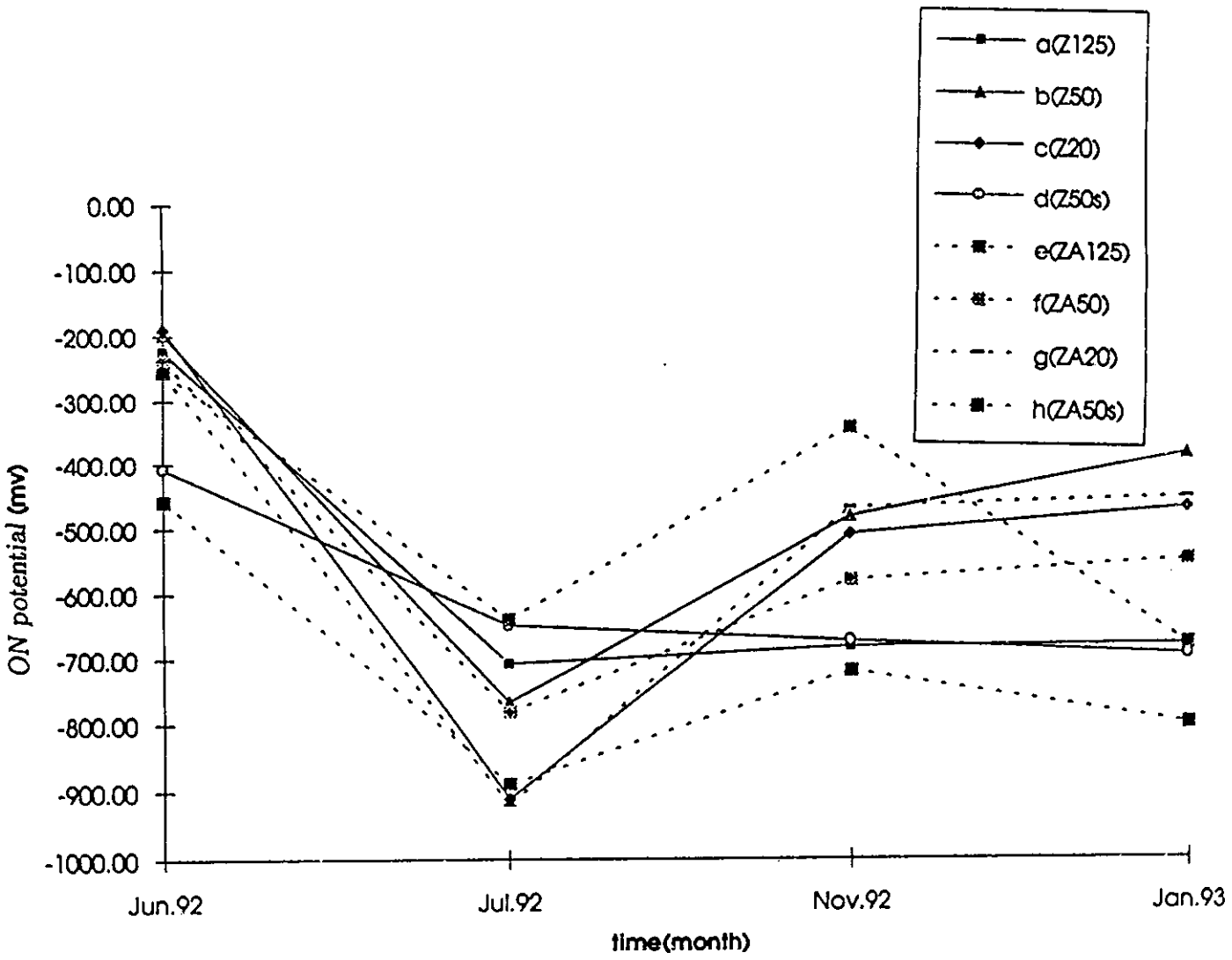

Figure A.4 : On-potential of steel-Cu/$CuSO_4$ vs. time measured in Phase 2 samples in 100% humidity.

Table A.5 : E_{corr} and I_{corr} of zinc, z-Alumi. (78:22), steel bar measured in Phase 3 samples. Z: Zn, ZA: Zn-Al. The number following Z and ZA represents the thickness of concrete cover in mm. (continued on next page)

Feb.12-25,1993. Measure Ecorr and Icorr of zinc; z-Alium.(78:22); steel bar.
The experiment is called polarization resistance,Rang -0.2mv to 0.2mv.
Reference(low)

	area(cm^	eq. wt(g)	density(g/cm^3)
Fe	200.00	18.62	7.87
Zn	250.00	32.69	6.51
Zn-Al	250.00	13.74	2.83

50%RH on zinc	**Ave.Z20**		**Ave.Z50**		**Ave.Z125**		**Ave.z125d**		
	Zinc	Steel	Zinc	Steel	Zinc	Steel	Zinc	Steel(up)	Steel(down)
Eco(mv) vs.CSE	**-770.29**	**-352.66**	**-640.01**	**-303.23**	**-695.36**	**-384.75**	**-663.91**	**-373.13**	**-326.50**
Pol Res.(K-o cm^2)	962.54	57.93	1715.50	54.98	1530.90	71.90	1164.28	86.96	109.34
Icor (uA/cm^2)	0.05	0.45	0.02	0.48	0.02	0.37	0.03	0.32	0.24
Corr Rate(mpy)	0.03	0.14	0.01	0.15	0.01	0.11	0.02	0.10	0.07
Correlation	1.00	0.94	0.99	0.95	0.99	33.62	0.99	0.88	0.92

50%RH z-alium.	**Ave.ZA20**		**Ave.ZA50**		**Ave.ZA125**		**Ave.ZA125D**		
	z-alium.	steel	z-alium.	steel	z-alium.	steel	z-alium.	steel(up)	steel(down)
Eco(mv) vs.CSE	**-815.84**	**-341.11**	**-758.60**	**-329.76**	**-826.36**	**-382.99**	**-813.74**	**-414.52**	**-414.72**
Pol Res.(K-o cm^2)	1094.94	65.29	1394.71	43.52	1112.65	60.43	1158.98	161.77	1003.44
Icor (uA/cm^2)	0.03	0.41	0.02	0.60	0.02	0.45	0.02	0.16	0.03
Corr Rate(mpy)	0.02	0.13	0.01	0.18	0.02	0.14	0.01	0.05	0.01
Correlation	0.99	0.94	0.98	0.88	0.99	0.93	0.99	0.98	1.00

100%RH on zinc	Ave.Z20		Ave.Z50		Ave.Z125		Ave.z125d		
	Zinc	Steel	Zinc	Steel	Zinc	Steel	Zinc	Steel(up)	Steel(down)
Eco(mv) vs.CSE	-791.12	-417.88	-780.70	-461.28	-653.53	-346.13	-814.09	-462.43	-500.66
Pol Res.(K-o cm^2)	311.05	76.14	347.98	93.02	508.52	85.96	632.62	79.04	99.86
Icor (uA/cm^2)	0.05	0.37	0.09	0.38	0.05	0.31	0.04	0.37	0.26
Corr Rate(mpy)	0.06	0.11	0.05	0.12	0.03	0.09	0.03	0.11	0.08
Correlation	1.00	0.93	1.00	0.95	1.00	0.96	0.99	0.92	0.93

100%RH z-alium.	Ave.ZA20		Ave.ZA50		Ave.ZA125		Ave.ZA125d		
	Z-Alium.	Steel	Z-Alium.	Steel	Z-Alium.	Steel	Z-Alium.	Steel(up)	Steel(down)
Eco(mv) vs.CSE	-1040.33	-378.50	-989.88	-402.85	-927.62	-331.26	-902.34	-397.28	-259.26
Pol Res.(K-o cm^2)	425.15	95.15	547.79	63.58	661.97	69.78	738.76	66.59	118.68
Icor (uA/cm^2)	0.06	0.32	0.05	0.41	0.04	0.38	0.04	0.39	0.22
Corr Rate(mpy)	0.04	0.10	0.03	0.13	0.03	0.12	0.02	0.12	0.07
Correlation	0.99	0.89	0.98	0.94	0.98	0.91	0.99	0.93	0.95

Table A.6 : Ac impedance between anode and steel bar measured in Phase 3 samples. Z: Zn, ZA: Zn-Al. The number following Z and ZA represents the thickness of concrete cover in mm.

Ac impedence measurement between Zn-Fe

	50% on Feb.23,1993		100% on Feb.24,1993	
name	R(ohm)	Ave.	R(ohm)	Ave.
z20-1	70.26		75.35	
z20-2	67.82	75.78	76.10	75.21
z20-3	89.26		74.19	
za20-1	60.63		73.86	
za20-2	76.15	70.05	75.04	74.82
za20-3	73.38		75.55	
z50-1	118.00		118.35	
z50-2	124.00	113.36	111.44	115.79
z50-3	98.07		117.58	
za50-1	119.03		133.36	
za50-2	120.69	125.04	133.71	134.47
za50-3	135.39		136.35	
z125-1	233.69		205.09	
z125-2	227.89	233.13	202.72	202.31
z125-3	237.80		199.13	
za125-1	233.11		207.69	
za125-2	240.14	238.26	207.68	215.22
za125-3	241.53		230.30	
z125dT-1	90.93	90.59	77.55	77.03
z125dT-2	90.25		76.50	
z125dB-1	254.13	255.44	199.40	203.88
z125dB-2	256.74		208.36	
za125dT-1	93.54		73.25	
za125dB-1	279.30		198.65	

Table A.7 : Half cell potential (V) between $Cu/CuSO_4$ and graphite in 50% and 100% humidities measured in Phase 3 samples. Z: Zn, ZA: Zn-Al. The number following Z and ZA represents the thickness of concrete cover in mm.

high on CuSO4, low on graphite

50%	Feb.12,93	May10,93	July 8,93	100%	Mar.1,93	May5,93	July 8,93
name	potential(v)	potential(v)	potential(v)	name	potential(v)	potential(v)	potential(v)
lz20-1	0.196	0.095	0.092	hz20-1	0.234	0.093	0.064
lz20-2	0.242	0.093	0.085	hz20-2	0.353	0.067	0.075
lz20-3	0.242	0.082	0.082	hz20-3	0.277	0.065	0.077
lza20-1	0.227	0.088	0.081	hza20-1	0.273	0.025	0.038
lza20-2	0.225	0.076	0.075	hza20-2	0.177	0.052	0.028
lza20-3	0.155	0.091	0.089	hza20-3	0.369	0.046	0.031
lz50-1	0.171	0.084	0.079	hz50-1	0.298	0.076	0.054
lz50-2	0.211	0.082	0.044	hz50-2	0.234	0.086	0.036
lz50-3	0.175	0.043	0.083	hz50-3	0.286	0.058	0.024
lza50-1	0.195	0.079	0.078	hza50-1	0.365	0.091	0.056
lza50-2	0.195	0.048	0.048	hza50-2	0.278	0.063	0.043
lza50-3	0.225	0.093	0.061	hza50-3	0.126	0.108	0.092
lz125-1	0.185	0.177	0.147	hz125-1	0.140	0.088	0.062
lz125-2	0.248	0.064	0.085	hz125-2	0.091	0.092	0.062
lz125-3	0.176	0.082	0.091	hz125-3	0.138	0.095	0.043
lza125-1	0.161	0.077	0.068	hza125-1	0.225	0.072	0.033
lza125-2	0.255	0.098	0.092	hza125-2	0.245	0.052	0.030
lza125-3	0.175	0.157	0.097	hza125-3	0.200	0.024	0.011
lz125d-1	0.235	0.091	0.083	hz125d-1	0.363	0.037	0.032
lz125d-2	0.192	0.106	0.107	hz125d-2	0.289	0.031	0.024
lza125d-1	0.225	0.107	0.107	hza125d-1	0.136	0.110	0.056

Table A.8 : EMF (V) between anode and cathode in 50% humidity measured in Phase 3 samples. Z: Zn, ZA: Zn-Al. The number following Z and ZA represents the thickness of concrete cover in mm.

	time	Z20	ZA20	Z50	ZA50	Z125	ZA125	Z125dt	Z125db	ZA125dt	ZA125db
EMF(V)	3 days	0.446	0.673	0.450	0.697	0.461	0.686	0.445	0.458	0.689	0.721
EMF(V)	1st week	0.394	0.658	0.403	0.679	0.411	0.644	0.378	0.391	0.674	0.713
EMF(V)	2nd week	0.314	0.578	0.316	0.604	0.331	0.561	0.306	0.322	0.622	0.662
EMF(V)	3rd week	0.332	0.672	0.344	0.710	0.388	0.676	0.335	0.352	0.696	0.748
EMF(V)	4th week	0.300	0.637	0.295	0.690	0.334	0.646	0.286	0.306	0.672	0.721
EMF(V)	5th week	0.255	0.552	0.255	0.606	0.278	0.557	0.254	0.275	0.608	0.660
EMF(V)	6th week	0.233	0.519	0.239	0.571	0.254	0.527	0.241	0.263	0.582	0.623
EMF(V)	7th week	0.222	0.508	0.230	0.557	0.240	0.516	0.236	0.255	0.569	0.610
EMF(V)	8th week	0.214	0.497	0.253	0.548	0.229	0.504	0.232	0.250	0.562	0.596
EMF(V)	9th week	0.213	0.500	0.245	0.547	0.233	0.516	0.233	0.252	0.562	0.604
EMF(V)	10th week	0.208	0.511	0.222	0.555	0.235	0.508	0.229	0.247	0.559	0.598
EMF(V)	11th week	0.203	0.491	0.211	0.536	0.235	0.492	0.271	0.240	0.493	0.581
EMF(V)	12th week	0.200	0.482	0.225	0.529	0.231	0.485	0.221	0.237	0.535	0.544
EMF(V)	13th week	0.200	0.481	0.229	0.527	0.231	0.484	0.207	0.235	0.533	0.570
EMF(V)	14th week	0.201	0.489	0.221	0.533	0.232	0.489	0.221	0.235	0.535	0.570
EMF(V)	18th week	0.188	0.455	0.203	0.498	0.220	0.457	0.204	0.220	0.406	0.538

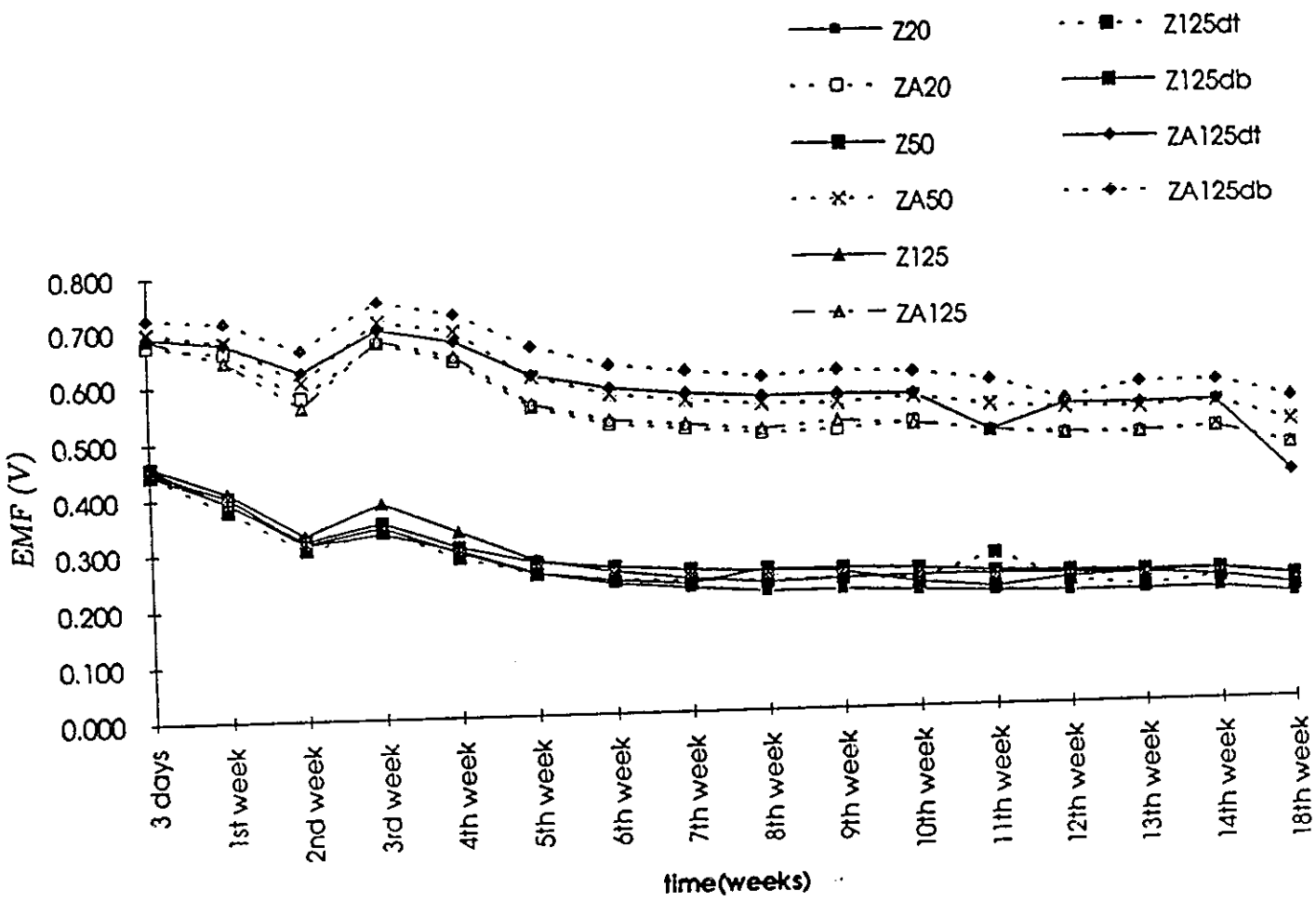

Figure A.5 : EMF (V) vs. time measured in Phase 3 samples in 50% humidity.

Table A.9 : EMF (V) between anode and cathode in 100% humidity measured in Phase 3 samples. Z: Zn, ZA: Zn-Al. The number following Z and ZA represents the thickness of concrete cover in mm.

	time	Z20	ZA20	Z50	ZA50	Z125	ZA125	Z125dt	Z125db	ZA125dt	ZA125db
EMF(V)	1st week	0.247	0.541	0.267	0.781	0.248	0.749	0.295	0.256	0.752	0.804
EMF(V)	2nd week	0.241	0.547	0.248	0.732	0.209	0.704	0.282	0.248	0.723	0.758
EMF(V)	3rd week	0.347	0.474	0.571	0.840	0.376	0.836	0.413	0.381	0.748	0.799
EMF(V)	4th week	0.255	0.457	0.524	0.809	0.297	0.735	0.320	0.275	0.699	0.738
EMF(V)	5th week	0.200	0.470	0.212	0.680	0.180	0.613	0.236	0.195	0.630	0.664
EMF(V)	6th week	0.378	0.476	0.483	0.726	0.341	0.700	0.556	0.536	0.728	0.765
EMF(V)	7th week	0.194	0.422	0.070	0.596	0.173	0.561	0.237	0.198	0.576	0.608
EMF(V)	8th week	0.226	0.419	0.247	0.606	0.270	0.614	0.336	0.346	0.567	0.611
EMF(V)	9th week	0.284	0.411	0.209	0.612	0.276	0.611	0.494	0.500	0.593	0.654
EMF(V)	10th wee	0.262	0.326	0.502	0.508	0.540	0.815	0.585	0.618	0.810	0.881
EMF(V)	11th wee	0.143	0.367	0.112	0.559	0.203	0.557	0.231	0.177	0.569	0.616
EMF(V)	12th wee	0.165	0.371	0.097	0.549	0.181	0.537	0.217	0.156	0.555	0.591
EMF(V)	13th wee	0.173	0.405	0.092	0.542	0.170	0.526	0.211	0.158	0.540	0.577
EMF(V)	14th wee	0.173	0.355	0.090	0.537	0.167	0.521	0.206	0.149	0.533	0.569
EMF(V)	18th wee	0.167	0.422	0.088	0.510	0.182	0.497	0.204	0.154	0.503	0.545

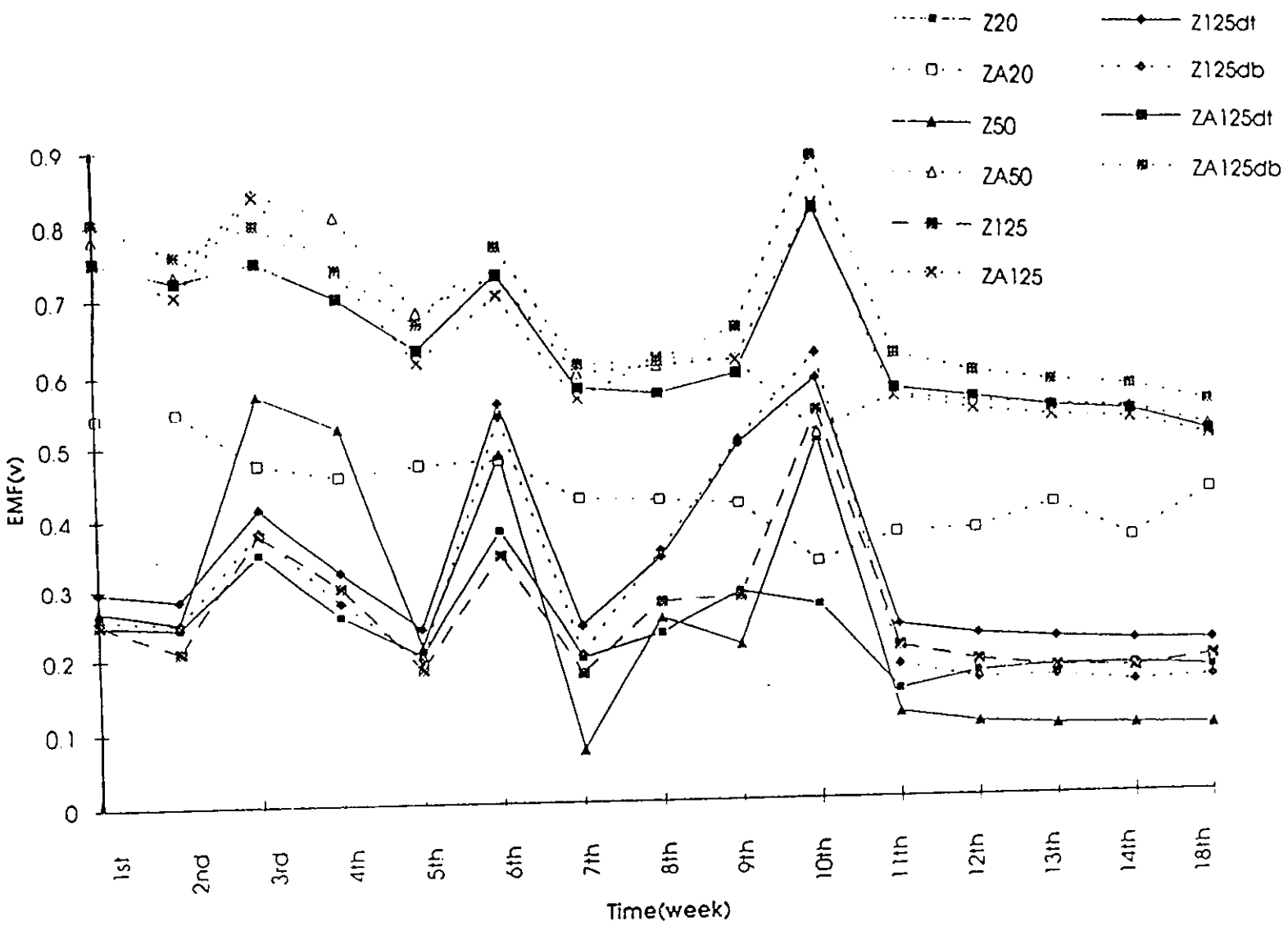

Figure A.6 : EMF (V) vs. time measured in Phase 3 samples in 100% humidity.

Table A.10 : On-potential (V) of two steel bars vs. $Cu/CuSO_4$ measured in Phase 3 samples in 50% humidity. Z: Zn, ZA: Zn-Al. The number following Z and ZA represents the thickness of concrete cover in mm.

	time	Z20	ZA20	Z50	ZA50	Z125	ZA125	Z125dt	Z125db	ZA125dt	ZA125db
on potential	3 days	-0.613	-0.564	-0.550	-0.546	-0.555	-0.567	-0.516	-0.518	-0.513	-0.513
on potential	1st week	-0.582	-0.546	-0.514	-0.514	-0.519	-0.502	-0.469	-0.470	-0.486	-0.486
on potential	2nd week	-0.524	-0.450	-0.451	-0.424	-0.452	-0.417	-0.426	-0.426	-0.418	-0.418
on potential	3rd week	-0.551	-0.573	-0.485	-0.569	-0.493	-0.554	-0.449	-0.449	-0.528	-0.528
on potential	4th week	-0.531	-0.523	-0.453	-0.525	-0.461	-0.508	-0.422	-0.422	-0.477	-0.477
on potential	5th week	-0.358	-0.328	-0.301	-0.300	-0.323	-0.330	-0.285	-0.285	-0.298	-0.298
on potential	6th week	-0.342	-0.307	-0.282	-0.277	-0.305	-0.302	-0.270	-0.272	-0.273	-0.273
on potential	7th week	-0.329	-0.301	-0.271	-0.268	-0.299	-0.292	-0.262	-0.262	-0.263	-0.261
on potential	8th week	-0.320	-0.296	-0.261	-0.261	-0.294	-0.286	-0.255	-0.256	-0.256	-0.254
on potential	9th week	-0.322	-0.298	-0.264	-0.264	-0.291	-0.296	-0.259	-0.259	-0.261	-0.261
on potential	10th week	-0.315	-0.309	-0.256	-0.272	-0.287	-0.294	-0.256	-0.256	-0.258	-0.258
on potential	11th week	-0.309	-0.297	-0.249	-0.260	-0.275	-0.284	-0.219	-0.250	-0.337	-0.251
on potential	12th week	-0.307	-0.294	-0.249	-0.258	-0.273	-0.282	-0.247	-0.247	-0.254	-0.256
on potential	13th week	-0.305	-0.292	-0.246	-0.256	-0.269	-0.281	-0.250	-0.248	-0.246	-0.246
on potential	14th week	-0.307	-0.300	-0.247	-0.262	-0.270	-0.287	-0.247	-0.247	-0.251	-0.251
on potential	18th week	-0.292	-0.278	-0.236	-0.235	-0.259	-0.244	-0.233	-0.233	-0.278	-0.278

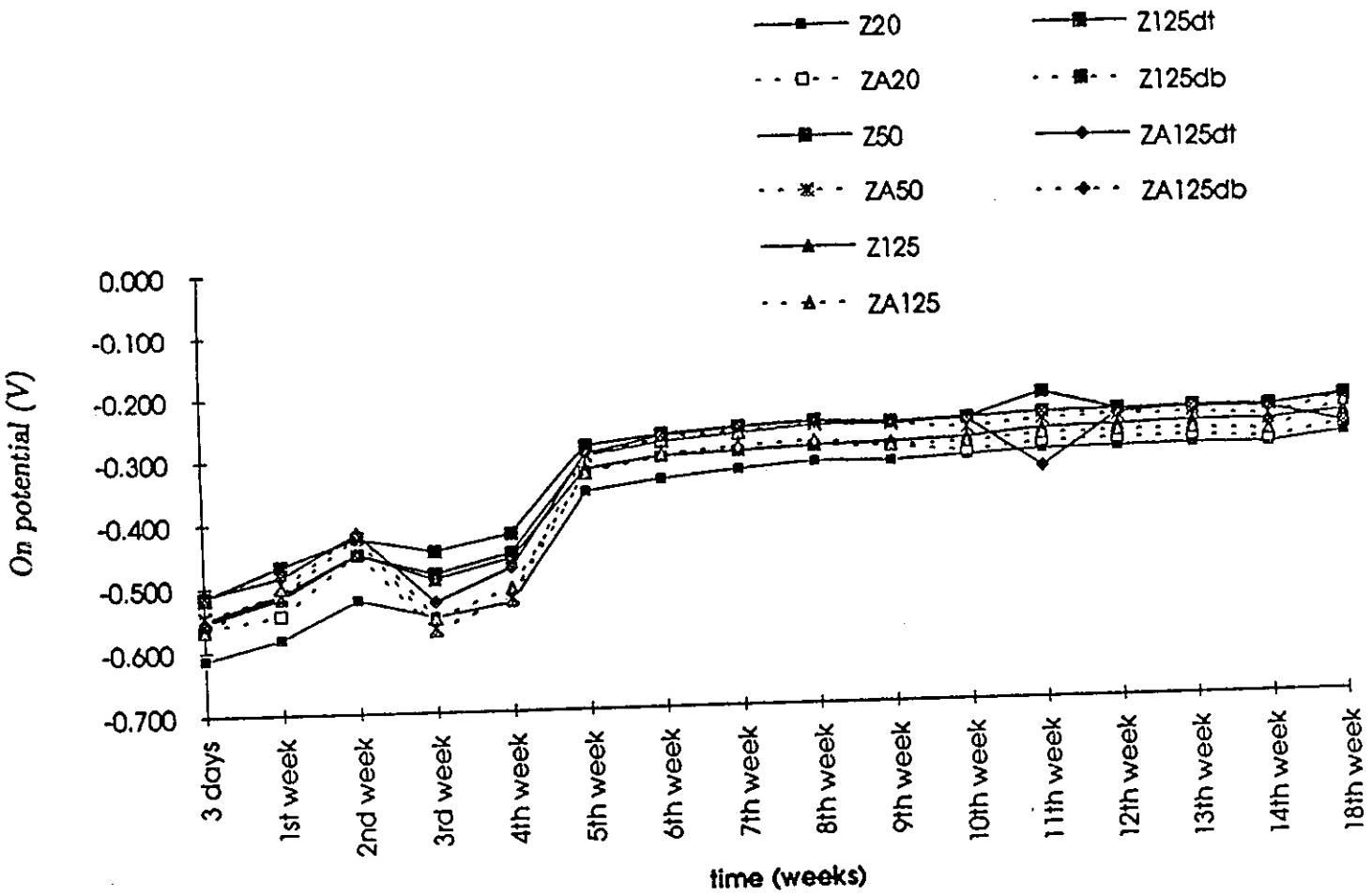

Figure A.7 : On-potential (V) of steel-Cu/$CuSO_4$ vs. time measured in Phase 3 samples in 50% humidity.

Table A.11 : On-potential (V) of two steel bars vs. $Cu/CuSO_4$ measured in Phase 3 samples in 100% humidity. Z: Zn, ZA: Zn-Al. The number following Z and ZA represents the thickness of concrete cover in mm.

	time	Z20	ZA20	Z50	ZA50	Z125	ZA125	Z125dt	Z125db	ZA125dt	ZA125db
on potential	1st week	-0.736	-0.739	-0.661	-0.652	-0.483	-0.652	-0.714	-0.714	-0.493	-0.493
on potential	2nd week	-0.722	-0.690	-0.645	-0.634	-0.467	-0.633	-0.707	-0.707	-0.478	-0.478
on potential	3rd week	-0.979	-0.973	-0.899	-0.717	-0.548	-0.694	-0.782	-0.782	-0.502	-0.502
on potential	4th week	-0.881	-0.898	-0.814	-0.706	-0.527	-0.680	-0.729	-0.729	-0.480	-0.483
on potential	5th week	-0.478	-0.491	-0.438	-0.482	-0.430	-0.466	-0.396	-0.396	-0.437	-0.437
on potential	6th week	-0.694	-0.614	-0.558	-0.511	-0.476	-0.499	-0.472	-0.472	-0.467	-0.467
on potential	7th week	-0.489	-0.478	-0.453	-0.453	-0.428	-0.460	-0.405	-0.405	-0.440	-0.437
on potential	8th week	-0.769	-0.635	-0.595	-0.481	-0.496	-0.527	-0.515	-0.515	-0.525	-0.525
on potential	9th week	-0.648	-0.551	-0.556	-0.451	-0.487	-0.496	-0.529	-0.529	-0.557	-0.557
on potential	10th weel	-0.711	-0.669	-0.696	-0.728	-0.520	-0.753	-0.567	-0.567	-0.584	-0.584
on potential	11th weel	-0.442	-0.492	-0.418	-0.458	-0.413	-0.448	-0.390	-0.390	-0.486	-0.486
on potential	12th weel	-0.417	-0.436	-0.393	-0.434	-0.396	-0.442	-0.389	-0.389	-0.469	-0.469
on potential	13th weel	-0.387	-0.375	-0.349	-0.398	-0.382	-0.428	-0.380	-0.380	-0.464	-0.462
on potential	14th weel	-0.438	-0.388	-0.407	-0.453	-0.420	-0.434	-0.383	-0.382	-0.464	-0.462
on potential	18th weel	-0.428	-0.369	-0.365	-0.421	-0.380	-0.404	-0.373	-0.371	-0.413	-0.413

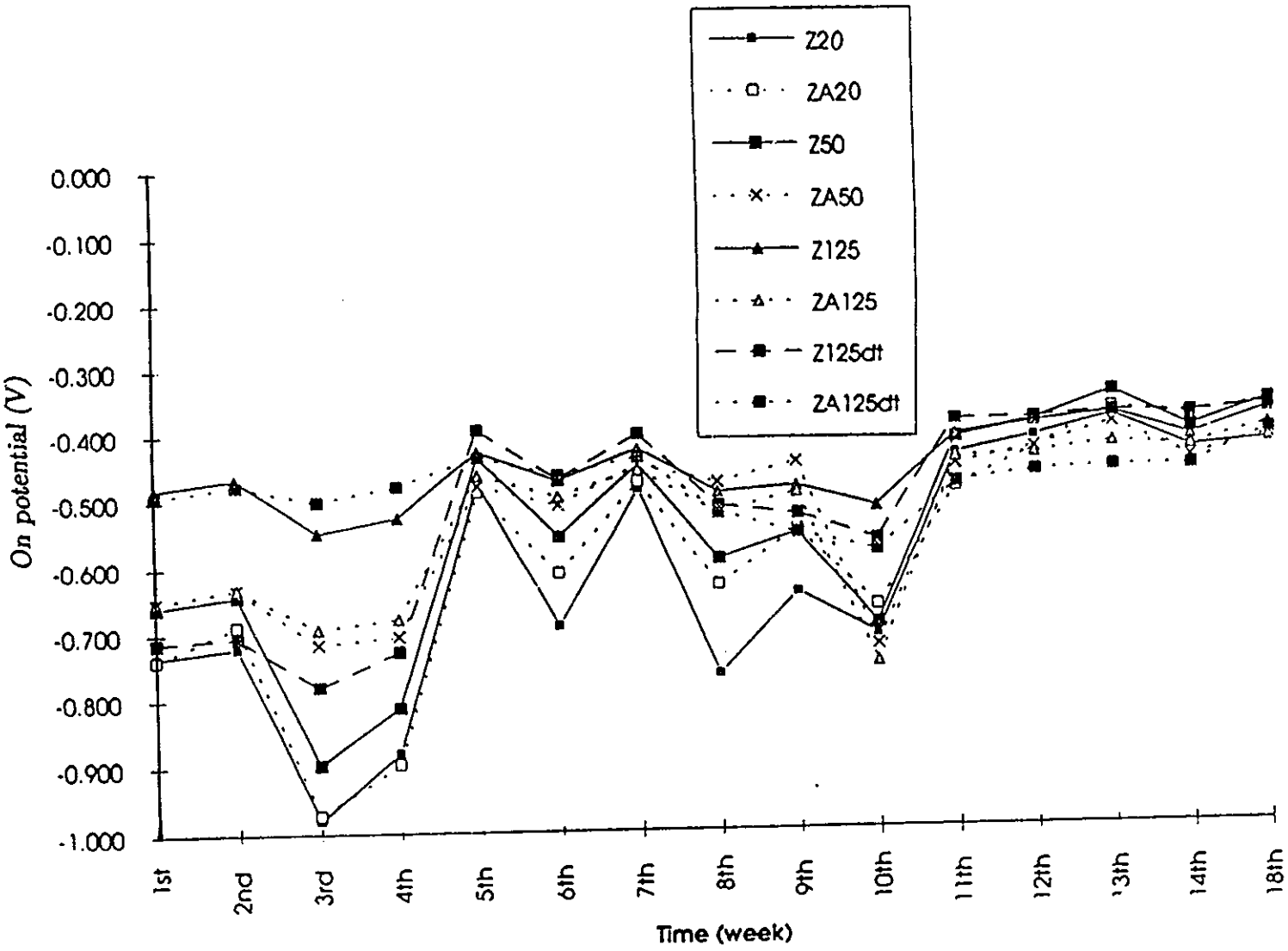

Figure A.8 : On-potential (V) of steel-Cu/$CuSO_4$ vs. time measured in Phase 3 samples in 100% humidity.

Appendix B

Practice Photo

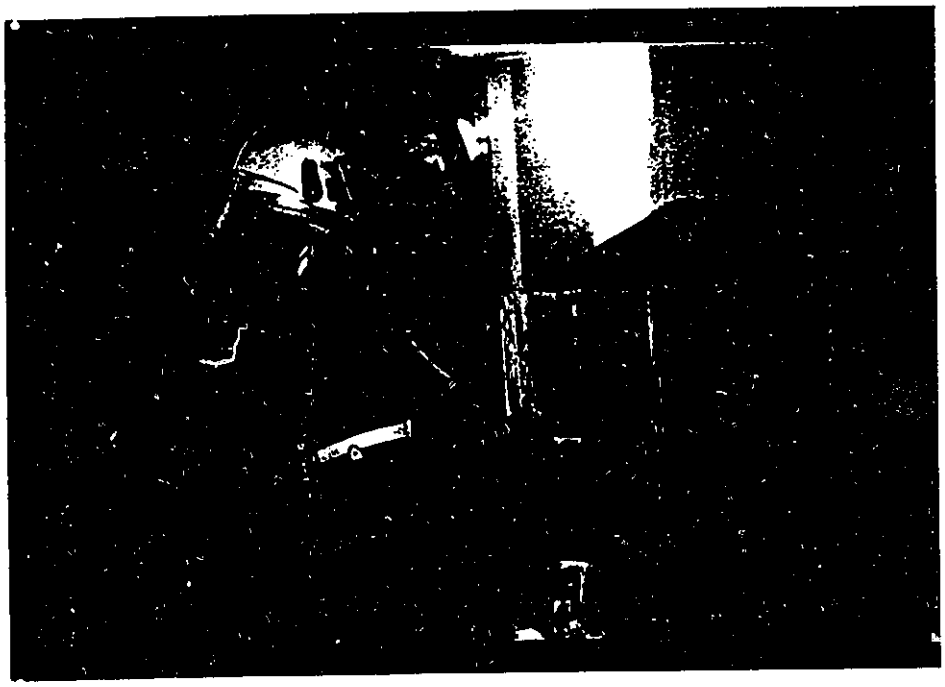

Figure B.1 : Metallized zinc spraying on Yaquina Bay Bridge, Newport, Oregon, U.S.A.

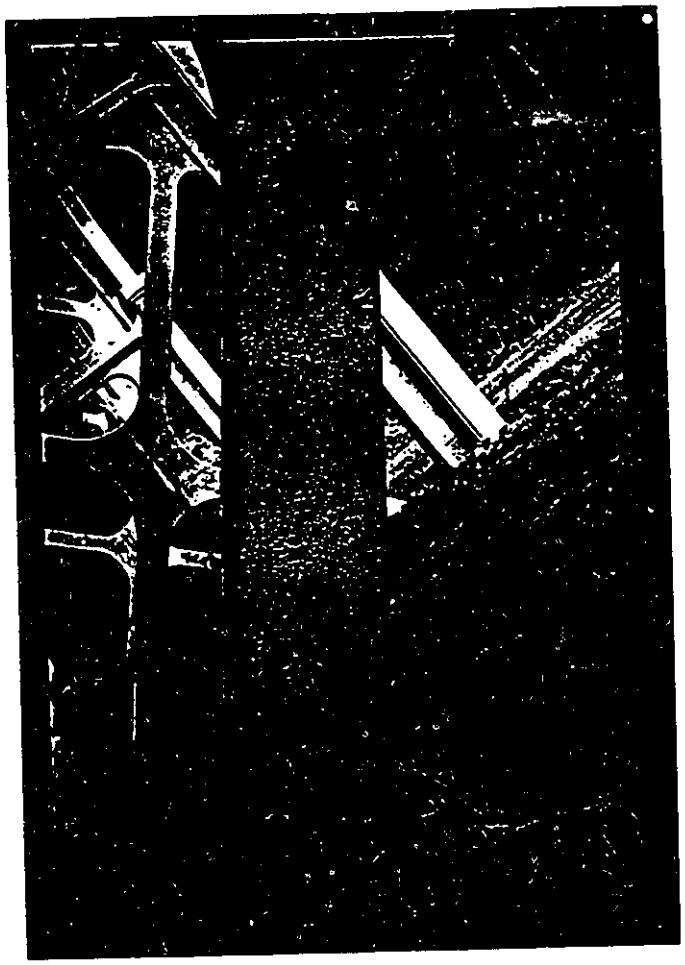

Figure B.2 : Partial galvanic cathodic protection on Cape Cveek Bridge, Devil's Elbow Park, Oregon, U.S.A.

Bibliography

[1] "Development, Testing and Field Application of Metallized Cathodic Protection Coatings on Reinforced Concrete Substructures," p. 1, by R.A. Carello, D.M. Parks, J.A. Apostolos. A research report, Office of Transportation Laboratory, Division of Construction, Department of Transportation, State of California.

[2] "Corrosion Basics, An Introduction", Chapter 3, by National Association Engineers, Houston, Texas, 1984.

[3] "Corrosion and Cathodic Protection of Steel Reinforced Concrete Bridge Decks" Chapter 1. by N.Dennis Burke, P.E. and James B.Bushman, P.E.

[4] "Evaluating the performance of conduction Coating Systems Applied to Reinforced Concrete Parking Decks" by R.A.Gommow, P.Eng. Consulting Engineer in Corrosion Correng Consulting Service Inc. Downsview, Ontario, November 1991.

[5] "Corrosion and Cathodic Protection of Steel Reinforced Concrete Bridge Decks" Chapter 2. by N.Dennis Burke, P.E. and James B.Bushman, P.E.

[6] "Repair and Protection of Concrete Structures" Chapter 11. by Noel P.Mailvaganam and Keith Cleary.

[7] "Repair and Protection of Concrete Structures" Chapter 3,10. by Noel P.Mailvaganam and John J.Deans.

[8] "Preventing Corrosion of Steel Reinforcement," pp. 29-33, by Dr. R. Brousseau. Construction Canada 92 09.

[9] "Corrosion of steel in concrete" Chapter 2. by P.Schiessl.

[10] "Metals Handbook" Ninth Edition. Volume 13, pp. 30-36. Corrosion. by ASM International.

[11] "Electrochemical methods, Fundamentals and applications" Chapter 1. by Allen J.Bard and Larry R.Faulkner.

[12] "Corrosion Basics, An Introduction", Chapter 9, by National Association Engineers, Houston, Texas, 1984.

[13] "Technical review of 100 mV polarization shift criteria for reinforcing steel in concrete" by M.Funahashi and J.B.Bushman.

[14] "A Proposal on Galvanic Cathodic Protection of Steel Reinforcement Using Metallized Zinc Coatings," by R. Brousseau, Y. Chen, S. Dallaire, R.F. Feldman, and M. Arnott. NRC report.

[15] "Galvanic Cathodic Protection of Steel Reinforcement Using Metallized Zinc Coatings," by J. Lawless. Report of Technical University of Nova Scotia Metallurgical Department.

[16] "Corrosion and Cathodic Protection of Steel Reinforced Concrete Bridge Decks" Chapter 2, 5. by N.Dennis Burke,P.E. and James B.Bushman, P.E.

[17] "Substructure Cathodic protection in Ontario: field trials 1982 to 1986" by D.G.Manning and H.C.Schell.

[18] "Metallizing provides cathodic protection to Florida bridge piers" by martin S. McGovern, on concrete repair digest June/July, 1992.

[19] K.W.J. Treadaway, B.L. Bron, and R.N. Cox, ASTM STP 713 (Philadelphia, PA: American Society of Testing and materials [ASTM],1980),p.102.

[20] A.R. cook and S. F. Radtke, ASTM StP 629 Philadelphia, PA: ASTM, 1977), p. 51.

[21] C. Andrade, A. Molina, F. Huete, and J.A. Gonzalez, in Corrosion of Reinforcement in Concrete Construction, ed. A.P. Crane (London, England: Ellis Horwood, 1983), p. 343.

[22] G.Sergi, N.R. Short, and C.L. Page, Corrosion 41, 11 (Nov.1985): p. 618.

[23] E. Maahn and B. Sorensen, Corrosion 42, 4 (April 1986): p. 187.

[24] A. Macias and C. andrade, Br. Corros. J. 22, 2 (1987): p. 113.

[25] A. Macias and C. andrade, ibid. 22, 2 (1987): p. 119.

[26] A. Macias and C. andrade, ibid. 22, 3 (1987): p. 162.

[27] A. Macias and C. andrade, Cement and Concrete Research 17, 2 (1987): p. 307.

[28] R.F. Lynch, J. Metals (Aug. 1987): p. 39.

[29] "Electrochemical Behavior of Galvanic Al-Zn Coatings in Saturated $Ca(OH)_2$ Solution" by T.P. Cheng, J.T. Lee, K.L.Lin, and W.T. Tsai.

[30] " Galvanic cathodic protection for reinforced concrete bridge decks" field evaluation by national cooperation highway research program report 234.

[31] "Sprayed-Zinc Galvanic Anodes for the Cathodic Protection of reinforcing Steel in Concrete" by Rodney G. Powers, Alberto A. sagues and Toshiya Murase, on Reinforcing Steel in Concrete.

[32] "Low-Cost Sprayed Zinc Galvanic of Reinforcing Steel in Marine Bridge Substructures" by Rodney G. Powers, Third quarterly report, Oct. 12, 1991.

[33] "Zinc Anodes to Control Bridge deck deterioration" by John L. Saner, State of Illinois Department of Transportation, Bureau of Material and Physical research.

[34] "Progress Report: Galvanic Cathodic Protection Using Metallized Coatings", by Mr. B. Baldock, Dr. R. Brousseau, Mr. M. Arnott, and Mr. R. Evraire.

[35] "ILZRO Project No. ZE-390 Flame Sprayed Zinc on Reinforced Concrete" by Dr.R.Brousseau.

[36] "Understanding electrochemical cells" Technical report number 017/85. by A.M.Kauffman, BSc, MSc, PGCE Solartron Instruments.

[37] "Metals Handbook" Ninth Edition. Volume 13, pp. 466-478, Corrosion. by ASM International.